University of Nebraska Medical Center
BREAKTHROUGHS FOR LIFE

University of Nebraska Medical Center
DigitalCommons@UNMC

Theses & Dissertations

Graduate Studies

Fall 12-18-2015

The Role of CXCR2 in Pancreatic Cancer Development and Progression

Abhilasha Purohit
University of Nebraska Medical Center

Tell us how you used this information in this short survey.

Follow this and additional works at: https://digitalcommons.unmc.edu/etd

 Part of the Cancer Biology Commons

Recommended Citation

Purohit, Abhilasha, "The Role of CXCR2 in Pancreatic Cancer Development and Progression" (2015). *Theses & Dissertations*. 48.
https://digitalcommons.unmc.edu/etd/48

This Dissertation is brought to you for free and open access by the Graduate Studies at DigitalCommons@UNMC. It has been accepted for inclusion in Theses & Dissertations by an authorized administrator of DigitalCommons@UNMC. For more information, please contact digitalcommons@unmc.edu.

THE ROLE OF CXCR2 IN PANCREATIC CANCER DEVELOPMENT AND PROGRESSION

By

Abhilasha Purohit

A DISSERTATION

Presented to the Faculty of

The Graduate College at the University of Nebraska Medical Center

In Partial Fulfillment of the Requirements

For the Degree of Doctor of Philosophy

The Department of Pathology and Microbiology

Under the Supervision of Professor Rakesh K. Singh

University of Nebraska Medical Center

Omaha, Nebraska

December, 2015

Supervisory Committee

Keith R. Johnson, Ph.D. **Surinder K. Batra, Ph.D.**

Joyce Solheim, Ph.D. **Audrey J. Lazenby, M.D.**

THE ROLE OF CXCR2 IN PANCREATIC CANCER DEVELOPMENT AND PROGRESSION

Abhilasha Purohit Ph.D.

University of Nebraska Medical Center, 2015

Supervisor: Rakesh K. Singh, Ph.D.

This dissertation examines the role of CXCR2, a seven transmembrane G-protein coupled receptor, in mediating autocrine as well as paracrine mechanisms during pancreatic cancer progression. Data presented in the initial section demonstrates the aberrant expression of the CXCR2 biological axis in human pancreatic cancer tissue specimens. A study performed within the first section of this dissertation investigates the contribution of CXCR2 signaling in pancreatic cancer initiation. These studies have identified a novel role of CXCR2 in mediating $KRAS^{(G12D)}$ -induced autocrine growth transformation of pancreatic cancer cells. The upregulation of the CXCR2 biological axis was found to be directly regulated by the $KRAS^{(G12D)}$ mutation using *in vitro* and *in vivo* model systems. Furthermore, the inhibition of CXCR2 by genetic and pharmacological tools was able to downregulate the protein level of KRAS.

The tumor microenvironment in pancreatic cancer is composed of heterogeneous populations of cells including endothelial, fibroblast and immune cells. CXCR2 is known to be expressed by a majority of these cell types. Besides, CXCR2 is also known to mediate immune responses in various diseases including cancer. The studies in the later section of this dissertation

investigate the role of CXCR2 in altering local and systemic host-mediated responses in pancreatic cancer. Two experimental strategies were used: 1) Evaluating the impact of host CXCR2 depletion on tumor growth in subcutaneous versus orthotopic tumor cell implants. 2) Examining the effect of host CXCR2 deletion on the infiltration of immune cells in orthotopic pancreatic tumors. The first approach identified a pancreatic-parenchyma specific role of CXCR2 in inhibiting fibrosis in pancreatic cancer. The second strategy unraveled an important role of CXCR2 in causing local immunosuppression where CXCR2 mediates the infiltration of myeloid-derived suppressor cells (MDSCs) in pancreatic cancer. However, CXCR2 was found to be important for inhibiting extramedullary hematopoiesis and expansion of MDSCs in the spleen. Overall, the results presented in this dissertation suggest that CXCR2 signaling functions as a double-edged sword in pancreatic cancer by mediating both tumor-promoting and -inhibitory effects.

TABLE OF CONTENTS

List of Figures

CHAPTER

List of Tables

List of abbreviations

BSA Bovine serum albumin

***Cxcr2*$^{+/-}$** *Cxcr2* heterozygous knock-out mouse

***Cxcr2*$^{-/-}$** *Cxcr2* homozygous knock-out mouse

DAB 3,3'-Diamino benzidine

DAPI 4'6-diamidino-2-phenylindole

DMSO Dimethyl sulfoxide

DMEM Dulbecco's Modified Eagle Medium

EDTA Ethylenediaminetetraacetic acid

ELISA Enzyme-linked immunosorbent assay

ELR Glutamic acid-leucine-arginine

EMH Extramedullary hematopoiesis

ERK Extracellular signal-regulated kinases

EtBr Ethidium bromide

GFP Green fluorescent protein

H&E Hematoxylin and eosin

IHC Immunohistochemistry

IFNγ Interferon gamma

IL Interleukin

KRAS Kirsten rat sarcoma viral oncogene homolog

MTT 3-(4,5-dimethylthiazol-2-yl)-2,5-diphenyltetrazolium bromide

NTB Non-tumor-bearing

PBS Phosphate-buffered saline

PanINs Pancreatic intraepithelial neoplasia

PC Pancreatic cancer

PDAC Pancreatic ductal adenocarcinoma

p-ERK Phosphorylated extracellular signal-regulated kinases

qRT-PCR Quantitative reverse transcription polymerase chain reaction

RIPA Radioimmunoprecipitation assay buffer

RPL13A Ribosomal protein large13A

RPMI Roswell Park Memorial Institute medium

TAL Tumor-associated lymphocytes

TME Tumor microenvironment

TNFα Tumor necrosis factor alpha

TMA Tissue microarray

TTBS Tris-buffered saline and Tween 20

WT Wild-type

Acknowledgements

I owe my mentor Dr. Rakesh K. Singh heartfelt thanks and an indebt of gratitude for guiding me through this journey of scholarly transition. I thank him for the initial incentive and constant encouragement that he provided during the course of my Ph.D. During the last four years, he has worked with me as my mentor on improving various aspects of my persona enabling me to become not just technically sound in my specialization but also to develop as an independent thinker in my field of research. Without his kind help, firm guidance, wisdom, valuable suggestions and a keen interest in the problems I faced at each step the present work would not have been possible.

I would like to thank my committee members Dr. Keith R. Johnson, Dr. Joyce Solheim, Dr. Surinder K. Batra and Dr. Audrey J. Lazenby for the time and efforts they have invested in me. Your suggestions and careful insights have helped me immensely in shaping this project. All I can say is that every single minute I have spent with you all has helped me to grow as a scientist. It is difficult for me to find appropriate words to thank Michelle Varney, whose timely assistance and support have been instrumental in the shaping of each and every experiment presented in this dissertation. I am extremely thankful to her for being patient with me and for enlightening me by teaching me almost everything I have learned during the last four years of my work in Dr. Singh's laboratory. It was wonderful working with you Michelle!

I would like to thank Dr. Philip Hexley from the UNMC Flow Cytometry and Cell Analysis Facility to help me analyze and present the flow cytometry data in a more appropriate way. I extend a hearty thanks to all the past and current members of Dr. Rakesh K. Singh's laboratory I have worked with: Dr. Bhawna Sharma, Dr. Sheng Wu, Dr. Hesham Hassan, Sugandha Saxena and Lingyun Wu for creating a healthy work environment. Special thanks go to Dr. Hesham Hassan, who has helped me resolve many of my dilemmas, related to the course work and also my routine laboratory work. I would like to take an opportunity to thank Dr. Thomas L. McDonald, my instructor for the Medical Immunology course, for stimulating my initial interest in immunology.

On a personal note, I thank my sister Dr. Vinee Purohit, who is a recent graduate from the Department of Pathology and Microbiology at UNMC. It was she who inspired, encouraged and guided me to join the graduate course at UNMC. I would like to thank my father and my brother for their constant encouragement and support. Last but not the least; I shall never be able to forget the love, encouragement and cooperation that have been extended by my maternal and paternal uncles and aunts and their families.

This dissertation is dedicated to my beloved mother.

A special thanks to all the rodents who sacrificed their lives for the present study.

Chapter 1

Introduction

Significance of the study:

Pancreatic cancer (PC) remains a challenging disease due to its aggressive tumor growth, early metastatic dissemination and late clinical presentation. Due to these factors, the prognosis of PC is extremely poor, leading to 100% mortality. In the pursuit to improve the clinical outcome of this disease, research focusing on the discovery of early detection markers is warranted. Extensive research efforts have led to significant insights into the genetic alterations occurring in PC. By understanding the molecular mechanisms linked with the early genetic events and further unraveling their phenotypic implementation, identification of novel diagnostic and therapeutic markers for the disease can be achieved. Several studies have established the importance of inflammatory cells and mediators in PC inception and progression. However, the molecules regulating the inflammatory responses in PC remain largely unknown. Here we present a research effort to identify therapeutically targetable inflammatory mediators regulating various autocrine and paracrine effects during the inception and progression of PC. The results generated in this study may aid in the development of novel therapeutic modalities for PC in the future.

Overview of the Anatomy and Histology of the Normal Pancreas:

Anatomy:

The pancreas is a 6 cm long, fish-shaped gland located in the abdomen and is anatomically divided into a head, body and tail. The head is the expanded portion that lies in the C-shaped curve of the duodenum, attached to the same by connective tissue. The centrally located body of the pancreas crosses the midline of the human body, and the tail extends towards the hilum of the spleen. The pancreatic duct (of Wirsung) extends through the length of the pancreas and empties into the duodenum at the hepatopancreatic ampulla (of Vater), through which the common bile duct from the liver and gallbladder also enters the duodenum. The hepatopancreatic sphincter (of Oddi) surrounds the ampulla and not only regulates the flow of bile and pancreatic juice into the duodenum but also prevents the reflux of intestinal contents into the pancreatic duct. In some individuals, an accessory pancreatic duct (of Santorini) is present as a vestige of pancreatic origin. A thin layer of moderately dense connective tissue forms the capsule around the glands. From this capsule, septa extend into the gland dividing it into ill-defined lobules.

Histology:

Microscopically the pancreatic tissue can be divided into two parts: the exocrine components (acinar glands and ducts) that produce and deliver digestive enzymes to the small intestine and the endocrine components (Islets of Langerhans) that secrete hormones (including insulin) into the blood stream. The

histology of these two parts is evidently discrete and can be seen as lightly stained and darkly stained tissue. The light stained Islets of Langerhans are comprised of alpha cells secreting glucagon, beta cells secreting insulin and delta cells that secrete somatostatin. Additionally, this tissue also includes PP cells that secrete pancreatic polypeptide. For the effective functioning as an endocrine tissue, this compartment of the pancreas is sufficiently vascularized, such that this tissue lies in close vicinity of blood vessels.

Pancreatic cancer:

PC is less frequent in occurrence compared with several other cancers including those of lungs, breast, stomach, liver, large bowel and prostate. However, the disease has a mortality rate in comparison to other cancer types (Lowenfels and Maisonneuve, 2006). The American Cancer Society estimates a total of 48,960 new cases and 40,560 deaths for both sexes in the year 2015. The incidence of PC is more prevalent in males than females. For the year 2015, estimated new cases for males and females are 24,840 and 24,120 respectively. The estimated death numbers for each sex are 24,120 for males and 19,850 for females. Overall PC is ranked as the fourth leading cause of cancer-related deaths for the year 2015. The combined five-year survival rate of all other cancer types has shown tremendous improvement in the last few decades. In 1977, the combined five-year survival rate of all cancer types was 49%, which improved to 68% in the year 2010. However, for the cancers of the pancreas this improvement rate is fairly small. In 1977, the five-year survival rate for PC was 3%, which improved to only 7% in the year 2010. One of the explanations for the

poor survival of PC patients is provided by the fact that 53% of patients (all races) have distant metastasis at the time of diagnosis (Siegel et al., 2015). Therefore, one of the major challenges in the field of PC is early detection at a stage where cancer has not metastasized and surgical resection is possible.

Risk factors for pancreatic cancer development:

Based on descriptive epidemiology:

Gender: Cancer of the pancreas is more common in males than in females. The life-time cumulative risk for development of PC is higher in males than in females (Lowenfels and Maisonneuve, 2006; Raimondi et al., 2009).

Geographical variations: The rate of PC is higher in northern countries like Iceland, Finland and the northern USA than the countries located closer to the equator such as Egypt, Zimbabwe and India (Raimondi et al., 2009). One of the proposed reasons for this variance is decreasing levels of Vitamin D due to less exposure to sunlight and UV rays in the populations located in the north (Raimondi et al., 2009).

Age: PC is a cancer of elderly people. The median age of diagnosis of PC is 72 years and only about 5-10% of patients develop PC before the age of 50 (Raimondi et al., 2009). The American Cancer Society reports the comparatively highest number of deaths 10,594 (males) and 9,076 (females) in the age group 60-79 years compared with other ages (Siegel et al., 2015).

Based on environmental factors:

Smoking: Exposure to tobacco smoke is known to cause about 25% of PC cases (Kamohara et al., 2007).

Dietary factors: Caloric consumption has been linked to the risk of PC (Lowenfels and Maisonneuve, 2006). Coffee and alcohol are not associated with the risk of PC. Vitamin D supplementation in the diet is known to have a protective role in PC (Raimondi et al., 2009).

Genetic risk factors: Germline mutations account for 5-10% cases of PC. Increased rate of PC is linked with various familial syndromes such as Peutz-Jeghers syndrome, familial atypical mole-multiple melanoma, cystic fibrosis and Li-Fraumeni syndrome (Raimondi et al., 2009).

Disease based: Preexisting diseases like diabetes, pancreatitis and obesity are linked with increased risk of PC (Lowenfels and Maisonneuve, 2006; Raimondi et al., 2009). An increased risk of PC, up to 50%, was reported in patients with type 2 diabetes for more than 10 years. An increased risk of PC (14 fold) was found in patients with chronic pancreatitis for at least 5 years (Raimondi et al., 2009).

Causative mutations of pancreatic cancer:

The signature genetic events of the evolving pancreatic ductal adenocarcinoma (PDAC) lesions include mutations of KRAS, CDKN2A, TP53, BRCA2 and SMAD4/DPC. As the precancerous lesions, pancreatic intraepithelial neoplasia (PanINs), progress to higher grades the number of genetic alterations

increase paralleled with atypical growth stages. Activating mutations in the KRAS oncogene are the first genetic events to be detected. Loss of heterozygosity at chromosome 9q, 17p and 18q are known to contribute to the mutations of CDKN2A, TP53 and SMAD4 respectively. As the focus of this thesis is to elucidate the early mechanisms of PC development, we will only discuss the details of KRAS mutations.

Activating mutations in KRAS are the earliest genetic events found in nearly 95% of PDAC cases. KRAS belongs to the family of small 21-30kDa GTPase, having the potential to cycle between a GTP-bound on-state and GDP-bound off-state. However, the event of a point mutation in this protein results in constitutive activation of RAS leading to persistent downstream signaling. The exclusively mutated form of RAS protein found in PC is KRAS and the predominant version occurs at position G12. Pharmacological approaches to block mutant KRAS have not transitioned into effective anti-KRAS therapies in clinics. Therefore, research focusing on targetable downstream effectors of RAS is necessary.

Histological classification of pancreatic cancer:

The histology of pancreatic tumors forms the foundation of not only the understanding these tumors but also their prognosis. The prognostic value of PC histology is reflected in the fact that the majority of cancers of the pancreas with a fatal prognosis are adenocarcinomas of the exocrine pancreas. The survival time among PC cases varies by histologic type; specifically patients diagnosed

with endocrine PC survive almost 2 years longer than those diagnosed with exocrine PC (Fesinmeyer et al., 2005). The apparent higher fatality of exocrine tumors is inexplicable, but may be attributed to their cellular or molecular behavior. For example, PDAC generally blocks the pancreatic duct, resulting in jaundice and cachexia. In contrast, endocrine pancreatic tumors often overproduce normally occurring substances such as insulin and glucagon. In this section, we will briefly review the histological classification of PC.

Tumors of the exocrine pancreas: The World Health Organization and International Agency for Research on Cancer has extensively classified tumors that affect the exocrine portion of the pancreas. The tumors of the exocrine pancreas are sub-classified into PDAC (75% cases), serous cystadenoma, mucinous cystadenocarcinoma, intraductal papillary-mucinous carcinoma and acinar cell carcinoma. PDAC is further subdivided into well differentiated or poorly differentiated types, and are the most frequent exocrine tumors with the poorest prognosis. Contrary to these, the next three are rare tumors. Finally, the group of rarest exocrine tumors arises from acinar cells. Additionally, pancreatoblastoma is a rare form of PC that affects children. For the purpose of this dissertation we will focus on the histology of the most malignant of all pancreatic epithelial tumors, PDAC.

(i) **Pancreatic ductal adenocarcinoma**: PDACs arise from and are phenotypically similar to pancreatic duct epithelia and constitute about 85-90% of all pancreatic neoplasms. Most ductal adenocarcinomas are moderately or well-differentiated tumors consisting of tubular or glandular structures formed by

mucous secreting columnar cells. The majority of ductal adenocarcinomas show KRAS mutations (Hruban et al., 2004).

Macroscopic view: Ductal adenocarcinomas are firm and poorly defined masses. PDACs are highly invasive cancers and have a tendency to invade the nearby tissues. Around 65% of PDACs arise in the head, 15% arise in the body and 10% in the tail. Based on the anatomy, the carcinomas of the head of the pancreas invade the common bile duct or the main pancreatic duct and produce stenosis. Advanced cases involve the ampulla of Vater or the duodenal wall. In contrast to these, the carcinomas in the pancreatic body and tail obstruct the main pancreatic duct only (Kloppel and Hruban et. al., WHO).

Histopathology of PDAC:

The hallmark feature of PDAC is the presence of a dense stromal response referred to as desmoplasia. Most ductal adenocarcinomas imitate normal pancreatic ducts embedded inside a thick stroma. The desmoplastic stroma in PDAC is known to be composed of fibroblasts, stellate cells, endothelial and immune cells. The large amount of fibrous stroma accounts for their firm consistency. To appreciate the histopathology of PDAC an understanding of the histological features is a must. The following is a summary of the key histological features of infiltrating ductal adenocarcinoma.

i) The presence of glandular tissue at places where it should not be found. Unlike the non-neoplastic tissue that consists of lobular units

with ducts at the center surrounded by acini, the growth pattern in PDAC is haphazard and the glands violate the lobular architecture.

ii) The presence of glands adjacent to muscular arteries without intervening pancreatic parenchyma.

iii) Perineural and intravascular invasion.

iv) The presence of nuclear polymorphism and the finding of nuclei in a single gland varying in area by more than 4 to 1.

v) Detection of necrotic debris within the lumen.

PanIN lesions:

Histological evaluation of areas surrounding PCs have revealed the presence of precursor lesions known as PanINs. PanINs are microscopic neoplastic proliferations in the pancreatic ducts and are subdivided into grades PanIN-1 to -3. Progression from PanIN-1 to -3 stage is accompanied by the onset of various mutations and increasing cellular and nuclear atypia. Discovery of these precursor lesions has provided a ray of hope that PC might be detected and cured in its preinvasive stages (Hruban et al., 2000; Hruban et al., 2008).

Tumors of the endocrine pancreas:

Tumors of the endocrine pancreas are relatively uncommon. They arise from the endocrine parts of the pancreas, the islets of Langerhans, and are sub-classified into insulinoma, glucagonoma, somatostatinoma and nonfunctional islet cell tumors (Gumbs et al., 2002).

CXCR2 and its ligands and introduction:

The members of the supergene family of chemotactic cytokines i.e. chemokines, are inflammatory mediators that recruit leukocytes to an area of evolving inflammation (Baggiolini, 1998; Epstein and Luster, 1998). They are small secreted proteins, 60-90 amino acids in length and 8-10 kilodaltons in mass. Chemokines were mainly discovered based on either the biological activity instigated by them or their ability to be expressed based on specific stimulation (Baggiolini et al., 1994b). Platelet factor 4 (PF4) was the first discovered chemokine reported in 1977 (Walz et al., 1977). Historically, chemokines were classified into sub-families based on the patterns of their N-terminal cysteine residues (Zlotnik and Yoshie, 2000). Currently, there are four main sub-families of chemokines known: CXC, CC, CX_3C and C (Zlotnik and Yoshie, 2000). Apart from their structures, the members of the different families of chemokines differ in their target cell selectivity (Baggiolini et al., 1994b) and the chromosomal location of their genes (Baggiolini et al., 1994a). Subsequent research efforts after the initial discovery of chemokines have highlighted their functions as and even beyond the initially identified role of immune cell recruiters (Slettenaar and Wilson, 2006). The CXC family of chemokines is comprised of 17 members, which are further classified into two groups based on the presence or absence of a three amino acid motif glutamic acid-leucine-arginine (ELR). Seven CXC chemokine receptors have been identified to date (CXCR1-7) (Lazennec and Richmond, 2010).

ELR motif-positive CXC chemokines:

Preceded by the discovery of PF4, CXCL8 was the first identified CXC chemokine (Baggiolini et al., 1994a). In 1987 Walz et al., isolated CXCL8 from the conditioned media of LPS-stimulated human blood mononuclear cells (Walz et al., 1987b). Further studies identified CXCL8 as a chemotactic factor and activator of neutrophils (Van Damme et al., 1988). Following the discovery of IL8 other CXC chemokines were discovered in rapid succession. CXCL7 (NAP-2) was identified in the conditioned media of monocytes cultured in the presence of blood platelets (Baggiolini et al., 1994a; Walz and Baggiolini, 1989). CXCL1 (GROα) was identified as a melanoma growth stimulator (MGSA) (Richmond and Thomas, 1988). Later GROβ (CXCL2) and GROγ (CXCL3) were also discovered (Haskill et al., 1990). CXCL5 was identified as a product of type II alveolar cells (Walz et al., 1991) and CXCL6 was isolated from the conditioned media of human osteosarcoma cells (Proost et al., 1993). Functionally, all these chemokines demonstrated the ability to attract and activate human neutrophils. CXCL8 shares 33 to 46% sequence identity with other ELR+ CXC chemokines (Baggiolini et al., 1994a). The N-terminal ELR motif preceding the first cysteine is necessary for the chemotactic activity towards neutrophils. The genes for these chemokines are co-localized on human chromosome 4q12-21(Raimondi et al., 2009). The activity of these CXC chemokines is mediated through two CXC receptors, CXCR1 and CXCR2 (Richmond and Thomas, 1988).

CXCR2: A synopsis:

CXCR2 is a seven-transmembrane G-protein coupled receptor having three extracellular and three intracellular loops (Hertzer et al., 2013). The extracellular N-terminal domain is necessary for ligand binding and the intracellular C-terminal domain is required for receptor internalization (Hertzer et al., 2013). Biochemically, CXCR2 is a 360 amino acid glycoprotein (Chapman et al., 2009). CXCR2 is known to have 78% amino acid homology with CXCR1 (Holmes et al., 1991). CXCR2 is known to bind with all the ELR^+ ligands; however, CXCR1 binds only CXCL6 and 8 (Lazennec and Richmond, 2010). Expression of CXCR2 has been detected in several cell types including epithelial cells, endothelial cells, fibroblasts, neuronal cells and immune cells like neutrophils, monocytes and mast cells (Raimondi et al., 2009). The normal physiological functions of CXCR2 include regulation of neutrophil homeostasis (Devalaraja et al., 2000; Slettenaar and Wilson, 2006). CXCR2 is also known to play key roles in wound-healing mechanisms (Devalaraja et al., 2000). CXCR2 is suggested to be a negative regulator of myeloid progenitor cell proliferation and their migration as CXCR2 knock-out (*Cxcr2*$^{-/-}$) mice show hyperproliferation of myeloid progenitor cells in the bone marrow, spleen and blood (Rollins, 1999).

Pathologically the CXCR2 biological axis is implicated in several autocrine and paracrine tumor-promoting roles in various cancers including melanoma (Singh et al., 2009; Varney et al., 2006), breast (Kitamura and Pollard, 2015; Sharma et al., 2015), colorectal (Desurmont et al., 2015; Wu et al., 2015) and

lung (Keane et al., 2004). As the focus of research presented in this dissertation is PC, we will provide a summary of existing information regarding CXCR2 in PC.

CXCR2 in Pancreatic cancer

Introduction:

In this section, we will give an overview of the current knowledge and the persisting gaps in understanding the role of CXCR2 and its ligands in PC. We will first provide information regarding the expression of CXCR2 and its ligands in human PC patient samples and cell lines. Later we will review the role of the CXCR2 biological axis in mediating tumor-associated phenotypes in PC. Lastly, we will summarize the oncogenes and signaling pathways stimulating the induction of CXCR2 and its ligands in PC.

CXCR2 in pancreatic cancer cell lines:

The expression of CXCR2 in human PC cell lines is still a matter of debate. In recent years, a number of research groups have identified expression of CXCR2 in PC cell lines (Le et al., 2000; Wang et al., 2013b). On the other hand, researchers have also reported that PC cell lines lack the expression of CXCR2 (Matsuo et al., 2009e). For instance, cell lines like Panc-1, MIA Paca-2, and Capan-2 have been reported as both positive and negative for CXCR2 expression by different research groups.

Expression of CXCR2 and its ligands in pancreatic cancer human samples:

Tissue Specimens:

CXCL1: Evaluation of protein lysates derived from human PC tissues demonstrated detectable levels of CXCL1 protein and showed a non-significant increase in relation to adjacent tumor-free neighboring tissue (Oliveira Frick et al., 2008).

CXCL5: Recent research reports have provided extensive evidence for the expression and pathological role of CXCL5 in PC using human tissue specimens. Significantly increased levels of CXCL5 were detected in the tumor tissue lysates of PC by ELISA compared with the surrounding normal tissue or other histopathologically distinct diseases of the pancreas including chronic pancreatitis. Furthermore, in the same study the authors confirmed the cellular location of CXCL5 in PC tissues by IHC. The expression of CXCL5 was extensively localized in the cytoplasm of the malignant ductal cells while the surrounding normal tissues demonstrated no substantial expression of the ligand except in some acinar cells and islets of Langerhans (Oliveira Frick et al., 2008). In a recent study Li et al., also identified the expression of CXCL5 in human tissue specimens and further established its correlation with disease progression and survival. They found that CXCL5 expression was occasionally present in PanIN-1 lesions but increased in PanIN-2 and PanIN-3 stages where 4 out of the total 11 specimens demonstrated high immunoreactivity for CXCL5 (Li et al., 2011c). Moreover, strong staining for CXCL5 was detected in 67% of PC

specimens. CXCL5 staining was found to be localized to the apical cytoplasm in the tumor cells while there was no immunoreactivity in the acinar and ductal epithelium of the normal pancreas. Based on these results, the authors concluded that the expression of CXCL5 correlates with tumor progression in PC. Furthermore, by performing Kaplan-Meier analysis they established that high CXCL5 expression shortened patient survival time. The authors also reported higher microvessel density in tumors with higher expression of CXCL5 suggesting its role in neoangiogenesis (Li et al., 2011c).

CXCL6: PC tumor lysates were shown to have detectable levels of CXCL6; however, there was no significant difference in its expression in tumors versus the surrounding normal tissue (Oliveira Frick et al., 2008).

CXCL7: CXCL7 protein demonstrated no differential in expression between the PC and the adjacent normal tissue (Oliveira Frick et al., 2008).

CXCL8: Compared with other members of its family, CXCL8 is the most extensively studied ligand for its pathological significance in human tissue specimens of PC. Xiangdong et al. for the first time, reported the higher expression of CXCL8 protein in human PC tissue specimens (n=45) compared with the normal pancreas (n=15). Its expression was localized to the ductal cells as well as the stroma (Le et al., 2000). Later, Kuwada et al. supported these observations by reporting the expression of CXCL8 in 20 out of 50 patient tissue specimens evaluated. CXCL8 was found primarily in the cytoplasm of the tumor cells (Kuwada et al., 2003). In further support of these observations, another

study identified higher expression of CXCL8 protein in PC tumor lysates compared to non-affected neighboring tissue. IHC analysis revealed that CXCL8 was located in the cytoplasm of the ductal epithelial cells as well as the infiltrating inflammatory cells. The authors evaluated the expression of CXCL8 in different tumor stages based on TMN classification of malignant tumors. Expression of CXCL8 was upregulated in the T3 and T4 versus the T1 and T2 stages (Oliveira Frick et al., 2008). In contrast to this report that did not detect CXCL8 in the normal pancreas a recent study detected expression of CXCL8 in both PC (55.6%) and non-cancer tissues (25.9%). They found positive signals localized in both normal and cancerous ducts (Chen et al., 2012).

CXCR2: Little focus has been placed thus far on the evaluation of the pathological significance of CXCR2 expression using human PC tissue specimens. Positive immunoreactivity for CXCR2 was reported by Kuwada et al. in 26 out of 40 (65%) surgically resected human PC tissues (Kuwada et al., 2003). However, the authors did not evaluate the expression of CXCR2 in normal tissue. In another study, Frick et al. reported that CXCR2 was expressed in PC tumor tissue and also in the corresponding non-affected tissue from the same patients (Oliveira Frick et al., 2008). A recent report by Hussain et al. evaluated the expression of CXCR2 along with CXCR1 and CXCL8 in PDAC and pancreatic neuroendocrine tumors by IHC (n = 52) and qRTPCR (n = 8). CXCR2 expression was detected in PDAC samples at both the mRNA and protein levels.

CXCR1:

A recent report by Chen et al. identified the presence of CXCR1 in human PDAC specimens. 61% of cases (40 out of 65) were positive for CXCR1 expression. On average, around 14.7% cells were positive in each of these specimens. The expression of CXCR1 significantly correlated with lymph node metastasis in these patients (Chen et al., 2014). However, there was no association found with other clinical prognostic features such as histopathological grade, depth of invasion or TMN stage. They also identified a positive correlation of CXCR1 with cancer stem cell markers like CD44 and CD133 (Chen et al., 2014).

Serum samples and body fluids:

O'Hayer et al. evaluated the expression of ELR^+ CXC chemokines hCXCL1, 5, 6, 7 and 8 in serum samples isolated from 20 PC patients and 19 age- and sex- matched healthy donors. Their results demonstrated significantly elevated expression of CXCL1 and CXCL7 in PC specimens. No change in the expression of CXCL5, 6 and 8 was observed in PC serum samples compared with healthy donors (O'Hayer et al., 2009). Moreover, a recent study reported significantly higher levels of CXCL8 in serum samples of PC patients compared with specimens derived from patients of acute or chronic pancreatitis (Chen et al., 2012). Matsuo et al. evaluated the levels of ELR^+ CXC chemokines (CXCL1, 5 and 8) in the secretin-stimulated pancreatic exocrine secretions of PC patients and healthy individuals. Their data demonstrates significantly enhanced secretion

of CXCL5 or cumulative expression of ELR^+ CXC in PC patients versus healthy individuals. However, they did not observe a significant change in the individual expression of CXCL1 and CXCL8 (Matsuo et al., 2009e).

CXCR2 ligands as autocrine growth factors in pancreatic cancer:

Presently the role of CXCR2 ligands as growth factors for PDAC tumor cells is an area of contention. While numerous data is supporting the theory of CXCR2-mediated tumor cell autochthonous growth, several of the recent reports highlight also the notion that CXCR2 agonists fail to provoke the growth of PC cells. Takamori et al. identified the expression of CXCR2 and its ligands, CXCL1 and 8 in Capan-1 cells. They found that treatment with anti-CXCL8 or anti-CXCL1 antibody inhibited the growth of Capan-1 cells (Takamori et al., 2000). In line with these observations, Kamohara et al. also demonstrated that neutralizing antibody for CXCL8 (1-100 µg/ ml) was sufficient to suppress significantly the autocrine growth of PC cell lines, including SUIT-2 and Capan-1 (Kamohara et al., 2007). Furthermore, while identifying the presence of a CXCR2 macromolecular signaling complex in PDAC cells, a recent study provided another functional evidence for the role of CXCR2 signaling in mediating *in vitro* and *in vivo* tumor cell growth. Their data revealed that treatment of PDAC cell lines HPAC and Colo357 with CXCR2 agonists (including CXCL1, 5 and 8) enhanced *in vitro* cell proliferation. Similarly, disruption of the CXCR2 macromolecular complex by using an exogenous CXCR2 C-tail sequence in HPAC cells significantly attenuated its *in vitro* and *in vivo* proliferation (Wang et al., 2013b).

In contrast to the studies described above, several groups have provided evidence that PDAC cell lines either lack the expression of CXCR2 (Matsuo et al., 2009d), or the receptor is unresponsive to its agonists (Ijichi et al., 2011a; Matsuo et al., 2009a). To reconcile this discrepancy, further experimenting with an advanced model system is required. For example, conditional *in vivo* deletion of CXCR2 in the ductal cells of spontaneous PDAC murine models can overcome the limitations of *in vitro* and orthotopic *in vivo* models systems used thus far.

Involvement of CXCR2 signaling in pancreatic cancer stroma:

In an *in vitro* co-culture system, CXCL8 produced by PC cells was shown to enhance angiogenesis in cooperation with CXCL12 produced by the fibroblasts (Matsuo et al., 2009d). More recently, Ijichi et al. reported the much higher expression of *CXCR2* mRNA transcripts in pancreatic fibroblasts compared with PDAC cells isolated from Ptf1a$^{cre/+}$;LSL-*Kras*$^{G12D/+}$ mice. Furthermore, the expression of Ctgf, a profibrotic factor, was found to be induced in pancreatic fibroblasts treated with PDAC-conditioned media and this induction was inhibited by incubating fibroblasts with PDAC-conditioned media containing CXCR2 antagonist. They also provided evidence for the role of CXCR2 signaling in accelerating PDAC progression by promoting tumor-stromal interaction. Subcutaneous implants of PDAC cells mixed with fibroblasts showed accelerated tumor growth compared with only PDAC cell implants. More importantly, CXCR2 knock-down in fibroblasts inhibited the subcutaneous tumor growth while CXCR2 knock-down in the tumor cells caused no effect. Based on these results, the

authors postulated that CXCR2 signaling indirectly supports PDAC progression by mediating tumor-stromal interaction and has no autocrine growth enhancing effect on tumor cells (Takamori et al., 2000).

CXCR2 in mediating pancreatic cancer angiogenesis:

The CXCR2 signaling axis has been well appreciated for its role in mediating angiogenesis in various cancers. Moritz et al. (2006) for the first time reported the angiogenic activity of CXCR2 signaling in PC by evaluating angiogenesis induced by culture supernatants of PC cell lines *in vivo* using the corneal micropocket assay. They demonstrated that CXCR2 antibody completely inhibited the *in vivo* angiogenic response stimulated by BxPC3 culture supernatants (Wente et al., 2006). In another study, Matsuo et al. identified a similar mechanism *in vitro* by demonstrating that the higher CXCL8-producing PC cell line BxPC3 enhanced the invasiveness and tube-forming ability of human umbilical vein endothelial cells (HUVECs) and that treatment with CXCL8 antibody abrogated this effect (Matsuo et al., 2009d). Another study by the same group demonstrated that CXCR2 antibody treatment significantly reduced microvessel density in an orthotopic nude mouse model (Matsuo et al., 2009e). Later they also established the role of CXCR2 axis in mediating KRAS-induced paracrine angiogenic effects in PC (Matsuo et al., 2009a). A recent study by Aihua Li et al. addressed the role of CXCR2 signaling in PC neovascularization with another view. Bone marrow-derived endothelial progenitor cells (EPCs) are known to differentiate into mature endothelial cells and form blood vessels. The authors found an increased presence of $CD133^+$ and $CD146^+$ cells in human PC

tissues compared with the normal pancreas. They also demonstrated increased subcutaneous tumor growth in mice implanted with a mixture of mouse PC cells with EPCs compared with the control group inoculated only with PC cells. Tumor-bearing *Cxcr2*$^{-/-}$ mice demonstrated a reduction in the levels of EPCs in bone marrow and blood. Congruent with this observation, the authors show that *Cxcr2*$^{-/-}$ reduced the proliferation and capillary tube formation of bone marrow-derived cells *in vitro* (Li et al., 2011a).

***In vivo* preclinical inhibition of CXCR2 in animal models: Approaches and outcomes:**

Numerous studies provide data for the effect of CXCR2 inhibition on *in vivo* growth of PC cells. In a study aimed to identify the role of the CXCR2 biological axis in PC, Matsuo et al. reported that treatment with CXCR2 antibody inhibited tumor growth and angiogenesis in an orthotopic nude mouse model having implantation of BxPC3 cells (Matsuo et al., 2009e). Using a subcutaneous tumor model generated by inoculation of BxPC3 cells in nude mice Li et al. demonstrated that treatment with CXCR2 antiserum decreased tumor volume and microvessel density. Furthermore, in the same study the authors demonstrated that nude mice inoculated with MIAPaCa-2 cells subcutaneously showed reduced tumor growth in response to treatment with CXCL5 siRNA (Li et al., 2011c). Another study by the same group provided data that mouse PC cells harboring a KRAS mutation implanted in the pancreas of C57BL6 *Cxcr2*$^{-/-}$ mice developed significantly smaller tumors compared with the control wild-type group (Li et al., 2011b). Unlike the systemic inhibition of CXCR2 in previous models, a

recent study by Wang et al. employed the technique of disrupting the CXCR2 macromolecular complex in tumor cells (HPAC) *in vitro* before subcutaneous implantation in CB17-SCID mice. They found that inhibition of CXCR2 in the tumor cells inhibited the tumor volume and *in vivo* tumor cell proliferation (Wang et al., 2013b). Treatment of Kras+TGFβr2-KO PDAC mice with the CXCR2 antagonists repertaxin or SB225002, inhibited tumor size and angiogenesis (Ijichi et al., 2011a). However, contrary to the above results, the authors of a review focused on the potential of targeting CXCR2 signaling in PC revealed that mice heterozygous for CXCR2 injected with PC cells developed larger tumors than the wild type (WT group) (Hertzer et al., 2013).

Oncogenes and CXCR2 signaling:

Upregulation of the ligands for CXCR2 is a well-known consequence of activating mutations in the KRAS oncogene. For the first time, Sparmann et al. reported that activation of the RAS pathway leads to substantially increased CXCL8 production in Hela cells. Furthermore, based on their *in vivo* results they concluded that CXCL8 is required for RAS-oncogene-dependent tumor growth by mediating angiogenesis. In rapid succession, similar findings were reported for cancers of the lungs and ovaries. Matsuo et al. identified the link between $KRAS^{(G12V)}$ and $KRAS^{(G12D)}$ mutations and upregulation of cumulative expression of CXCL1, 5 and 8 in PC. Later, Hayer et al. reported that knock-down of endogenous $KRAS^{(G12D)}$ in the PC cell line SW1990 resulted in the reduction of transcripts of CXCL1, 2, 3, 5, 6, 7 and 8. Activation of MEK and cJun pathways are known to induce the expression of CXCR2 ligands downstream of KRAS

activation. However, the role of KRAS in inducing the expression of CXCR1 and 2 remains less defined.

Potential roles of the CXCR2 biological axis in pancreatic cancer immune microenvironment

The previous section provides a summary of the currently known facts regarding the role of CXCR2 in PC. In summary, previous research efforts have addressed the potential involvement of CXCR2 in regulating the PC microenvironment by affecting the functions of fibroblasts and endothelial cells. However, the functional significance of CXCR2 in orchestrating the immune component within the PC tumor microenvironment (TME) remains unexplored. Therefore, in this section we focus on the well-identified roles of the CXCR2 biological axis in the regulation of myeloid cell populations. Each subsection presents information linking CXCR2 and one immune cell type. Furthermore, we also summarize relevant reports related to each cell type in PC. Taken together, this information might help in understanding the potential roles played by the CXCR2 biological axis in the immune microenvironment of PC.

Mast cells:

Mast cells are tissue resident cells of myeloid origin primarily known for their involvement in type I hypersensitivity reactions like allergy and anaphylaxis. However, mast cells also function to mediate the processes of wound healing and defense against pathogens. They are recruited to the target tissue as immature precursors where they remain sentinel and undergo terminal

differentiation in response to an external challenge (Collington et al., 2011; Maltby et al., 2009). Characteristically, mast cells degranulate upon stimulation and release an arsenal of effector molecules including histamine, heparin, tryptase and various cytokines (Gabrilovich and Nagaraj, 2009). Reports have recognized the presence of mast cell infiltrates in several cancer types including pancreatic tumors. Mast cells foster tumor growth primarily by mediating angiogenesis, remodeling the extracellular matrix to facilitate metastasis and suppressing anti-tumor immune responses (Khazaie et al., 2011; Maltby et al., 2009). In PDAC, mast cells can be detected at the infiltrating edges of tumors. Also, mast cells are detected in precursor PanIN lesions suggesting their role in the early stages of this disease. Detailed information regarding the role of mast cells in PC is reviewed elsewhere (Evans and Costello, 2012; Wörmann et al., 2014).

Mast cells are known to express both CXCR2 and its ligands. HMC1 cells, a human mast cell line, express CXCR2 and demonstrate concentration-dependent chemotaxis and F-actin polymerization in response to stimulation with *Cxcl2, 5, 7* and *8* suggesting a role for CXCR2 in mast cell trafficking (Lippert et al., 1998; Nilsson et al., 1999). In a recent report Jenny et al. revealed an indirect role for CXCR2 in mast cell recruitment beyond the induction of directed cell migration. Using a model of inflamed lung they demonstrated that the absence of CXCR2 signaling in lung endothelium impairs the expression of VCAM-1, a critical counter ligand for α4 integrins expressed on mast cell progenitors, leading to decreased recruitment of mast cells (Hallgren et al., 2007).

Evidence suggests that CXC chemokines can regulate mast cell-mediated regulation of other immune cells and thus exert effects beyond their chemotactic cell migration. CXCL1 and 2 released by mast cells are important for neutrophil recruitment *in vivo*. Furthermore, Wang et al. demonstrated that CXCL2-induced neutrophil recruitment was found to be mediated by TNF-α released from local mast cells (Wang and Thorlacius, 2005). Also, mast cell-derived CXCL2 was found to mediate the recruitment of neutrophils in T cell-mediated heparin-induced delayed-type hypersensitivity reactions of skin (Biedermann et al., 2000).

Lee et al. demonstrated that IL-1β evokes mast cells to produce CXCL8, which in turn induces angiogenesis (Lee et al., 2011). Interestingly, various studies on disease pathogenesis including psoriasis and rheumatoid arthritis identified mast cells as the predominant source of IL-17, which is a potent inducer of CXCR2 ligands (Lin et al., 2011). Thus, these IL-17-induced ligands can further cause infiltration of neutrophils or enhance the angiogenic response. Direct evidence for the role of CXCR2 signaling in the cross-talk between tumor and mast cells was demonstrated in a study using a thyroid cancer model. Mast cells were shown to enhance the *in vitro* survival and invasive ability of thyroid cancer cells via the secretion of CXCL1 (Melillo et al., 2010). Furthermore, conditioned media from thyroid cancer cell lines upregulated the secretion of CXCL1 from mast cells (Melillo et al., 2010).

The earliest study identifying the expression of CXCR2 in mast cells reported higher expression of this receptor in the intracellular compartment,

suggesting its presence on the granules (Lippert et al., 1998). Therefore, there is a possibility that CXCR2 might be involved in the degranulation of mast cells.

Taken together, these reports suggest a role for CXCR2 signaling in mast cell recruitment and also in mediating their cross-talk with stromal and tumor cells. Thus, based on this evidence it would be interesting to evaluate the role of this signaling axis in regulating mast cell pathology in various cancer types including PC.

Myeloid-derived suppressor cells:

Myeloid-derived suppressor cells (MDSCs) are a phenotypically heterogeneous population of immature myeloid cells having only one common feature i.e. their ability to induce immunosuppression by causing defective T cell function (Fujimura et al., 2010). Canonically, they are divided into granulocytic (mouse: $CD11b^{+}Ly6G^{+}$; human: $CD11b^{+}$ $CD15^{+}$) and monocytic (mouse: $CD11b^{+}Ly6C^{+}$; human: $CD11b^{+}$ $CD14^{+}$) sub-populations (Goedegebuure et al., 2011; Ostrand-Rosenberg and Sinha, 2009). In cancer, tumor-released factors stimulate myelopoiesis but block the differentiation of immature myeloid cells (IMCs) to mature myeloid cells like macrophages, dendritic cells and granulocytes. This IMC population is further activated by another group of factors resulting in the generation of immunosuppressive cells (with increased levels of ROS, arginase, and/or NO) collectively known as MDSCs (Gabrilovich and Nagaraj, 2009).

Patients with cancer are known to have a marked systemic expansion of MDSCs in spleen and lymph nodes and also in the number of circulating MDSCs in the blood (Gabrilovich and Nagaraj, 2009). These MDSCs then get recruited to the tumors. Of note, MDSCs can cause immunosuppression at the tumor site as well as when located systemically. However, the mechanism of immunosuppression caused by MDSCs can be either antigen-specific or -nonspecific depending on their location (Nagaraj and Gabrilovich, 2008). At the tumor site the immunosuppressive activity of MDSCs is mainly antigen-nonspecific mediated primarily by the production of inducible nitric oxide synthase (iNOS) and arginase 1. iNOS and arginase 1 produced by MDSCs are known to suppress the proliferation and activation of T cells by inhibiting the expression of MHC class II on antigen-presenting cells and CD3-ζ chains on T cells respectively (Fujimura et al., 2010; Gabrilovich and Nagaraj, 2009; Goedegebuure et al., 2011; Nagaraj and Gabrilovich, 2008). However, in the peripheral tissues MDSCs function as antigen-presenting cells and induce reactive oxygen species (ROS)-mediated T cell suppression during the antigen-specific interaction between MDSCs and T cells (Nagaraj and Gabrilovich, 2008). MDSCs are also known to cause indirect immunosuppression by promoting the recruitment of Tregs to the tumor sites and by blocking the entry of effector T cells (Goedegebuure et al., 2011).

Several studies in cancer and other diseases have elaborated the role of CXCR2 signaling axis in MDSC trafficking. Chemotherapy in breast cancer induced TNF-α in the stromal compartment of tumors, which further upregulated

CXCL1 and 2 in the tumor cells both in tumors and the lung microenvironment. These upregulated chemokines in turn recruited $CXCR2^{+}$ MDSCs, which enhanced the viability of cancer cells through S100 A8/9 factors (Acharyya et al., 2012). MDSCs isolated from tumors of mice inoculated with B16-F10 melanoma demonstrated higher levels of CXC chemokines compared with bone marrow MDSCs from the same mice suggesting the role of these chemokines in trafficking of MDSCs to the tumors (Wang et al., 2015). A report from Weiss et al. demonstrated that IL-2/αCD40 treatment caused a reduction in tumor-associated MDSCs, which was accompanied by reduced CXCL5 protein expression in tumor lysates (Weiss et al., 2009). Furthermore, Toh et al. also demonstrated the role of CXCL1, 2 and 5 in the recruitment of granulocytic MDSCs to the primary tumors (Toh et al., 2011). Likewise, in a colitis-associated colon cancer model the levels of CXCR2 ligands were found to be elevated in inflamed mucosa and the loss of CXCR2 diminished the infiltration of granulocytic MDSCs from the circulatory system to colonic inflamed mucosa (Katoh et al., 2013). A recent report by Highfill et al. also demonstrated that CXCR2 deficiency inhibited the trafficking of granulocytic MDSCs to the tumors resulting in compensatory accumulation in the spleen and peripheral blood. They further concluded that $CXCR2^{+}$ granulocytic MDSCs mediate local immunosuppression in murine rhabdomyosarcoma and that inhibiting CXCR2 signaling can enhance the efficacy of checkpoint inhibitors (Highfill et al., 2014).

The presence of MDSCs has been recognized in both human specimens and mouse models of PC. In human PDAC specimens MDSCs were found to be

present in the tumor stroma and systemically in the peripheral blood, bone marrow and spleen (Porembka et al., 2012). Furthermore, Clark et al. (2007) identified the presence of MDSCs as early as the PanIN stage and found further increased infiltration in PDAC (Clark et al., 2007a). As several reports in PC suggest for enhanced CXCR2 signaling, further work is required to characterize the role of CXCR2 in MDSC trafficking in PC.

Macrophages:

Tumor-associated macrophages (TAMs) are derived either from tissue resident macrophages or circulating blood monocytes. The primary recruiter of macrophages is monocyte chemotactic protein (MCP-1). The direct role of CXCR2 in inducing chemotaxis of monocytes for recruitment to tumors is not well defined. While CXCR2 is expressed by monocytes and macrophages (Moser et al., 1993; Murdoch et al., 2004; Patel et al., 2001), these cells do not respond to the stimulus provided by the CXCR2 ligands. The human monocytic cell line THP-1 demonstrated no chemotaxis in response to stimulation with different doses of rhCXCL8 (Bailey et al., 2007). Instead, there is evidence for indirect roles of CXCR2 signaling in the recruitment of macrophages. CXCL8 was shown to mediate the adhesion of rolling monocytes to endothelial cells expressing E-selectin under flow conditions. However, these effects did not correlate with calcium induction or chemotaxis in monocytes (Gerszten et al., 1999). Interestingly, there is another mode of CXCR2-mediated monocyte recruitment via neutrophils.CXCR2-positive neutrophils recruited to tumors can secrete MCP-

1, which in turn recruits monocytes from the blood. This indirect mechanism is discussed in detail in the coming paragraphs.

Both the M1 and M2 activation stages of macrophages are linked with CXCR2 signaling. Treatment of monocytes with LPS and IFN-γ leads to the induction of the M1 phenotype and also of the ligands for CXCR2 like CXCL8 (Gordon, 2003; Mantovani et al., 2004a; Mantovani et al., 2004b). However, the M1-activated macrophages are not known to express CXCR2 (Bonecchi et al., 2000; Mantovani et al., 2004a). Thus, the ligands produced can exert paracrine effects by influencing CXCR2 positive elements of the TME. Although there is no direct evidence for the role of CXCR2 signaling in inducing M1- to M2-phenotypic switch, intracellular CXCR2 signaling is activated in M2 macrophages unlike M1 counterparts (Melillo et al., 2010). IL-4 and IL-13 induce the M2a phenotype (alternatively activated) that demonstrate an inhibited CXCL8 production but make monocytes exquisitely sensitive to CXCR2 ligands by inducing the expression of the receptor CXCR2 (Mantovani et al., 2004b). Therefore, alternatively activated M2a macrophages have activated intracellular CXCR2 signaling. On the other, hand M2c (deactivated) phenotype of macrophages has decreased expression of both CXCR2 and its ligands. Thus, in this receptor-deprived state, macrophages are insensitive to exogenous CXCR2 ligands and also cannot affect the microenvironment by secreting ligands. Overall, while the evidence is indirect it is not unreasonable to conclude that based on the induction stimuli, the M1- to M2- macrophage switch might be mediated by CXCR2 signaling.

CXCR2 signaling is a well-known facilitator in macrophage-neutrophil crosstalk. In 1989, CXCL8 was firstly identified in culture supernatants of stimulated human blood monocytes and it's biological activity was demonstrated by its ability to attract and activate human neutrophils (Walz et al., 1987a). More recently, Kaur and Singh (2013) identified CXCL8 as the major neutrophil chemoattractant produced by alveolar macrophages in chronic obstructive pulmonary disease, a condition characterized by neutrophilic airway inflammation (Kaur and Singh, 2013). Apart from neutrophils, CXCR2 signaling is also important for the crosstalk of macrophages with other cell types including endothelial cells. IL-1β-induced corneal neovascularization was found to be mediated by macrophages. Furthermore, the levels of the CXC chemokines KC (CXCL1), Mip-2 (CXCL2/3) and CXCL5 were found to be elevated in IL-1β implanted corneas. Depletion of macrophages by clodronate liposomes and the also treatment of these mice with an anti-mouse CXCR2 antibody inhibited IL-1β implanted corneal angiogenesis. These data provide indirect evidence that IL-1β induced CXC chemokines produced from macrophages enhance angiogenesis (Nakao et al., 2005). CXCR2 ligands secreted by macrophages can also generate interlinked networks between more than one cell types. For example, Zheng and Green reported the upregulation of CXCL8 in macrophages exposed to thrombin, an enzyme produced by leaky blood vessels. This thrombin-induced upregulation of CXCL8 was found to be regulated via PAR-1 by the Rho/Jnk pathway coupled to the activation of NF-κB and AP-1 transcription factors (Zheng and Martins-Green, 2007). Importantly, thrombin-induced expression of CXCL8

from the tissue-resident macrophages subsequently recruits neutrophils. These neutrophils in turn produce monocyte chemotactic protein (MCP-1) also known as CCL2, which further recruits monocytes (Gillitzer and Goebeler, 2001). Once recruited, monocytes differentiate into macrophages and produce CXCL8 that enhances angiogenesis and in turn maintains a paracrine crosstalk network in tumors. Thus, this evidence suggests that CXCR2 signaling is an important molecular mechanism involved in crosstalk between macrophages and cellular components of the tumor microenvironment including indirectly infiltrating monocytes.

Dendritic cells:

Dendritic cells are antigen-presenting cells (APCs) capable of coordinating both innate and adaptive immune responses. They arise from hematopoietic stem cells in bone marrow as precursor cells and further differentiate into immature dendritic cells (iDCs). These iDCs are recruited to tumors where they encounter tumor-specific antigens and differentiate to mature dendritic cells (mDCs). The maturation of dendritic cells enables their migration to the next site of action, the secondary lymphoid organs, where they activate effector T cells leading to the generation of an adaptive anti-tumor immune response (Pinzon-Charry et al., 2005). Tumor-derived factors are known to induce dysfunction of dendritic cells by affecting either their migration or maturation. Both anti- and pro-tumor effects of dendritic cells have been reported in PC. High levels of circulating myeloid DCs were related to improved survival in PC (Hirooka et al., 2011) and low levels of dendritic cell markers were negatively correlated with

survival rate (Tjomsland et al., 2011; Wörmann et al., 2014). On the contrary, a dendritic cell population was shown to accelerate pancreatic tumorigenesis by polarizing the T cell response to a protumorigenic Th-2 type (Ochi et al., 2012; Wörmann et al., 2014).

Evaluating the receptor expression and chemoattractant responsiveness of human dendritic cells isolated from peripheral blood monocytes, Sozzani et al. revealed the presence of detectable levels of CXCR2 and CXCR1 mRNA in dendritic cells. However, they concluded that dendritic cells do not respond biologically to CXCR2 signaling as the agonist CXCL8 failed to induce chemotaxis and calcium fluxes in dendritic cells *in vitro* (Sozzani et al., 1997; Sozzani et al., 1995). Parallel to these reports, other observers also reported the presence of CXCL7 and 8 binding sites on dendritic cells but demonstrated a lack of migratory response induced by these chemokines (Xu et al., 1996). Contrary to these observations, a recent study presented results of CXCL8-induced chemotactic attraction of dendritic cells. The authors concluded that this discrepancy can be attributed to the dissimilarity in the conditions employed to differentiate dendritic cells in the two studies (GM-CSF and IL-13 vs. GM-CSF and IL-4) highlighting the relevance of the *in vivo* cytokine milieu in altering the functional contribution of CXCR2 signaling in dendritic cell biology in tumors (Feijoó et al., 2005). In the same report, the authors observed that intratumoral injections of dendritic cells transfected to produce IL-12 failed to migrate to secondary lymphoid organs. As they detected high expression of IL-8 in serum samples of human patients (including PC) and tissue culture supernatants of

various cancer cell lines, they suggested IL-8 was the candidate molecule mediating the retention of dendritic cells inside the tumors. They further supported their conclusion by *in vitro* classical chemotaxis assays where they found that chemotaxis of dendritic cells towards MIP-3β was diminished by culture supernatants of colon cancer cells and that this effect was overcome by treatment with a neutralizing anti-IL8 specific monoclonal antibody (Feijoó et al., 2005). These data provide evidence for the potential role of CXCR2 signaling in causing tumor immunoevasion by impeding dendritic cell-activated anti-tumor T cell responses. CXCR2 is suggested to indirectly mediate circulating dendritic cell recruitment via adhesion to endothelial cell-displayed ligands like CXCL8 and CXCL1 (Cavanagh and Von Andrian, 2002; Krishnaswamy et al., 1999). CXCR2 signaling did not influence the maturation of dendritic cells, as the stimulation of immature dendritic cells with CXCL8 caused no change in the expression of CD86, MHC II and CD83 on these cells (Feijoó et al., 2005). However, Th2 cytokines IL-13 and IL-4 strongly induced the expression of CXCR2 on human dendritic cells suggesting the role of CXCL8 in intratumoral positioning at Th2 response-dominated sites (Bonecchi et al., 2000).

Conclusion:

To conclude, CXCR2 seems to play diverse roles in the pathobiology of the immune component of the TME ranging from chemotaxis to functional activation to mediating their cross talk with surrounding cells **(Fig. 1.1)**. Therefore, the overall impact of inhibiting CXCR2 signaling would be cumulative

in terms of how an individual cell is affected and how the overall interactions mediated by this signaling are influenced.

Hypothesis and Specific Aims:

The two major challenges faced by clinicians and researchers in PC today are the scarcity of early biomarkers for the detection of PC in the preinvasive stages and lack of proper understanding of the tumor microenvironment of PC for the discovery of novel therapeutic targets. Addressing these problems by specific research efforts may improve the prognostic outcome by enabling the targeting of PC in early stages and by improving the therapeutic delivery for the later stages of the disease.

Oncogenic mutations in KRAS are present in 95% of PDAC cases. Expression of ELR+ CXC chemokines is linked to oncogenic mutations in different isoforms of RAS in various malignancies, for example, lung, ovarian, colorectal and pancreatic cancers (Ancrile et al., 2008). Of note, KRAS mutations are required for both initiation and maintenance of PDAC (Collins et al., 2012). While recent reports in PDAC have identified a KRAS-CXC chemokine link, it remains unclear if this signaling can serve as an early biomarker for PDAC progression. Reports in recent past have demonstrated the roles of CXCR2 and its ligands in mediating tumor-stromal interactions in PC, but the primary focus of these studies was endothelial cells. Nevertheless, the events regulating the inflammatory response and the pathological effects mediated by immune cells remain elusive in PC.

Based on evidence from the literature the **central hypothesis** of this project is that CXCR2 and its ligands play important pro-tumorigenic roles during

a) PC initiation by mediating *KRAS*$^{(G12D)}$-induced tumor growth and b) PC progression by their ability to recruit immune cells of myeloid origin **(Figure 1.2)**.

To test this hypothesis I pursued the following specific aims.

Specific Aim 1: Define the role of CXCR2 in *KRAS*$^{(G12D)}$-induced tumor growth in PC.

Specific Aim 2: Evaluate the role of host CXCR2 in regulating tumor growth by altering the inflammatory responses in PC.

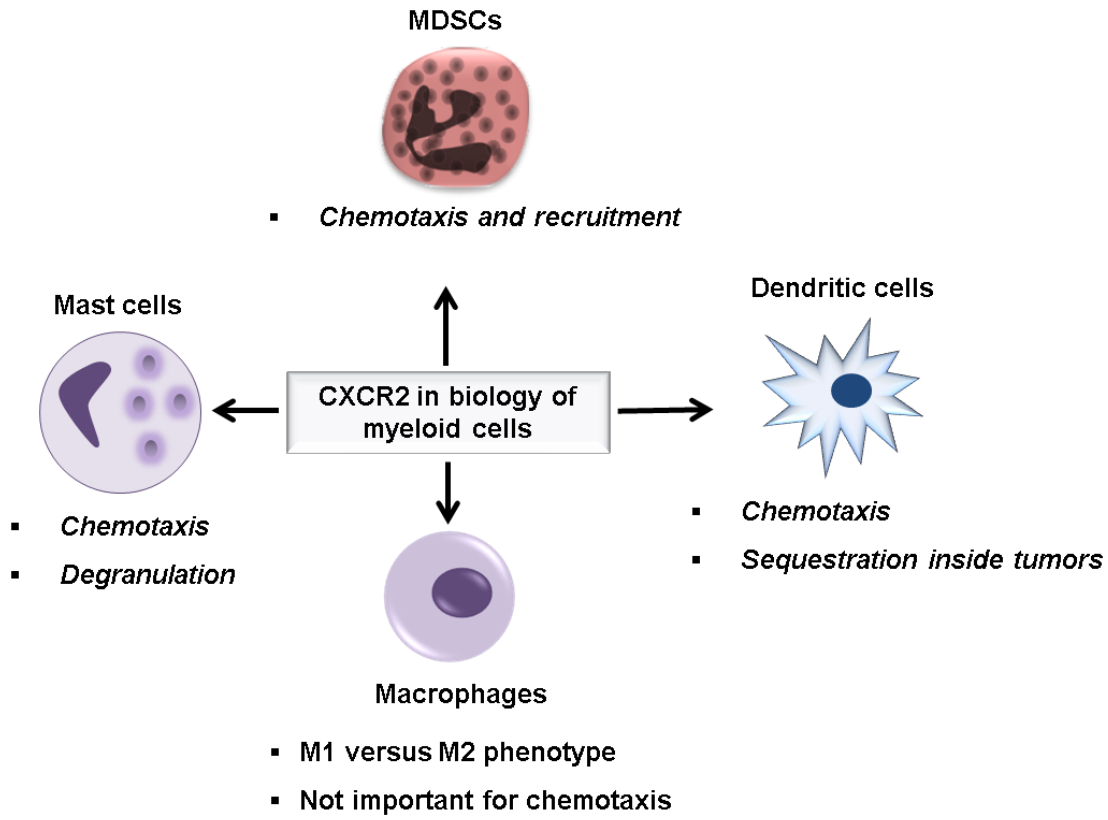
MDSCs
Chemotaxis and recruitment
Mast cells
Chemotaxis
Degranulation
CXCR2 in biology of myeloid cells
Dendritic cells
Chemotaxis
Sequestration inside tumors
Macrophages
M1 versus M2 phenotype
Not important for chemotaxis

Figure 1.1. CXCR2 in the biology of myeloid cells.

Schematic representation of known roles for CXCR2 in the biology of myeloid cells including myeloid-derived suppressor cells (MDSCs), macrophages, dendritic cells and mast cells.

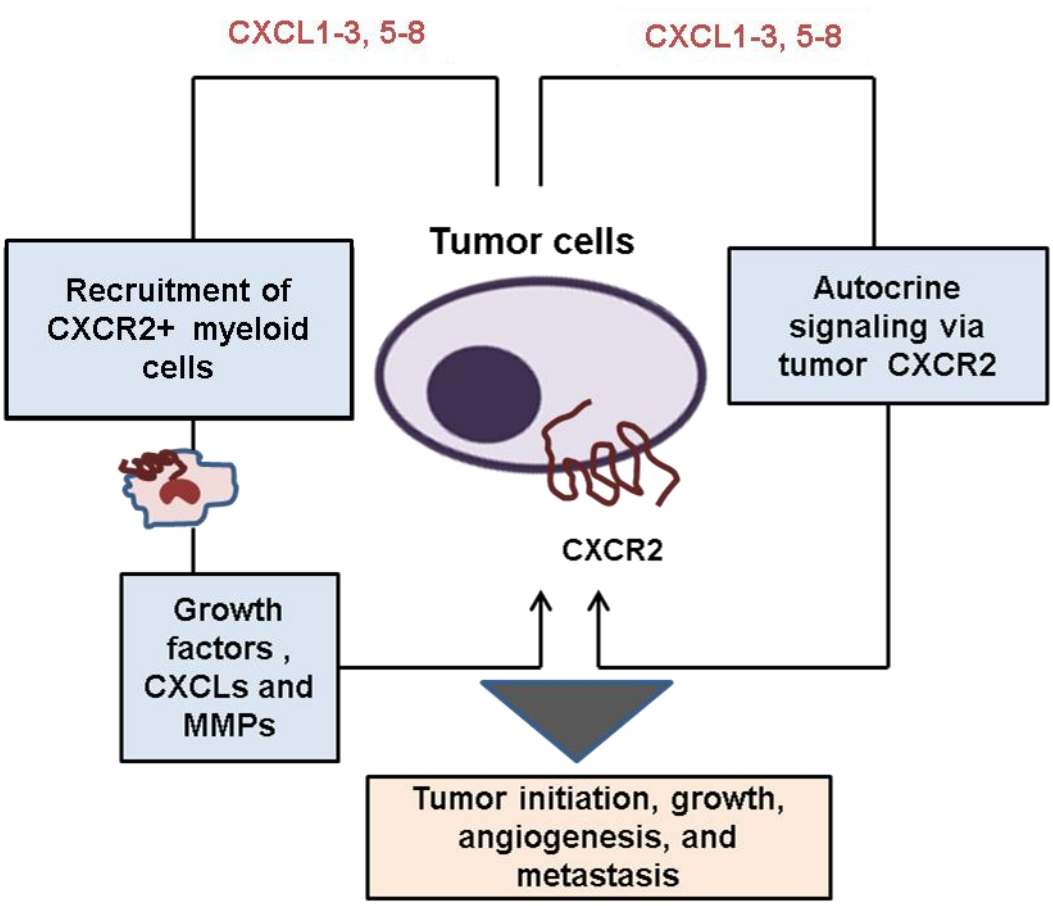
CXCL1-3, 5-8
CXCL1-3, 5-8
Tumor cells
Recruitment of CXCR2+ myeloid cells
Autocrine signaling via tumor CXCR2
CXCR2
Growth factors , CXCLs and MMPs
Tumor initiation, growth, angiogenesis, and metastasis

Figure 1.2. Hypothesis figure summarizing the proposed roles for CXCR2 in pancreatic cancer.

The central hypothesis for the research presented in this dissertation was that CXCR2 regulates both autocrine and paracrine mechanisms during the progression of pancreatic cancer (PC). Ligands produced by PC cells can bind to CXCR2 expressed on the surface of the tumor cells to enhance tumor cell proliferation. CXCR2 signaling in the host can also mediate the recruitment of immune suppressive cells, which can then lead to the growth of tumor cells by paracrine mechanisms.

Chapter 2

Materials and Methods

Human pancreatic cancer specimens:

Tissue microarray (TMA) slides were obtained from the University of Nebraska Medical Center (UNMC) rapid autopsy program. TMAs were constructed from paraffin blocks containing tumor cores, non-cancerous pancreas and control specimens of gastric tissue. The study was approved by the Institutional Review Board of the UNMC.

Cell line cultures and transfections:

Cell lines and culture conditions:

Murine cell lines.

Panc02 cells and UN-KC-6141 cell line (Torres et al., 2013a) (referred to as KRAS-PDAC cells in this study, a kind gift from Dr. Surinder K. Batra's laboratory at UNMC) were maintained in Roswell Park Memorial Institute Medium (RPMI) (HyClone®, GE Life Sciences, UT) and Dulbecco's Modified Eagle Medium (DMEM) (HyClone®, Thermo Scientific, UT) respectively. These media were supplemented with fetal bovine serum (FBS) (Atlanta Biologicals, GA), L-Glutamine (MediaTech, VA), two-fold vitamin solution (MediaTech) and Gentamycin (Gibco, Life Technologies, NY).

Human cell lines.

We used a model of immortalized human pancreatic duct-derived cell lines, with or without exogenous expression of $KRAS^{(G12D)}$. The model consisted of four cell lines hTERT-HPNE (HPNE), hTERT-HPNE-$KRAS^{(G12D)}$ (HPNE-KRAS)

[both cell lines referred to as HPNE/-KRAS], hTERT-HPNE-E6/E7/st (E6-E7-st) and hTERT-HPNE-E6/E7/st/KRAS$^{(G12D)}$ (E6-E7-st-KRAS) [both cell lines referred to as E6-E7-st/-KRAS]. Generation and maintenance of hTERT-HPNE, E6-E7-st and E6-E7-st-KRAS cells have been previously described (Campbell et al., 2007).

Transfection of murine pancreatic cancer cell lines:

Panc02 cells: Expression of Gaussia luciferase vector.

A lentiviral vector containing an expression cassette encoding gaussia luciferase (GLUC) and green fluorescent protein (GFP) was a kind gift from Dr. Bakhos A. Tannous, Harvard Medical School, Boston. Panc02 cells were transduced as described previously (Tannous, 2009). After the transduction GFP positive cells were sorted at the flow cytometry facility at UNMC and maintained in culture.

KRAS-PDAC cells: Expression of Luciferase GFP vector.

HEK293 cells were maintained in DMEM. The retroviral vector containing luciferase GFP expression was generated by infecting HEK293 cells with pBABE-luciferase hygromycin, pBABE-luciferase EGFP and helper virus plasmid (kind gifts from Dr. Kay Wagner's laboratory, UNMC). KRAS-PDAC cells were transfected using $CaCl_2$. Transfected GFP-expressing cells were flow sorted in the Flow Cytometry Facility at UNMC and cultured.

Transfections of human pancreatic cancer cell lines:

Generation of CXCR2 knock-down cells.

Six human GIPZ lentiviral shRNAmir anti-CXCR2 individual clones were obtained from Thermo Scientific Open Biosystems (Grand Island, NY). A scrambled shRNA was used as a non-silencing control (NSC). Lentiviral particles were generated by us and cells were infected according to the manufacturer's protocol. Stable knock-down of CXCR2 was achieved in E6-E7-st-KRAS cells by pooling together the six different anti-CXCR2 shRNA individual clones.

Animal models and details of *in vivo* studies:

***Study approval*.**

Mice were maintained under specific pathogen-free conditions. All procedures performed were in accordance with institutional guidelines and approved by the University of Nebraska Medical Center Institutional Animal Care and Use Committee (IACUC).

***Breeding strategy for the generation of Cxcr2$^{-/-}$ mice and genotyping PCR*.**

C57BL6 mice heterozygous (+/-) and knock-out (-/-) for *Cxcr2* were obtained from Charles Rivers (Wilmington, MA). Breeding pairs used to produce *Cxcr2*$^{-/-}$ mice were *Cxcr2*$^{-/+}$ female and *Cxcr2*$^{-/-}$ male **(Fig. 2.1A)**. All the colonies were maintained in the pathogen-free transgenic mouse facility at UNMC. Genomic DNA was isolated from tail clippings performed on 2- to 3-week-old mice. The tail clippings were digested overnight at 55ºC by incubating in 300 µl

digestion buffer containing 5 mM EDTA, pH 8.0, 200 mM NaCl, 100 mM Tris, pH 8.0 and 0.2% sodium dodecyl sulfate (Wang and Storm, 2006). Genomic DNA was amplified with specific primers for wild-type *Cxcr2* (forward: GGT CGT ACT GCG TAT CCT GCC TCAG, reverse: TAG CCA TGA TCT TGA GAA GTC CATG) and neomycin resistance gene (forward: CTT GGG TGG AGA GGC TAT TC, reverse: AGG TGA GAT GAC AGG AGA TC). PCR amplification products were electrophoresed on 1.5% agarose gel containing 0.25 µg/ml ethidium bromide (EtBr) **(Fig. 2.1B)**.

***Syngeneic mouse models*.**

In order to understand the role of CXCR2 in mediating the host immune response towards PC, we generated a syngenic immunocompetent mouse model having intact CXCR2 in the tumor cells and CXCR2 deletion in the tumor-bearing host mouse. Two different murine PC cell lines Panc02-GLUC-GFP and KRAS-PDAC-GFP were inoculated orthotopically in the pancreas of *Cxcr2*$^{+/+}$, *Cxcr2*$^{-/+}$ and *Cxcr2*$^{-/-}$ mice, male or female, 6- to 8-week-old. Mice were sacrificed after 4 to 6 weeks. A part of the tumor was processed to isolate tumor-associated lymphocytes (TALs), and a part was fixed in 10% formalin and processed for histological analysis.

***Xenogenic mouse models*.**

6- to 8-week-old female nude mice were obtained from Charles River Laboratories (Wilmington, MA). E6-E7-st-KRAS-NSC and E6-E7-st-KRAS-shCXCR2 cells (1 x 10^6 in 50 µl HBSS) were injected into the pancreas

(orthotopic) or flanks (subcutaneous) of nude mice. For subcutaneous implants, the tumors were measured twice a week for 50 days with a caliper. The tumor volume was calculated using the formula: volume = (length x width^2)/2. Subcutaneous tumors (50 days post inoculation) and orthotopic tumors (8 weeks post inoculation) were resected, fixed in 10% formalin and paraffin embedded.

***In vivo monitoring of growth of orthotopic tumors*.**

Gaussia luciferase assay.

Secreted levels of GLUC were measured as described previously (Chung et al., 2009; Tannous, 2009). Briefly, blood was collected from the tail vein of mice and transferred directly to the wells of a 96-well plate containing 2 µl of EDTA solution. GLUC activity was measured using a plate luminometer.

Reagents and antibodies.

The two CXCR2 antagonists SCH-527123 and SCH-479833 were obtained from Schering-Plough Research Institute and were dissolved in 20% hydroxypropyl-β-cyclodextrin (HPβCD) from Acros Chemical (St. Louis, MO, USA). All the antibodies used for the present study are listed in supplementary table 1.

Gene expression analysis:

RNA isolation.

Total RNA was isolated from cells and homogenized tissues using the standard Trizol (Invitrogen, Carlsbad, CA) protocol.

***PCR analysis*.**

Reverse Transcription was performed with 1-5 µg RNA using oligo (dT) (Fermentas, Hanover, MD, USA) and Superscript® II RT (Invitrogen) or iScript™ Reverse Transcription Supermix for RT-qPCR (BIO-RAD, Hercules, CA, USA). Regular PCR reactions were performed using Fast Start Taq dNTPack (Roche Diagnostics, IN, USA). Quantitative real-time PCR reactions were performed using FastStart SYBR Green Master Mix (Roche; Indianapolis IN, USA) using the MyIQ™ iCycler (BIO-RAD). Primer sets used for the study are listed in table 2.2 and 2.3. For regular PCR, amplified cDNA was resolved on EtBr-containing agarose gels. For real-time PCR mean C_t values of the target genes were normalized to mean C_t values of the endogenous control, ribosomal protein large 13 A (RPL13A); [$-\Delta C_t = C_t$ (RPL13A) – C_t (target gene)]. The ratio of mRNA expression of target genes versus RPL13A was defined as $2^{(-\Delta Ct)}$. Melting curve analysis was performed to check the specificity of the amplified product.

Protein analysis:

Protein isolation.

Total protein was isolated by lysing cells with RIPA buffer. Tumor tissues were homogenized in mammalian protein extraction reagent (M-PER®, Pierce, Rockford, IL). Protein concentrations were determined using BCA kit (Pierce™ BCA Protein Assay Kit (Thermo Scientific, Rockford, IL, USA).

***Western blot analysis*.**

Protein samples (40 µg or 25 µg) were electrophoresed on sodium dodecyl sulfate (SDS) polyacrylamide gels (10% or 15%) and transferred onto Immobilon-P Transfer membrane (Millipore, Billerica, Massachusetts, USA). Membranes were blocked with 3% BSA in PBS for 1 hour at room temperature. Membranes were probed with specific primary antibodies **(Table 2.1)** overnight at 4˚C. Membranes were washed with TTBS buffer, thrice and probed with respective secondary antibodies. Following washing with TTBS buffer membranes were visualized using SuperSignal® West Femto Kit (Thermo Scientific).

Enzyme linked immunosorbent assay (ELISA).

Equal numbers (1 x 10^6) of cells CD18/HPAF-scram (control), CD18/HPAF-shKRAS$^{(G12D)}$, HPNE, HPNE-KRAS, E6-E7-st, E6-E7-st KRAS, E6-E7-st KRAS-NSC, E6-E7-st KRAS-shCXCR2 and KRAS-PDAC cells were plated in 60 mm dishes in complete medium. After attachment of cells to the plate the medium was changed to serum free DMEM. Supernatants of cultured cells were collected at 24 hours or 72 hours. ELISA assays for hCXCL8 and hCXCL1 were performed as described previously (Varney et al., 2011). ELISAs for hCXCL5, mCXCL2, mCXCL5 and mCXCL7 were performed using a duoset kit (R & D Systems, Minneapolis, MN, USA) according to the manufacturer's protocol. All the experiments were performed in duplicate.

Immunofluorescence.

Cells were cultured on 8-well chamber slides and were allowed to adhere overnight. The following day, cells were fixed using 4% paraformaldehyde, blocked with antibody diluent (BD Biosciences), and probed with anti-CXCR2 antibody (4˚C overnight). The next day, slides were incubated with Cy3-conjugated anti-mouse antibody. Nuclei were counterstained with DAPI (4, 6 diamidino-2-phenylindole). Finally, slides were mounted with Vectashield® mounting medium (Vector Laboratories, Burlingame, CA, USA) and observed under a fluorescence microscope.

Immunohistochemistry.

4 µm thick, formalin-fixed, paraffin-embedded sections were deparaffinized. Antigen retrieval was performed using sodium citrate buffer (pH = 6.0) and microwaving for 10 minutes. Endogenous peroxidase was blocked by incubating with 3% hydrogen peroxide in methanol for 30 minutes. After blocking non-specific binding by incubating with serum, slides were probed with primary antibody **(Table 2.1)** overnight at 4ºC. Slides were washed and appropriate secondary antibodies were added. Immunoreactivity was detected using the ABC Elite Kit and 3, 3 diaminobenzidine substrate kit (DAB) (Vector Laboratories, Burlingame, CA) as per the manufacturer protocols. A reddish brown precipitate indicated positive staining. Nuclei were counter stained with hematoxylin. For quantitative evaluation positive cells were counted in five independent areas at 400X. For human PC specimens, immunostaining was evaluated by a

semiquantitative system. Extent (percentage of positive cells) were scored using the following grading system 0 (negative), 1+ (1%–10% of cells positive), 2+ (11%–50% of cells positive), and 3+ (>50% of cells positive). Furthermore, intensity was designated as weak (1 point), moderate (2 points), or strong (3 points). IHC composite score (IHC-CS) was calculated by multiplying extent with intensity.

***In vitro* cell based assays:**

In vitro cell proliferation assay.

Cells were seeded at the indicated densities in 96-well plates and were allowed to adhere. Cells were washed with HBSS and were incubated with medium alone or medium containing different serum concentrations or medium containing specified concentrations of the CXCR2 antagonists for 72 hours. Cell viability was determined by MTT assay (3-(4, 5 dimethylthiazol-2-yl)-2, 5-dipehnylate-tetrazolium bromide, tetrazole) as previously described (Li et al., 2001). Percent inhibition of cell growth was calculated by the formula: [100 - (A/B) x 100], where ‘A’ and ‘B’ are the absorbance of the treated and untreated cells, respectively. Percentage of cell growth was calculated by the formula: [(A/B) x 100], where ‘A’ and ‘B’ are the absorbance of treatment and control group respectively.

Anchorage-dependent and -independent growth assay.

To evaluate anchorage-dependent (clonogenic) potential, KRAS-PDAC cells were plated at a density of 2500 cells/well in a 6-well plate and treated with

different concentrations of CXCR2 antagonists in 10% DMEM. Clonogenicity was evaluated after ten days by fixing cells in methanol and staining with crystal violet.

Anchorage-independent growth (colony formation) was assessed by plating 3000 cells per well in 0.3% agarose with a 0.6% agarose underlay in a 6-well plate. CXCR2 antagonists were added at the indicated concentrations to both 0.3% agarose layer and the medium covering the 3% agarose layer. Cells were incubated for two weeks at 37º C in a 5% CO_2 incubator. Media was changed once every week. Colonies were fixed in a solution of acetone with methanol and stained with 0.5% crystal violet and counted under an inverted microscope at 4X magnification.

Cell migration-wound healing assay.

A wound healing assay was conducted to assess the migratory potential of the cells. Cells were plated in 60 mm dishes. After the cells reached 90-95% confluence, a wound was generated using 1 ml pipette tip. Cells were washed with HBSS and incubated with either serum-free medium or with serum free medium with the indicated concentrations of CXCR2 antagonists for 24 hours. Cells were photographed under an inverted microscope at 4X magnification at time T = 0 hours and T = 24 hours. The width of wound was measured using NIH image J software. Distance migrated was calculated by the formula: Initial wound width (T = 0 hours) – Final wound width (T = 24 hours).

Isolation of tumor-associated lymphocytes:

A part of the harvested tumor was digested and TALs were isolated using the lympholyte®-M density separation medium (CEDARLANE®, Ontario, Canada). TALs were further processed for RNA isolation or flow cytometry **(Fig. 6.1)**

Flow cytometry:

In order to characterize immune cells isolated from the pancreas and spleens, multicolored flow cytometry was performed. Single cell suspensions were prepared from freshly isolated spleens by crushing them and passing the mixture through a cell strainer. TALs were isolated from the pancreas as described above. Immune cells were stained using the following antibodies: anti-CD11b (APC); anti-Ly6C (PE/Cy7); anti-Ly6G (Alexa Flour 700); anti-F4/80 (FITC); anti-CD3 (FITC); anti-CD4 (PE); anti-CD8 (APC); anti-CD25 (Alexa Flour 700); anti CD49b (Pan-NK) (PErCP/Cy5.5) all from BioLegend® (San Diego, CA). Flow cytometry was performed using BDLSR II and data were analyzed with BD FACS DIVA and FlowJo software **(Fig. 6.1)**.

Statistical analysis:

Statistical analysis was conducted using Excel or GraphPad Prism software. The significance was determined by the Student's t-test or the nonparametric Mann-Whitney *U*-test. For all statistical tests, a p-value of ≤ 0.05 was considered significant.

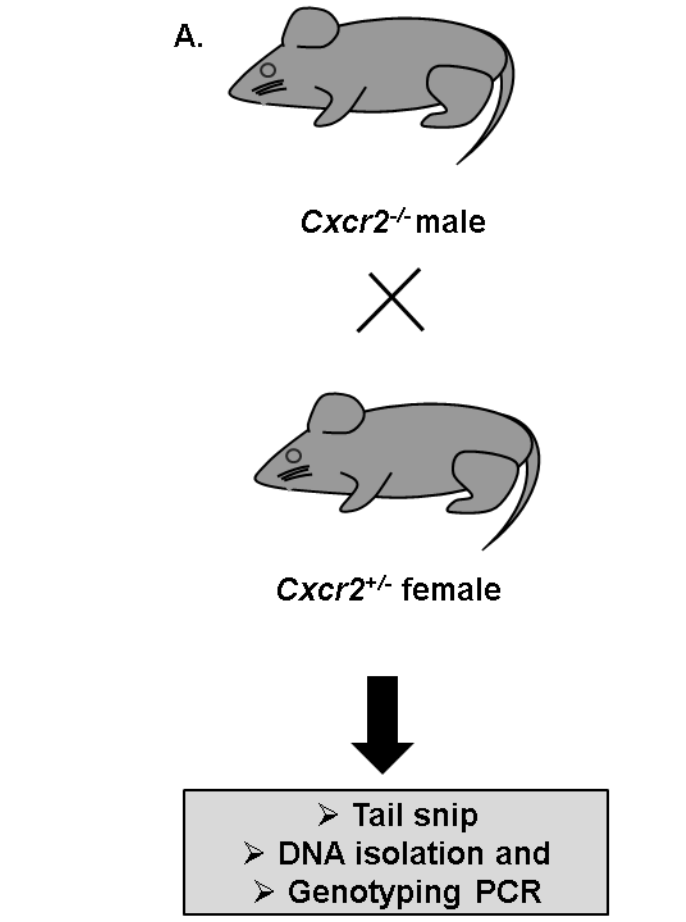
A.
Cxcr2$^{-/-}$ male
Cxcr2$^{+/-}$ female
➢ Tail snip
➢ DNA isolation and
➢ Genotyping PCR
B.
Cxcr2$^{+/-}$
Cxcr2$^{+/+}$
Cxcr2$^{-/-}$
360 bp
280 bp

Figure 2.1. Breeding strategy and genotyping PCR for the generation of *Cxcr2*$^{-/-}$ mice.

A) The mouse colony was maintained by crossing *Cxcr2*$^{-/-}$ male mice with *Cxcr2*$^{-/+}$ female mice. **B)** Genotyping PCR was performed on DNA isolated from the snipped tails of mice.

Table 2.1. List of antibodies used for the study

Species reactivity	Antibody	Supplier	Catalogue number	Host species	Dilution
Mouse	mCXCR2	Kind gift from Dr. Strieter		Goat	1:1000
Mouse	Gro alpha	Abcam	ab86436	Rabbit	1:500
Mouse and human	mCXCL3	Bioss	bs-2547R	Rabbit	1:500
Mouse	mCXCL5	Cloud-clone corp.	PAA860Mu01	Rabbit	1:100
Mouse	mCXCR1	Novous Biologicals	NB600-1142	Rabbit	1:100
Human	Ki-67	Santa cruz	sc-15402	Rabbit	1:50
Human	Cleaved caspase 3	Cell Signaling	Asp175	Rabbit	1:200
Mouse	Cytokeratin	Dako	Z0622	Rabbit	1:500
Mouse	F4/80	Abcam	Ab6640	Rat	1:100
Mouse	Ly6	Thermo Scientific	MA1-40038	Rat	1:50
Human	hCXCR2	Santa cruz	Sc-7304	Mouse	1:200
Human	hCXCL1	Abcam	Ab86436	Rabbit	1:500
Human and mouse	Erk	Santa cruz	Sc-94	Rabbit	1:200
Human and mouse	p-Erk	Cell Signaling	#9101	Rabbit	1:2000
Human and mouse	KRAS	Santa cruz	F234-sc-30	Mouse	1:1000
Human and mouse	Actin	Sigma	A2066	Rabbit	1:5000

Table 2.2. List of human primers used for the study

Human Primers			
Gene	**Temperature**	**In this study used for**	**Primer sequence**
CXCR2	59˚	PCR (regular)	Forward-5'-ACC CAG GTG ATC CAG GAG AC-3' Reverse-5'- CCA ATG AAG GCG TGA AAA GG-3'
RPL13A	59˚	Real-time PCR and regular PCR	Forward-5'- GGCTGAAGCCTACCAGAAAG-3' Reverse- 5'-CTTTGCCTTTTCCTTCCGTT-3

Table 2.3: List of murine primers used for the study.

Murine Primers			
Gene	**Temperature**	**In this study used for**	**Primer sequence**
Cxcr2	60˚	Regular PCR	Forward 5'- CACCGATGTCTACCTGCTGA -3' Reverse 5'- CACAGGGTTGAGCCAAAAGT -3'
Cxcl1	55˚	Regular PCR	Forward 5'-TCGCTTCTCTGTGCAGCGCT-3' Reverse 5'- GTGGTTGACACTTAGTGGTCT C-3'
Cxcl2	57˚	Regular PCR	Forward 5'-AGTGAACTGCGCTGTCAATG-3' Reverse 5'-TTCAGGGTCAAGGCAAACTT-3'
Cxcl3	68˚	Regular PCR	Forward 5'-GCAAGTCCAGCTGAGCCGGGA-3' Reverse 5'-GACACCGTTGGGATGGATCGCTTT-3'
Cxcl5	68˚	Regular PCR	Forward 5'-ATGGCGCCGCTGGCATTTCT-3' Reverse 5'-CGCAGCTCCGTTGCGGCTAT-3'
Cxcl7	57˚	Regular PCR	Forward 5'-CTCAGACCTTACATCGTCCTGC-3' Reverse 5'-AGCGCAACAAGGATCGTCCTGC-3'
Ccl5	56˚	Real-time PCR	Forward 5'-GCTGCTTTGCCTACCTCTCC-3' Reverse 5'-TCGAGTGACAAACACGACTGC-3'
Ccl3	56˚	Real-time PCR	Forward 5'-TTCTCTGTACCATGACACTCTGC-3' Reverse 5'-CGTGGAATCTTCCGGCTGTAG-3'
Ccl2	56˚	Real-time PCR	Forward 5'-TTAAAAACCTGGATCGGAACCAA-3' Reverse 5'-GCATTAGCTTCAGATTTACGGGT-3'
IL-12	57˚	Real-time PCR	Forward 5'-TGGGTTTGCCATCGTTTTGCTG-3' Reverse 5'-ACAGGTGAGGTTCACTGTTTCT-3'
IL-10	57˚	Real-time PCR	Forward 5'-GCTCTTACTGACTGGCATGAG-3' Reverse 5'-CGCAGCTCTAGGAGCATGTG-3'
IFN-γ	57˚	Real-time PCR	Forward 5'-ATGAACGCTACACACTGCATC-3' Reverse 5'-CCATCCTTTTGCCAGTTCCTC-3'
TNF-α	57˚	Real-time PCR	Forward 5'-CCCTCACACTCAGATCATCTTCT-3' Reverse 5'-GCTACGACGTGGGCTACAG-3'
APO-2	58˚	Regular PCR	Forward 5' –GGATATGGCCTGGCTGTAGA-3' Reverse 5'-TTGGCGGAAAGAAAGCAAGT-3'
Bcl2	58˚	Regular PCR	Forward 5'-AATGTCCAGGTGGGTCAGAG-3' Reverse 5'-TCCTGCTGGATCTGCCTAGT-3'
Bax	58˚	Regular PCR	Forward 5'-TGCAGAGGATGATTGCTGAC-3' Reverse 5'-GGAGGAAGTCCAGTGTCCAG-3'
Rpl13a	58˚	Regular PCR	Forward 5'-ACTCTGGAGGAGAAACGGAAGG-3' Reverse 5'- CAGGCATGAGGCAAACAGTC-3'

Chapter 3

The expression of CXCR2 and its ligands in human and murine pancreatic cancer

Abstract:

The aim of this section of the study was to evaluate the localization of the expression of CXCR2 and its ligands in tissue specimens of human and mouse pancreatic cancer (PC). Human tissue specimens were obtained from the rapid autopsy program at UNMC. PC progression model was built from tumors isolated form Pdx1-cre;LSL-*Kras*$^{(G12D)}$ mice at different ages. Immunohistochemistry (IHC) for CXCR2 and its ligands was performed. Our results demonstrate an increased staining for hCXCR2 and hCXCL1 and 3 in PC versus the normal pancreas. In the Pdx1-cre;LSL-*Kras*$^{(G12D)}$ mouse model the expression of mCXCR2 and ligands mCXCL1, 3 and 5 was found to be upregulated at the early stages of the disease. Overall, we conclude that CXCR2 and its ligands are expressed early during the course of PC progression. Furthermore, there expression was found to be located on the malignant ductal cells as well as the surrounding stroma.

Introduction:

Precise identification of the cell types expressing CXCR2 and its ligands in PC can help in making any targeted therapies in the future to be more accurate. PC is associated with a) high frequency of mutations in the KRAS oncogene in the malignant ductal cells and b) dense production of stroma. CXCR2 and its ligands are known to be expressed by several cell types in the body including those that are a part of the PC TME such as fibroblasts, immune cells and endothelial cells.

Expression of CXCR2 and its ligands in PC cell lines has been well documented (Matsuo et al., 2009c; Wang et al., 2013b). Furthermore, reports in PC have also identified the expression of CXCR2 and its ligands CXCL8 and 5 in human PC patient tissue specimens (Kuwada et al., 2003; Li et al., 2011c). However, currently there is no study evaluating the expression of CXCL1 and CXCL3 in PC tissue specimens. Animal models of PC have widely expanded our understanding of the progression of this disease in relation to the most frequently mutated genes like *KRAS* and *P53* (Hingorani et al., 2005). The Pdx1-cre;LSL-*Kras*$^{(G12D)}$ mouse model, having pancreas specific knock-in for the *Kras*$^{(G12D)}$ mutation is known to closely recapitulate the histological and molecular pathology of the human PC (Hingorani et al., 2003a). This model enables the evaluation of not just the cellular pattern for the expression of molecular targets but also helps in identification of the time points of their expression during the course of disease development. However, the expression of CXCR2 biological axis during the

disease progression in the animal model Pdx1-cre;LSL-*Kras*$^{(G12D)}$ has not been reported yet.

In order to conceive a clear picture of the probable pathological roles of CXCR2 and its ligands in PC we firstly evaluated the expression pattern of hCXCR2 and its ligands hCXCL1, 3 and 8 in the human PC tissue specimens. Furthermore, using pancreatic tissues derived from Pdx1-cre;LSL-*Kras*$^{(G12D)}$ mouse model we recognize the kinetics of their expression during the development and progression of PC.

Results:

Expression of hCXCR2 in human pancreatic cancer specimens:

IHC analysis revealed the presence of hCXCR2 in human PC specimens. We observed an intense immunoreactivity for hCXCR2 both in the ducts and the stroma of the human PC specimens. CXCR2 was also expressed in the normal pancreas; however, this expression was localized only to the acinar cell compartment and normal pancreatic ducts were negative for hCXCR2 expression **(Fig. 3.1A and B)**. 83.33% ducts (10\12) and 88.235% stroma (15\17) in the primary tumors were positive for CXCR2 expression. Overall the average composite score of CXCR2 IHC was higher in the PC tissue specimens versus the normal pancreas ($p = 0.075$) **(Fig. 3.1C)**.

Expression of hCXCL1 in human pancreatic cancer specimens:

Expression of hCXCL1 was detected both in the ducts and the stroma of human PC tissues. Normal pancreatic acinar cells also showed immunoreactivity for hCXCL1; however the normal pancreatic ducts were negative for its expression **(Fig. 3.2A and B)**. In primary tumors, both ductal and stromal cells in 100% specimens were positive for hCXCL1. Overall composite score for IHC remained unchanged in the normal pancreas versus the PC tissue ($p = 0.4211$) **(Fig. 3.2C)**.

Expression of hCXCL3 in human pancreatic cancer specimens:

Malignant ductal cells of PC tissue and surrounding stroma showed an enhanced expression of hCXCL3 compared with the normal pancreas. The average IHC composite score for hCXCL3 was significantly higher in pancreatic tumors versus the normal pancreas ($p = 0.049$) **(Fig. 3.3A and B)**. In normal pancreas the ducts were negative for hCXCL3; however, the malignant ductal cells showed high immunoreactivity for the ligand **(Fig. 3.3C)**.

Enhanced expression of CXCR2 and cognate ligands in the cancerous lesions of Pdx1-cre;LSL-*Kras*$^{(G12D)}$ mice.

Earlier reports have highlighted the role of KRAS mutations in upregulation of CXCR2 ligands in various cancers (Ancrile et al., 2008). The majority of reports in PC have used *in vitro* cell line based model systems and hence the precise spatiotemporal pattern of expression of CXCR2 and its ligands in the context of introducing the *KRAS*$^{(G12D)}$ mutation remains unclear (Matsuo et

al., 2009a). In the present study we used Pdx1-cre;LSL-*Kras*$^{(G12D)}$ mice having pancreas-specific expression of the *KRAS*$^{(G12D)}$ mutation, which is known to recapitulate the histological and pathological features of human PDAC progression (Hingorani et al., 2003b). Our primary objective was to evaluate the cellular location and time points for the expression of CXCR2 and its ligands in the lesions of Pdx1-cre;LSL-*Kras*$^{(G12D)}$ mice. Pancreatic tissues derived from mice sacrificed at different time points (10, 25 and 50 weeks) were used to generate a progression model. We observed no expression of mCXCL1, 3 and 5 in the normal pancreas, derived from the control Pdx1-cre mice. However, in Pdx1-cre;LSL-*Kras*$^{(G12D)}$ mice, beginning at 10 weeks of age expression of mCXCL1 and mCXCL3 was observed **(Fig. 3.4A)**. This expression was further intensified in the tumors of mice at 25 and 50 weeks age, which represent fully developed PDAC. The expression was localized in both PDAC (duct) cells as well as the surrounding stroma. Next, we determined the expression levels of mCXCR2. Similar to the ligands, while normal pancreas showed no immunoreactivity for the protein, expression of mCXCR2 was observed in 10 week old animals, and it further intensified in the 25- and 50- week old animals **(Fig. 3.4A)**. mCXCR2 was expressed in the ducts as well as the surrounding stromal cells. Figure 3.4B summarizes the expression pattern of CXCR2 and its ligands at different time points during PDAC development.

Discussion:

In this section of the dissertation, we have identified the expression of the CXCR2 biological axis in both human and murine PC tissues and normal

pancreas. Our results demonstrate expression of hCXCR2 and its ligands hCXCL1 and hCXCL3 in the human PC tissue as well as the normal pancreas. However, the expression of hCXCR2 and hCXCL3 was higher in the PC tissues versus the normal pancreas. Furthermore, we also identified the expression of mCXCR2, mCXCL1, 3 and 5 in the pre-cancerous lesions of Pdx1-cre;LSL-*Kras*$^{(G12D)}$ mice. However, unlike the human tissues the normal murine pancreas was negative for the expression of mCXCR2, mCXCL1 and 5.

Previous reports have identified the expression of hCXCR2, hCXCL5 and 8 in human PC specimens by IHC (Kuwada et al., 2003). Similar to our observations, expression of hCXCR2 has been reported in both PC tissues and normal pancreas (Oliveira Frick et al., 2008). We observed positive immunoreactivity for hCXCR2 only in the acinar cells of the normal pancreas; however, both malignant ducts and stroma were positive in the PC tissues. A previous report by Frick et al. demonstrated a non-significant increase in the expression of hCXCL1 in the PC tissues versus the surrounding normal pancreas (Oliveira Frick et al., 2008). We for the first time identify the expression of hCXCL1 using IHC analysis and demonstrate that this protein is expressed in malignant ductal cells and surrounding stroma of the PC tissues. We also for the first time identify the expression of hCXCL3 in human PC tissues. The expression of hCXCL3 was expressed both in the ducts as well as surrounding stromal compartment; furthermore, its expression was significantly enhanced compared with the normal pancreatic tissue.

Oncogenic mutations in KRAS are present in 95% of PDAC cases (Bryant et al., 2014). Expression of ELR+ CXC chemokines is linked to oncogenic mutations in different isoforms of RAS in various malignancies, for example lungs, ovaries, colorectal and pancreas (Ancrile et al., 2008). Of note, KRAS mutations are required for both initiation and maintenance of PDAC (Collins et al., 2012). While recent reports in PDAC have identified a KRAS-CXC chemokine link, it remains unclear if this signaling can serve as an early biomarker for PDAC progression. Using Pdx1-cre;LSL-*Kras*$^{(G12D)}$ mice as a model system we identify the time point of upregulation of CXCR2 signaling during *KRAS*$^{(G12D)}$-induced PDAC progression. Our data provides evidence for the expression of mCXCR2 and its ligands mCXCL1, 3 and 5 in the precursor lesions of 10-week old Pdx1-cre;LSL-*Kras*$^{(G12D)}$ mice (PanIN-1 stage) and that their expression is further enhanced as these precursor lesions advanced to PDAC. Additionally, we identify the cellular sources for the expression of CXCR2-CXCL axis. mCXCR2, mCXCL1, mCXCL3 and mCXCL5 were expressed by the malignant ductal cells in the earliest stages and further in the stromal cells as the lesions advanced. The expression of mCXCR2 and mCXCL1 has been previously reported *in vivo* in tumors of Ptf1a$^{cre/+}$;LSL-*Kras*$^{(G12D)}$ mice (Ijichi et al., 2011a). Our results further elaborate these finding by identifying the spatial-temporal pattern of the expression of mCXCR2, mCXCL1 and two additional ligands mCXCL3 and mCXCL5 during the PDAC progression.

Taken together, we here identify the expression of CXCR2 biological axis in the ductal as well as the stromal compartment of PC tissues. These results

suggest a possible autocrine as well as paracrine roles of this signaling axis during PC progression. We also report the presence of CXCR2 and its ligands in the precursor lesions of Pdx1-cre;LSL-*Kras*$^{(G12D)}$ mice suggesting that the upregulation of CXCR2 biological axis is an early event during PC progression.

A.

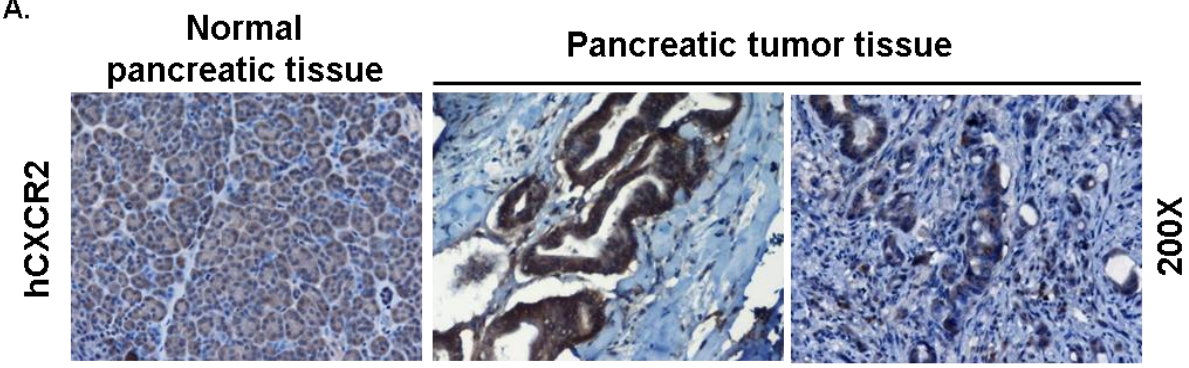

B.

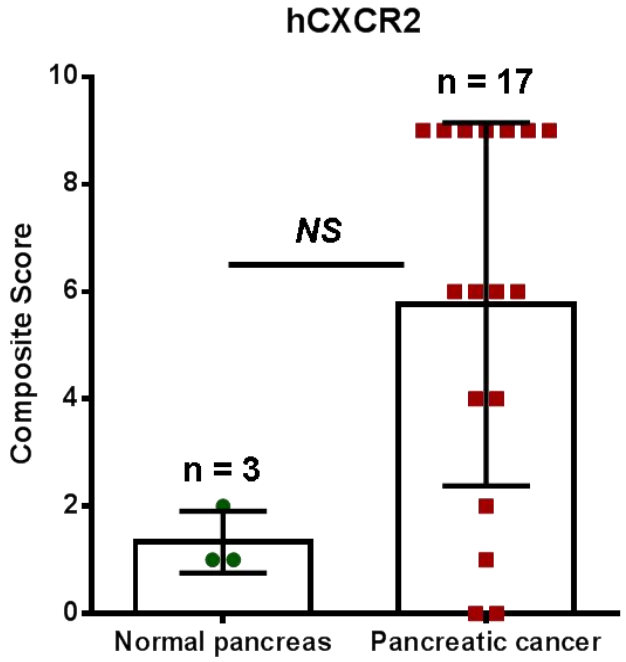

C.

	Normal pancreas		Primary tumor	
	Ducts	Other cells	Ducts	Stroma
CXCR2 +VE	0/3 (0%)	3/3 (100%)	10/12 (83.33%)	15/17 (88.235%)
CXCR2 -VE	3/3 (100%)	0/3 (0%)	2/12 (16.66%)	2/17 (11.76%)

Figure 3.1. Expression of hCXCR2 in human pancreatic cancer tissue specimens:

A) Representative pictures of human pancreatic cancer tissue specimens stained for hCXCR2. **B)** Higher mean composite score (extent x intensity) of hCXCR2 staining in human pancreatic cancer tissues (n = 17) compared with the normal pancreas (n = 3). Each dot on the graph represent composite score of one tissue specimen. **C)** Table summarizing the percent distribution of hCXCR2 staining in different cell types in normal pancreas and tumor tissue. Statistical significance determined by non-parametric Mann-Whitney *U* test. (* $p \leq 0.05$, ** $p \leq 0.01$, *** $p \leq 0.001$, *NS* $p > 0.05$).

A.

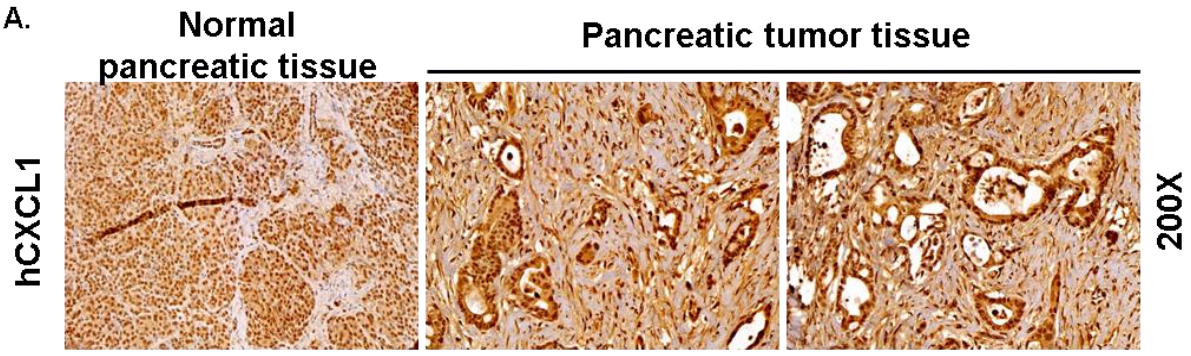

B.

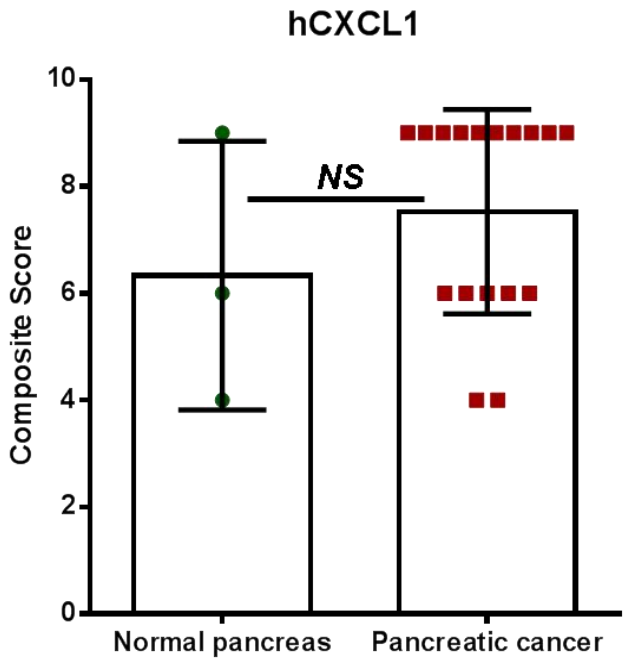

C.

	Normal pancreas		Primary tumor	
	Ducts	Other cells	Ducts	Stroma
CXCR2 +VE	0/3 (0%)	3/3 (100%)	14/14 (100%)	16/16 (100%)
CXCR2 -VE	3/3 (100%)	0/3 (0%)	0/14 (0%)	0/16 (0%)

Figure 3.2. Expression of hCXCL1 in human pancreatic cancer tissue specimens.

A) Representative pictures of human pancreatic cancer tissue specimens stained for hCXCL1. **B)** Higher mean composite score (extent x intensity) of hCXCL1 staining in human pancreatic cancer tissues (n = 17) compared with the normal pancreas (n = 3). Each dot on the graph represent composite score of one tissue specimen. **C)** Table summarizing the percent distribution of hCXCL1 staining in different cell types in normal pancreas and tumor tissue. Statistical significance determined by non-parametric Mann-Whitney *U* test. (* $p \leq 0.05$, ** $p \leq 0.01$, *** $p \leq 0.001$, *NS* $p > 0.05$).

A.

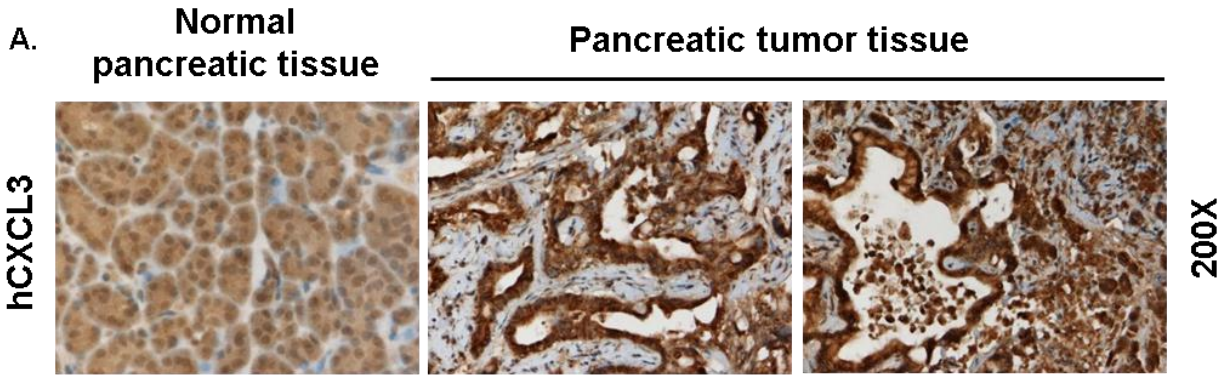

B.

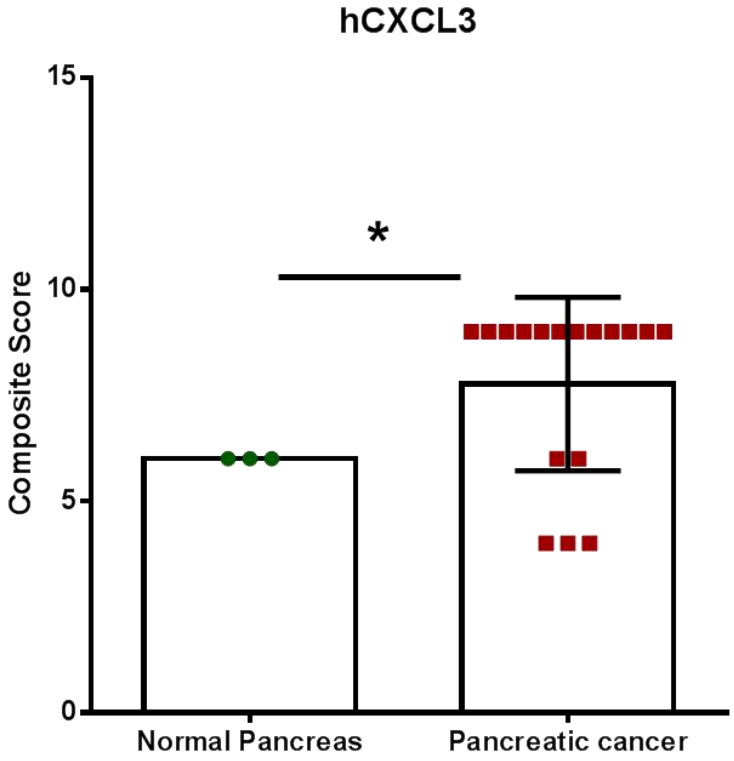

C.

	Normal pancreas		Primary tumor	
	Ducts	Other cells	Ducts	Stroma
CXCR2 +VE	0/3 (0%)	3/3 (100%)	1212 (100%)	17/17 (100%)
CXCR2 -VE	3/3 (100%)	0/3 (0%)	0/12 (0%)	0/17 (0%)

Figure 3.3. Expression of hCXCL3 in human pancreatic cancer tissue specimens.

A) Representative pictures of human pancreatic cancer tissue specimens stained for hCXCL3. **B)** Higher mean composite score (extent x intensity) of hCXCL3 staining in human pancreatic cancer tissues (n = 17) compared with the normal pancreas (n = 3). Each dot on the graph represent composite score of one tissue specimen. **C)** Table summarizing the percent distribution of hCXCL3 staining in different cell types in normal pancreas and tumor tissue. Statistical significance determined by non-parametric Mann-Whitney *U* test. (* $p \leq 0.05$, ** $p \leq 0.01$, *** $p \leq 0.001$, *NS* $p > 0.05$).

A.

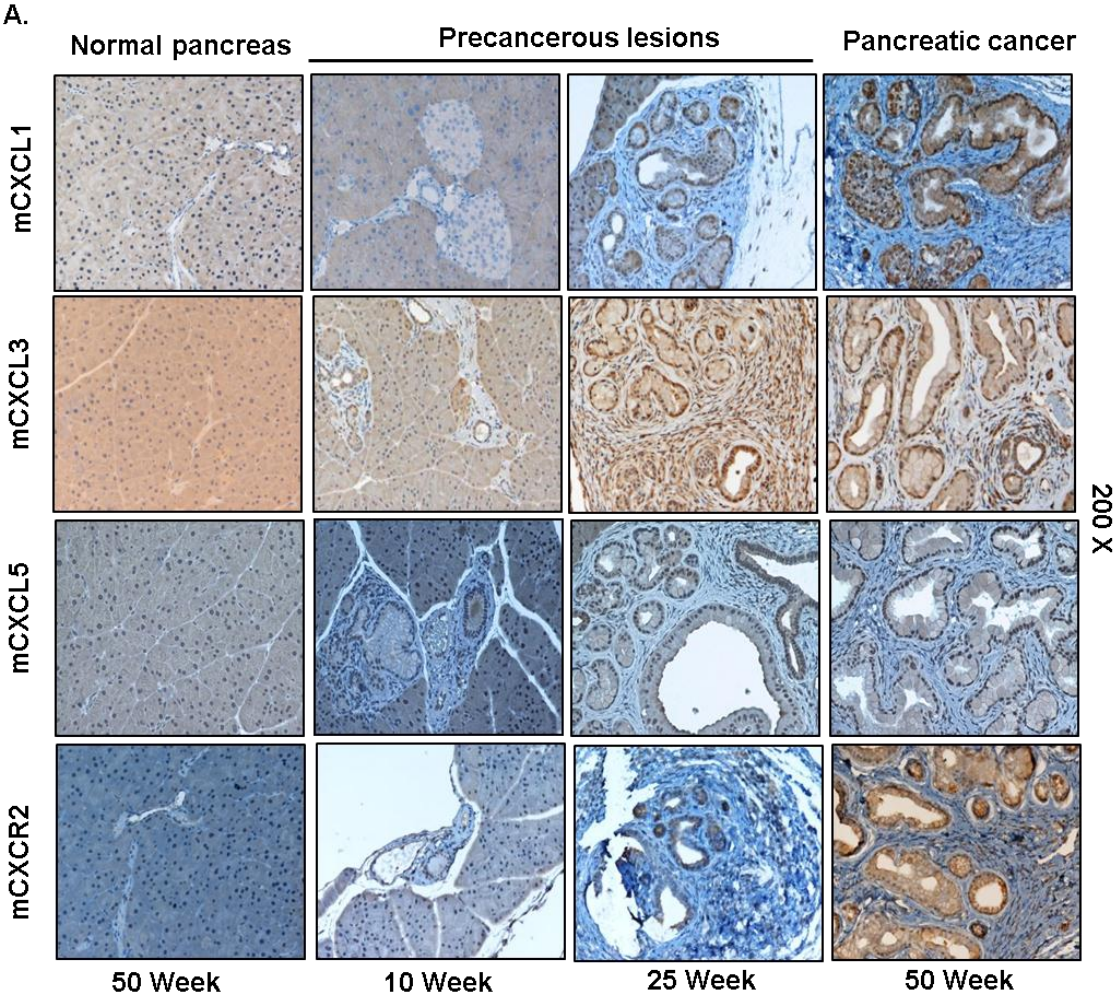

B.

Expression	Normal	10 Weeks	25 Weeks	50 Weeks
mCXCR2	-	+	++	+++
mCXCL1	-	+	++	+++
mCXCL3	+	+	++	+++
mCXCL5	-	+	++	+++

Figure 3.4. Expression of mCXCR2 and its ligands progressively increases in the developing cancerous lesions of Pdx1-cre;LSL-*Kras*$^{(G12D)}$ mouse model. A) Representative images of immunohistochemistry performed on progression model derived from tumors of Pdx1-cre;LSL-*Kras*$^{(G12D)}$ mice at different ages (n = 5 mice per group), demonstrating progressively increasing expression of mCXCL1, mCXCL3, mCXCL5 and mCXCR2. Normal pancreas is negative for the expression. **B)** Table summarizing the time points of expression of CXCR2 biological axis in Pdx1-cre;LSL-*Kras*$^{(G12D)}$ mice.

Chapter 4

CXCR2 signaling mediates *KRAS*$^{(G12D)}$-induced autocrine growth in pancreatic cancer

This chapter is derived from:

Abhilasha Purohit[1], Michelle Varney[1], Satyanarayana Rachagani[2], Michel M. Ouellette[3], Surinder K. Batra, Rakesh K. Singh[1]"CXCR2 signaling mediates *KRAS*$^{(G12D)}$-induced autocrine growth in pancreatic cancer"**.** *Oncotarget* (Accepted)

Abstract:

Pharmacological inhibition of *RAS*, the master regulator of pancreatic ductal adenocarcinoma (PDAC), continues to be a challenge. Mutations in the various isoforms of the *RAS,* including *KRAS,* are known to upregulate CXC chemokines; however, their potential role in KRAS-driven pancreatic cancer remains unclear. In this report, we reveal a tumor cell-autonomous role of $KRAS^{(G12D)}$-induced CXCR2 signaling in mediating growth of neoplastic PDAC cells. Knocking-down *CXCR2* in $KRAS^{(G12D)}$-bearing human pancreatic duct derived cells demonstrated a significant decrease in the *in vitro* and *in vivo* tumor cell proliferation. Furthermore, CXCR2 antagonists demonstrated selective growth inhibition of $KRAS^{(G12D)}$-bearing cells *in vitro.* Intriguingly, both genetic and pharmacological inhibition of CXCR2 signaling in $KRAS^{(G12D)}$-bearing pancreatic ductal cells reduced the levels of KRAS protein, strongly implying the presence of a KRAS-CXCR2 feed-forward loop. Together, these data demonstrate role of CXCR2 signaling in $KRAS^{(G12D)}$-induced growth transformation and progression in PDAC.

Introduction

PC is a disease with extremely poor prognosis (Siegel et al., 2015). It is the late clinical presentation which makes the disease extremely difficult to treat, leading to high mortality. Therefore, elucidating the molecular entities that regulate the early stages of this disease may facilitate the development of novel diagnostic and therapeutic strategies for PC. PDAC is the most frequent (90%) histological subtype of PC. PDAC arises in a step-wise manner from precursor lesions, collectively known as PanINs (Vincent et al., 2011). The detection and targeting of PDAC at the PanIN stages may therefore provide a curative window for this disease.

The histological progression of PanINs to PDAC involves a complex interplay of various genetic mutations and molecular mediators. *KRAS*, a member of *RAS* family of GTPases, is known to be mutated in 95% cases of PDAC. The predominant version of this earliest tumor-promoting mutation is the substitution of Glycine to Aspartic acid at codon 12 ($KRAS^{(G12D)}$). Inhibiting KRAS, the driver of PDAC development and progression, appears to be a very appealing approach to target the earliest stages of this disease. However, till date the strategies to pharmacologically block the aberrant RAS functions have turned futile (Bryant et al., 2014). Thus, to develop alternative approaches to target KRAS-induced PDAC initiation and progression it is requisite to understand the molecular intermediaries that execute the actions of mutant *KRAS*.

Initiation and progression of cancer is intimately connected with inflammation. Cytokines including IL6 and ELR^+ CXC chemokines are known targets of oncogenic RAS signaling (Ancrile et al., 2008). ELR^+ CXC chemokines includes the ligands CXCL1-3, 5, 6, 7 and 8. A seven transmembrane G protein coupled receptor CXCR2 is the cognate receptor for all the ELR^+ CXC chemokines. However, CXCL6 and 8 are also known to bind to CXCR1, having structural homology with CXCR2 (Chapman et al., 2009). CXCR2 signaling is known to contribute to tumor progression via a variety of mechanisms, including promoting growth of tumor cells, angiogenesis and infiltration of immune suppressive cells in the TME (Highfill et al., 2014; Luppi et al., 2007; Waugh and Wilson, 2008). Aberrant expression of CXCR2 and its ligands has been reported in various malignancies including cancers of lungs (Saintigny et al., 2013), melanoma (Wu et al., 2012), gastric (Lee et al., 2014), prostate (Salazar et al., 2013) and pancreas (Li et al., 2011a). A higher expression of CXCL5 and CXCL8 has been reported in patient-derived tumor samples (Li et al., 2011d; Takamori et al., 2000; Wente et al., 2006). In fact, CXCL5 was detected in the precursor PanIN lesions of human PC tissue, suggesting its role in the early stages of the disease (Li et al., 2011d). Also, CXCL1 and CXCL5 were found to be upregulated in serum samples of PDAC patients (O'Hayer et al., 2009). With respect to connecting them with the *RAS* mutation, a recent report by Matsuo et al., identified $KRAS^{(G12D)}$ to be sufficient for the upregulation of cumulative expression of CXCL1, 5 and 8 (Matsuo et al., 2009a). Collectively, these reports identified that $KRAS^{(G12D)}$-induced CXCLs play paracrine roles in mediating

tumor-stromal cross talk during PDAC genesis and that they do not exert autocrine effects in context of *KRAS*$^{(G12D)}$-induced mitogenic growth transformation. Contrary to these conclusions, some of the earlier research efforts have indicated the role of CXCR2 signaling in mediating autonomous growth of tumor cells in PC. Expression of both CXCR2 and its ligands is detected on PC cell lines (Matsuo et al., 2009e; Wang et al., 2013a). More importantly, Takamorie et al., identified CXCL1 and 8 as growth factors having autocrine effect on the proliferation of PC cell line Capan-1, through the receptor CXCR2 (Takamori et al., 2000). Growth stimulatory downstream signaling of RAS protein is primarily mediated by the activation of ERK pathway (Thompson and Lyons, 2005). Interestingly, CXCR2 signaling is also known to induce activation of ERK pathway (Li et al., 2008). More specifically, reports in gastric cancer and melanoma provide evidence for the direct role of CXCL1 (a CXCR2 ligand) in regulating the protein levels of KRAS (Cheng et al., 2011; Wang et al., 2000). Taken together, these lines of evidence strongly support the theory that CXCR2 signaling might play identifiable roles in KRAS-induced autonomous cell growth by directly contributing to its intracellular signaling during PDAC development and progression.

The objective of the current study was to shed light on the previously unidentified autocrine effects of CXCR2 signaling in regulating *KRAS*$^{(G12D)}$-induced mitogenic cell growth.

Results

Expression of CXCR2 and cognate ligands in the ductal cells isolated from the lesions of Pdx1-cre;LSL-*Kras*$^{(G12D)}$ mice.

The PDAC-cell specific expression of mCXCR2 was confirmed by performing dual staining for cytokeratin and CXCR2. Co-localization of the two proteins confirmed the expression of CXCR2 in PDAC cells **(Fig. 4.1A)**. To establish an *in vitro* system for further experimentation, we used PDAC cells isolated from Pdx1-cre;LSL-*Kras*$^{(G12D)}$ mice (Torres et al., 2013b). We confirmed the expression of transcripts of *Cxcr2* and *Cxcl1, 2, 3, 5* and *7* in the KRAS-PDAC cells by PCR **(Fig. 4.1B)**. ELISA on culture supernatants of KRAS-PDAC cells detected mCXCL5, which was previously detected by IHC. Furthermore, two additional ligands mCXCL2 and 7 were also detected **(Fig. 4.1C)**. Expression of mCXCR2, mCXCL1 and 3 proteins was confirmed by immunofluoresence **(Fig. 4.1D)**. Collectively, these data demonstrate that ductal cells of Pdx1-cre;LSL-*Kras*$^{(G12D)}$ mice express mCXCR2 and its ligands.

KRAS$^{(G12D)}$ mutation-bearing human pancreatic cancer cells show higher expression of CXCR2 and its ligands.

We next assessed whether *KRAS*$^{(G12D)}$ alters the expression of CXCR2 and its ligands using immortalized human pancreatic ductal cells having exogenous expression of *KRAS*$^{(G12D)}$ [HPNE/-KRAS and E6-E7-st/-KRAS]. In culture supernatants of both HPNE/-KRAS and E6-E7-st/-KRAS cell line models we detected significantly higher expression of hCXCL1, 5 and 8 in the

KRAS$^{(G12D)}$-bearing cells compared with their control counterparts **(Fig. 4.2A and B)**. We next looked for the presence of hCXCR2 expression in both cell line models. The E6-E7-st-KRAS cells demonstrated upregulation of the *CXCR2* mRNA transcript in comparison to the control counterpart **(Fig. 4.2C)**. The presence of CXCR2 was further confirmed by immunofluorescence, where we observed enhanced expression on the *KRAS*$^{(G12D)}$-bearing cells compared with the control cells **(Fig. 4.2D)**. Further evaluation of hCXCR2 protein level by western blot confirmed these findings **(Fig. 4.2E and F)**. Together, these data demonstrate that the *KRAS*$^{(G12D)}$ mutation directly induces the expression of hCXCR2 and its ligands in the PDAC cells.

Blocking CXCR2 signaling inhibits *KRAS*$^{(G12D)}$ -induced *in vitro* cell growth and migration.

Thus far we established the presence of the CXCR2 receptor as well as its ligands in *KRAS*$^{(G12D)}$-bearing PDAC cell models. These data suggested the possible existence of a self-sufficient CXCR2 signaling loop on PDAC cells, which may act as a mediator of *KRAS*$^{(G12D)}$-induced autocrine growth transformation. Based on these observations the goal of the next set of our experiments was to investigate whether the inhibition of CXCR2 signaling modulates *KRAS*$^{(G12D)}$-induced autocrine cell growth. To investigate this, we generated stable CXCR2 knock-down clones of E6-E7-st-KRAS cells **(Fig. 4.3A)**. Knocking down CXCR2 significantly inhibited the *in vitro* cell viability (**Fig. 4.3B)** and anchorage-independent growth **(Fig. 4.3C)**. Furthermore, E6-E7-st-KRAS-

shCXCR2 cells demonstrated markedly reduced *in vitro* cell migration potential **(Fig. 4.3D)**.

Next, we used a pharmacological approach to inhibit CXCR2 signaling using SCH-527123, a potent CXCR2 and CXCR1 antagonist. It is known to bind to CXCR2 at a higher affinity (picomolar) than CXCR1 (nanomolar). It has demonstrated high efficacy in a variety of pulmonary inflammatory models and is currently in phase II of clinical trials (Chapman et al., 2009). We also used SCH-479833, which binds to both CXCR2 and CXCR1 but is CXCR2 selective (Singh et al., 2009). Since RAS is a crucial signaling pathway known to regulate the homeostatic proliferation of normal cells, it was important for us to evaluate if the CXCR2 antagonists provide a selective growth disadvantage to mutant KRAS-bearing tumor cells versus normal cells (Downward, 2003). To examine this, we treated our two cell models, HPNE/-KRAS and E6-E7-st/-KRAS, with the above mentioned CXCR2 antagonists and evaluated percent inhibition in viability at a time point of 72 hours. As demonstrated in **fig. 4.4 A and B**, at a lower dose of the CXCR2 antagonist there was a significant specific difference in the growth inhibition of the $KRAS^{(G12D)}$-bearing cells versus the control cells. Furthermore, this difference remained even at the highest dose.

Taken together, these results demonstrate I) the role of CXCR2 signaling in $KRAS^{(G12D)}$-induced autocrine cell growth and II) the specificity of CXCR2 antagonists in facilitating growth inhibition in $KRAS^{(G12D)}$-bearing cells versus the control counterparts.

CXCR2 knockdown in *KRAS$^{(G12D)}$* -bearing pancreatic cancer cells affects tumor growth in subcutaneous and orthotopic implants.

As a logical extension to our *in vitro* findings we evaluated the role of CXCR2 in *KRAS$^{(G12D)}$*- induced autocrine cell growth *in vivo*. For the first set of our experiments, we performed subcutaneous injections of 1 x 10^6 E6-E7-st-KRAS-NSC and E6-E7-st-KRAS-shCXCR2 cells in the flanks of nude mice and measured the tumors twice a week for 50 days **(Fig. 4.5A)**. We found that the E6-E7-st-KRAS-shCXCR2 cells demonstrated a non-significant reduction in the tumor growth compared to the E6-E7-st-KRAS-NSC cells **(Fig. 4.5B)**. Mice were sacrificed on day 50. We observed a decreased proliferation index and an enhanced apoptotic index, as observed by quantification of the IHC for Ki-67 and cleaved caspase3 (CC3), respectively, in the tumors from E6-E7-st-KRAS-shCXCR2 and E6-E7-st-KRAS-NSC cells **(Fig. 4.5C)**.

Subcutaneous implantation of PDAC cells can serve as advancement to the *in vitro* cell culture based studies. Yet it does not provide precise information as the organ microenvironment is absent and hence organ-specific responses cannot be evaluated. Therefore, we implanted 1 x 10^6 E6-E7-st-KRAS-NSC and E6-E7-st-KRAS-shCXCR2 cells in the pancreas of nude mice. The tumors from E6-E7-st-KRAS-shCXCR2 cells demonstrated inhibited proliferation and increased apoptotic index compared with the tumors from the E6-E7-st-KRAS-NSC cells (**Fig. 4.6)**.

Inhibiting CXCR2 signaling alters KRAS protein levels and inhibits the activation of the ERK pathway.

As we observed a direct contribution of CXCR2 signaling in KRAS-induced autocrine growth, we hypothesized that inhibition of the CXCR2 pathway may alter the levels of KRAS protein and activation of its downstream effectors. Our results demonstrate reduced protein levels of KRAS in E6-E7-st-KRAS-shCXCR2 versus E6-E7-st-KRAS-NSC cells as evaluated by western blotting. Furthermore, E6-E7-st-KRAS-shCXCR2 cells showed reduced activation of the downstream ERK pathway, due to decreased levels of p-ERK **(Fig. 4.7A)**. Treatment of E6-E7-st-KRAS$^{(G12D)}$ cells with increasing doses of SCH-527123 (for 24 hours) showed a similar trend for the expression of KRAS and p-ERK protein in a dose-dependent manner **(Fig. 4.7B)**.

Discussion

In the present section of the study, we aimed to investigate the role of CXCR2 signaling in mediating *KRAS*$^{(G12D)}$-induced autocrine growth transformation of PDAC cells. Our results lead us to two novel findings i) Upregulation of CXCR2 signaling by *KRAS*$^{(G12D)}$ enhances autonomous proliferation of tumor cell in PDAC; and ii) the *KRAS*$^{(G12D)}$-induced CXCR2-CXCL axis in tumor cells upregulates the expression of KRAS protein maintaining a feed-forward loop in PDAC cells.

Expression of CXCR2 and allied ligands was detected in the malignant ductal cells derived from Pdx1-cre;LSL-*Kras*$^{(G12D)}$ mice. In addition, we

experimentally validated the role of *KRAS*$^{(G12D)}$ in altering the expression of CXCR2, CXCL1, 5 and 8 in human pancreatic duct-derived cells. By expression of exogenous *KRAS*$^{(G12D)}$, we provide experimental evidence directly linking this mutation with CXCR2 signaling. A recent study by Matsuo et al. reported the role of *KRAS*$^{(G12D)}$ in upregulating the cumulative expression of CXCL1, 5 and 8 in the E6-E7-st- KRAS cell line model (Matsuo et al., 2009a). In another report, knocking-down *KRAS*$^{(G12D)}$ in a tumor derived cell line (SW1990) down-regulated the transcripts of CXCR2 ligands (O'Hayer et al., 2009). Our results are consistent with previous findings. We advance the current knowledge by providing the first evidence for the role of *KRAS*$^{(G12D)}$ in upregulating the expression of not just CXCLs but also CXCR2. We used the human pancreatic duct-derived hTERT-HPNE/-KRAS cell model having *KRAS*$^{(G12D)}$ as the only genetic alteration. As mutations in KRAS are known to occur in PanIN1 stage, this cell line represents the initial stages of the disease. Consequently, based on these results we conclude that CXCR2 signaling axis is directly linked with the *KRAS*$^{(G12D)}$ and thus may contribute to the PDAC development during the initial stages.

Cancer progression involves a complex interplay of various autocrine and paracrine signaling pathways, which lead to the stimulation of tumor cell growth. *RAS* mutations in cancer primarily permit the uncontrolled proliferation and survival of tumor cells. Additionally, oncogenic RAS also induces the secretion of various cytokines from tumor cells that promote the tumor cell growth by altering the TME (Bryant et al., 2014). Previous reports implicating *RAS* mutations in

inducing the expression of CXCLs have concluded that these upregulated ligands fail to provoke any autonomous growth-promoting effects on the cancer cells and mediate paracrine effects by interacting with the TME. Using the Hela cell line, Sparmann and Sagi demonstrated that *HRas*^{V12}-induced hCXCL8 can mediate tumorigenesis by enhancing angiogenesis (Sparmann and Bar-Sagi, 2004). In ovarian cancer, *HRAS*^{V12}-induced upregulation of hCXCL1 was found to promote tumor growth through the induction of senescence in the stromal fibroblasts (Yang et al., 2006). Furthermore, a report in lung cancer demonstrated that *KRAS*$^{(G12D)}$-induced CXCLs mediated tumorigenesis by recruiting inflammatory and endothelial cells (Wislez et al., 2006). More relevant to the current study, recent reports in PC have implicated *KRAS*$^{(G12D)}$-induced CXCLs as mediators of angiogenesis (Matsuo et al., 2009a) or fibrosis (Ijichi et al., 2011a) and noted a lack of autocrine growth-promoting effects on PC cells. Succinctly, the two fundamental reasons for the absence of CXCLs-mediated autocrine effects in all these studies were a) lack of the receptor CXCR2 on these cells and b) dysfunctionality of the receptor. We detected the expression of mCXCR2 in the KRAS-PDAC cells isolated from Pdx1-cre;LSL-*Kras*$^{(G12D)}$ mice and also the *KRAS*$^{(G12D)}$-bearing human pancreatic ductal cells. Therefore, we were prompted to evaluate the role of CXCR2 signaling in mediating *KRAS*$^{(G12D)}$-induced autocrine growth transformation in PDAC. Knocking-down CXCR2 in E6-E7-st-KRAS demonstrated a significant growth inhibition *in vitro* and *in vivo.* Tumors obtained from subcutaneous and orthotopic implants demonstrated

reduced cell proliferation and enhanced apoptosis in the shCXCR2 cells versus the tumors of control cells.

Cumulatively these results clearly indicated that *KRAS*$^{(G12D)}$-induced expression of CXCR2 and its ligands mediate autocrine growth transformation in PDAC. These results are opposite to the previous findings in PDAC. *KRAS*-induced expression of CXCLs on PC cells was reported to lack an autocrine growth-promoting effect on PC cells (Matsuo et al., 2009a). This inconsistency can be mainly explained by two facts. Firstly, they have used the HPDE cell line versus the HPNE cell line used in our study. Secondly, unlike the *KRAS*$^{(G12D)}$ in our report they have studied the effects of *K-Ras4B*^{G12V} on these cells. Importantly, it has been reported that not all mutant KRAS proteins effect the downstream signaling in a similar way, which may lead to different functional patterns (Garassino et al., 2011). In a recent study Ijichi et al. reported that CXCR2 inhibition in mPanIN cell lines isolated from Ptf1a$^{cre/+}$;LSL-*Kras*$^{(G12D)}$ mice demonstrated no inhibition in cell growth (Ijichi et al., 2011a). This contrariety can be explained by the fact that we have cell lines isolated from Pdx1-cre;LSL-*Kras*$^{(G12D)}$ mice, which employs a Pdx1 promoter for inducing the expression of *KRAS*$^{(G12D)}$ versus the Ptf1a promoter used by them. Therefore, taken together these findings describe a novel autocrine role of CXCR2 signaling in mediating *KRAS*$^{(G12D)}$-induced cell growth in PDAC.

Our results demonstrate that pharmacological inhibition of CXCR2 by two antagonists SCH-527123 and SCH-479833 (Chapman et al., 2009) engenders selective growth inhibition and toxicity on the *KRAS*$^{(G12D)}$-bearing cells versus the

normal RAS-bearing control cells. Studies in several cancer types have documented anti-tumor effects of CXCR2 antagonists. We previously reported anti-tumor and anti-metastatic effects of CXCR2 antagonists in melanoma (Singh et al., 2009) and colon cancer (Varney et al., 2011) respectively. Additionally, in a recent study by Ning et al., SCH-527123 was shown to demonstrate *in vitro* and *in vivo* anti-tumor effects either alone or in combination with Oxaliplatin in colon cancer (Ning et al., 2012b). Also, in a proof-of-principle study on ozone-challenged healthy human subjects, SCH-527123 was found to inhibit pulmonary neutrophilia. Importantly, with only a few mild adverse effects, the oral administration of SCH-527123 was well tolerated by human subjects (Holz et al., 2010). By reason of information provided above, we anticipate that further experimenting based on results in the current study may enable the development of clinically effectual treatments for KRAS-induced PDAC in future.

The RAS protein transmits signals received from the stimulation of receptors on the cell surface to the nucleus via activating various signaling pathways. One of the key downstream mediators of RAS activation is the ERK pathway. The ERK pathway has been implicated in RAS-mediated autocrine and paracrine cell growth (Thompson and Lyons, 2005). In furtherance of understanding the mechanism of CXCR2 inhibition-mediated reduction in the $KRAS^{(G12D)}$-induced growth potential of PDAC cells, we evaluated the activation of the ERK pathway and the total levels of KRAS. Our results demonstrated a marked reduction in the activation of ERK pathway, as evaluated by p-ERK

levels on inhibiting the CXCR2 signaling in the E6-E7-st-KRAS cells both genetically and pharmacologically.

These results are in agreement with various reports identifying CXCR2 signaling as a regulator of the activation of the ERK pathway (Li et al., 2008). Importantly, in a study performed to evaluate gastric cancer metastasis, Cheng et al., have demonstrated that the ectopic expression of CXCL1 in the cell line AAZ521 enhanced the expression of NRAS and KRAS in the total cell lysates (O'Hayer et al., 2009). Likewise, a study in melanoma revealed elevated levels of KRAS and NRAS leading to an overall increase in activated RAS levels in CXCL1-expressing clones of immortalized murine melanocytes. These reports are in agreement with our results of reduction in KRAS levels by inhibiting CXCR2, as it is the specific receptor for CXCL1 (Waugh and Wilson, 2008).

Overall, our work shows for the first time the novel role of CXCR2 signaling in mediating $KRAS^{(G12D)}$-induced autocrine growth transformation of tumor cells by directly modulating the levels of KRAS protein and its downstream signaling. Figure 4.8 provides a schematic representation and summary. These findings may have clinical application as CXCR2 antagonists are currently in clinical trials for the treatment of chronic obstructive pulmonary disease. To conclude, these results demonstrate that targeting CXCR2 signaling might be a feasible approach to inhibit $KRAS^{(G12D)}$-induced PDAC tumor cell growth.

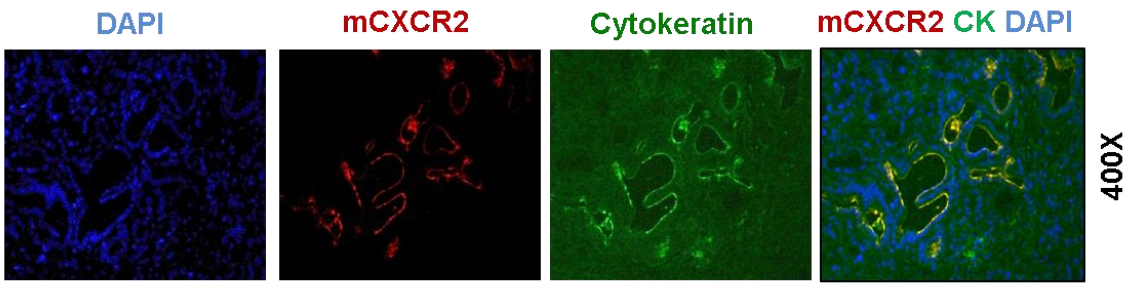

Pdx1-cre;LSL-Kras(G12D)

B.

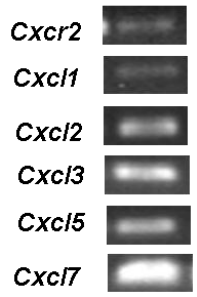

C.

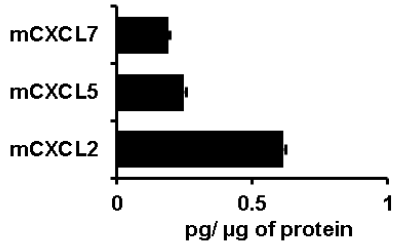

D.

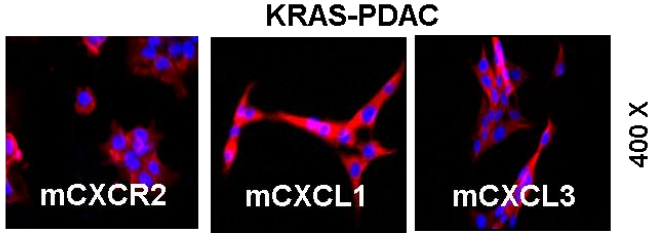

Figure 4.1. Expression of CXCR2 and its ligands in the ductal cells of cancerous lesions of the Pdx1-cre;LSL-*Kras*$^{(G12D)}$ mouse model.

A) Dual immunofluorescence staining demonstrating co-localization of mCXCR2 (Cy3) and cytokeratin (FITC) on the ductal cells. Nuclei are counterstained by DAPI. **B)** Expression of transcripts of *Cxcr2* and its ligands *Cxcl1, 2, 3, 5* and *7* in the KRAS-PDAC cells. **C)** Expression of mCXCL2, 5 and 7 in culture supernatants of KRAS-PDAC cells, as measured by ELISA. **D)** Immunofluorescence for mCXCR2, mCXCL1 and mCXCL3 on KRAS-PDAC cells. Error bars represent standard error of mean.

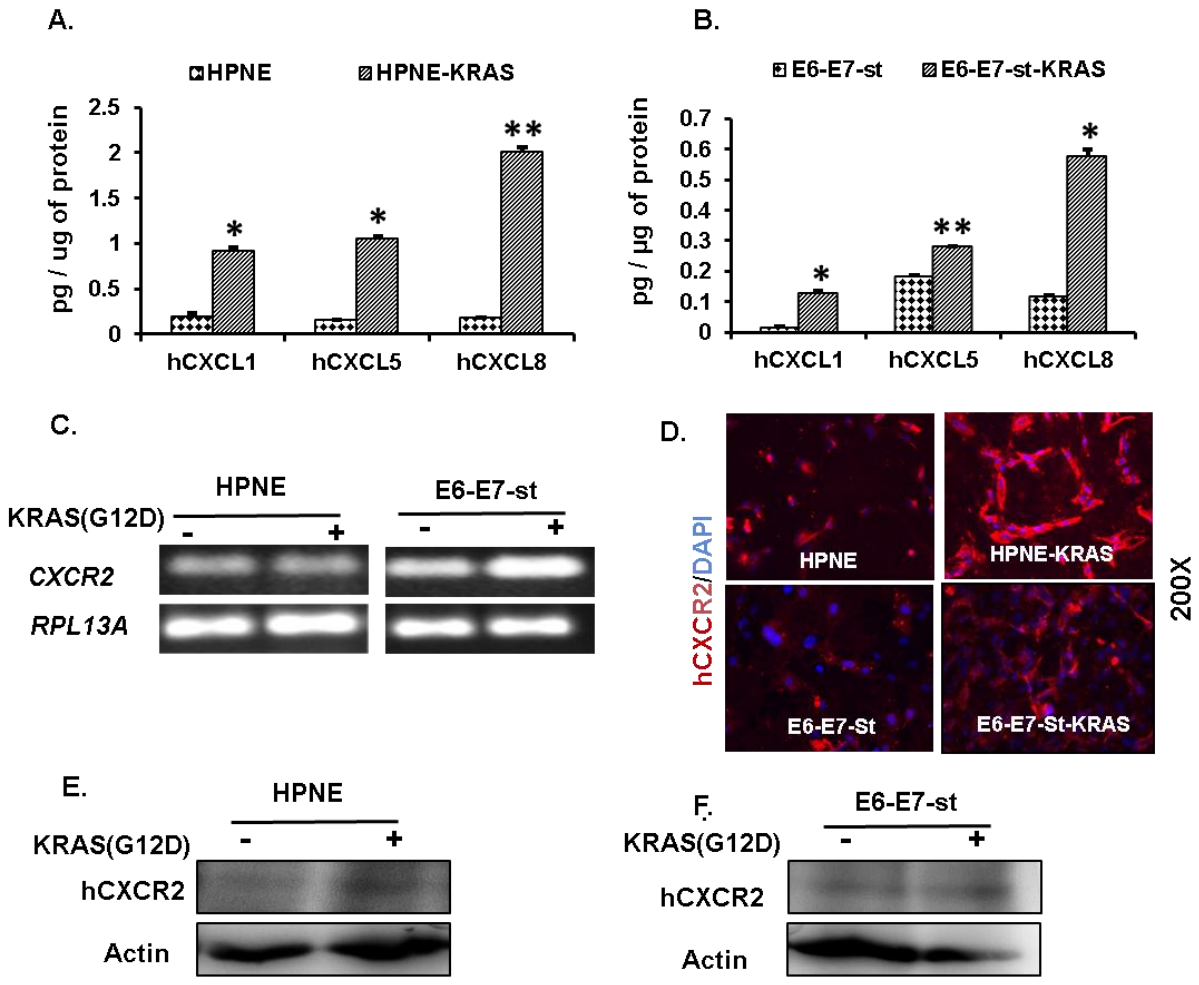
A.
HPNE
HPNE-KRAS
pg / ug of protein
2.5
2
1.5
1
0.5
0
hCXCL1
hCXCL5
hCXCL8
B.
E6-E7-st
E6-E7-st-KRAS
pg / µg of protein
0.7
0.6
0.5
0.4
0.3
0.2
0.1
0
hCXCL1
hCXCL5
hCXCL8
C.
HPNE
E6-E7-st
KRAS(G12D)
-
+
-
+
CXCR2
RPL13A
D.
hCXCR2/DAPI
HPNE
HPNE-KRAS
E6-E7-St
E6-E7-St-KRAS
200X
E.
HPNE
KRAS(G12D)
-
+
hCXCR2
Actin
F.
E6-E7-st
KRAS(G12D)
-
+
hCXCR2
Actin

Figure 4.2. The *KRAS*$^{(G12D)}$ mutation regulates the expression of CXCR2 and its ligands in human pancreatic cancer cells.

Expression levels of hCXCL1, 5 and 8 in culture supernatants of **A)** HPNE and HPNE-KRAS **B)** E6-E7-st and E6-E7-st-KRAS cells, as detected by ELISA. Values are normalized to total µg of protein. **C)** PCR to detect the transcript levels of *CXCR2* in HPNE, HPNE-KRAS and E6-E7-st, E6-E7-st-KRAS cells. **D)** Immunofluorescence for CXCR2 in HPNE, HPNE-KRAS and E6-E7-st, E6-E7-st-KRAS cells. Western blots to detect the protein levels of hCXCR2 in whole cell lysates of **E)** HPNE, HPNE-KRAS and **F)** E6-E7-st, E6-E7-st-KRAS. Error bars represent standard error of mean. Statistical significance determined by Student's t test (* $p \leq 0.05$, ** $p \leq 0.01$, *** $p \leq 0.001$, *NS* $p > 0.05$).

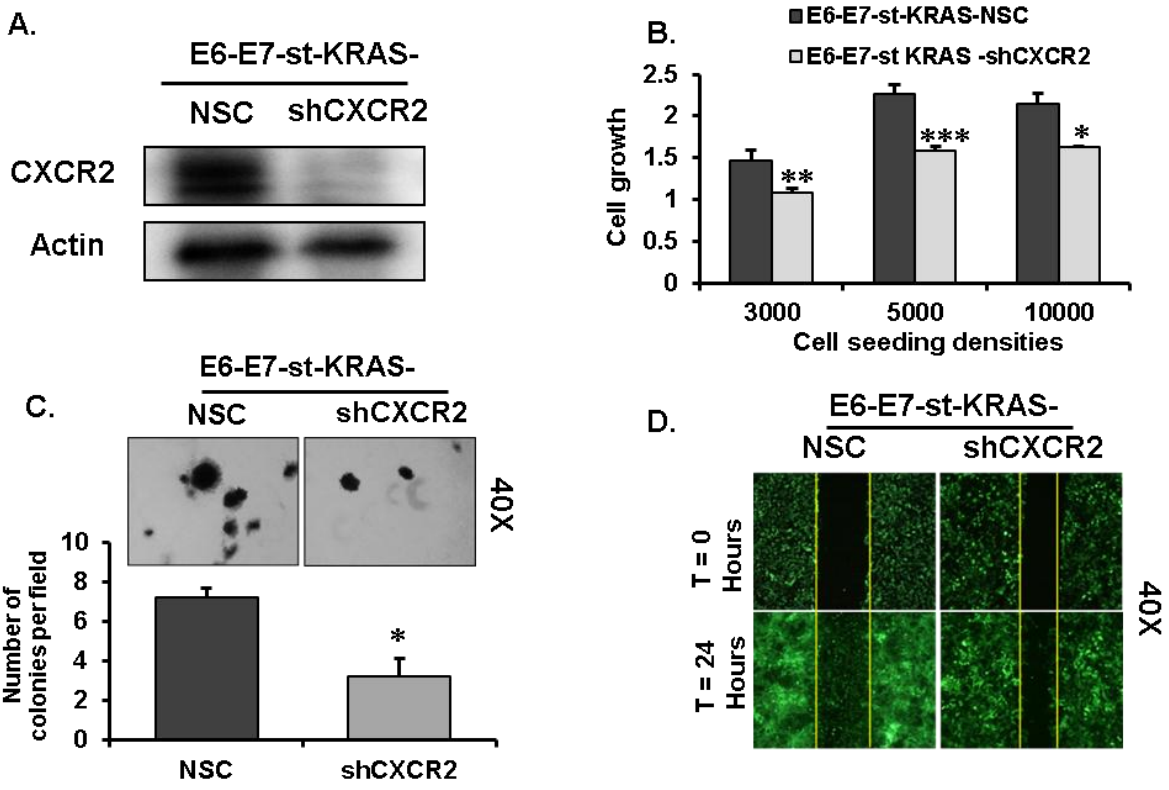
A.
E6-E7-st-KRAS-
NSC
shCXCR2
CXCR2
Actin
B.
E6-E7-st-KRAS-NSC
E6-E7-st KRAS -shCXCR2
Cell growth
2.5
2
1.5
1
0.5
0
**
***
*
3000
5000
10000
Cell seeding densities
C.
E6-E7-st-KRAS-
NSC
shCXCR2
40X
Number of colonies per field
10
8
6
4
2
0
*
NSC
shCXCR2
D.
E6-E7-st-KRAS-
NSC
shCXCR2
T = 0 Hours
T = 24 Hours
40X

Figure 4.3. CXCR2 signaling mediates *KRAS*$^{(G12D)}$-induced autocrine cell growth and migration.

A) Western blotting on total cell lysates of E6-E7-st KRAS-NSC/-shCXCR2 cells, demonstrating deletion of hCXCR2 at the protein level in the knock-down cells. **B)** Cell viability of E6-E7-st-KRAS-NSC/-shCXCR2 cells at different seeding densities at 72 hours evaluated by MTT assay **C)** Anchorage-independent growth potential of E6-E7-st-KRAS-NSC/-shCXCR2 cells was evaluated by soft agar colony formation assay. **D)** Wound healing assay to evaluate migratory potential of E6-E7-st-KRAS-NSC/-shCXCR2 cells. Error bars represent standard error of mean. Statistical significance determined by Student's t test (* $p \leq 0.05$, ** $p \leq 0.01$, *** $p \leq 0.001$, *NS* $p > 0.05$).

A.

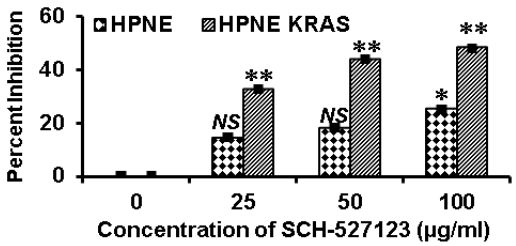
HPNE
HPNE KRAS
Percent Inhibition
60
40
20
0
NS
**
NS
**
*
**
0
25
50
100
Concentration of SCH-527123 (µg/ml)

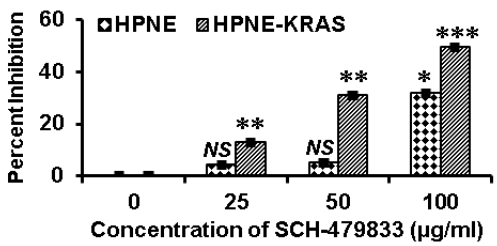
HPNE
HPNE-KRAS
Percent Inhibition
60
40
20
0
NS
**
NS
**
*
***
0
25
50
100
Concentration of SCH-479833 (µg/ml)

B.

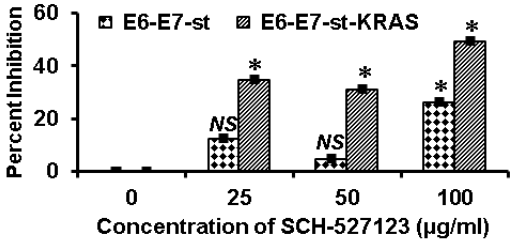
E6-E7-st
E6-E7-st-KRAS
Percent Inhibition
60
40
20
0
NS
*
NS
*
*
*
0
25
50
100
Concentration of SCH-527123 (µg/ml)

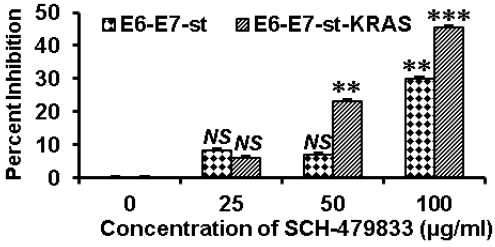
E6-E7-st
E6-E7-st-KRAS
Percent Inhibition
50
40
30
20
10
0
NS
NS
NS
**
**
***
0
25
50
100
Concentration of SCH-479833 (µg/ml)

Figure 4.4. Treatment with CXCR2 antagonist preferentially inhibits the growth of *KRAS*$^{(G12D)}$ mutant cells versus the control counter parts.

Percent inhibition in cell viability of **A)** HPNE, HPNE-KRAS and **B**) E6-E7-st, E6-E7-st-KRAS cells incubated with the indicated doses of SCH-527123 or SCH-479833 for 72 hours. Error bars represent standard error of mean. Significance of the data for each cell line was evaluated by comparing the treatment group with the no treatment control of the same cell line. Statistical significance determined by paired Student's t test (* $p \leq 0.05$, ** $p \leq 0.01$, *** $p \leq 0.001$, *NS* $p > 0.05$).

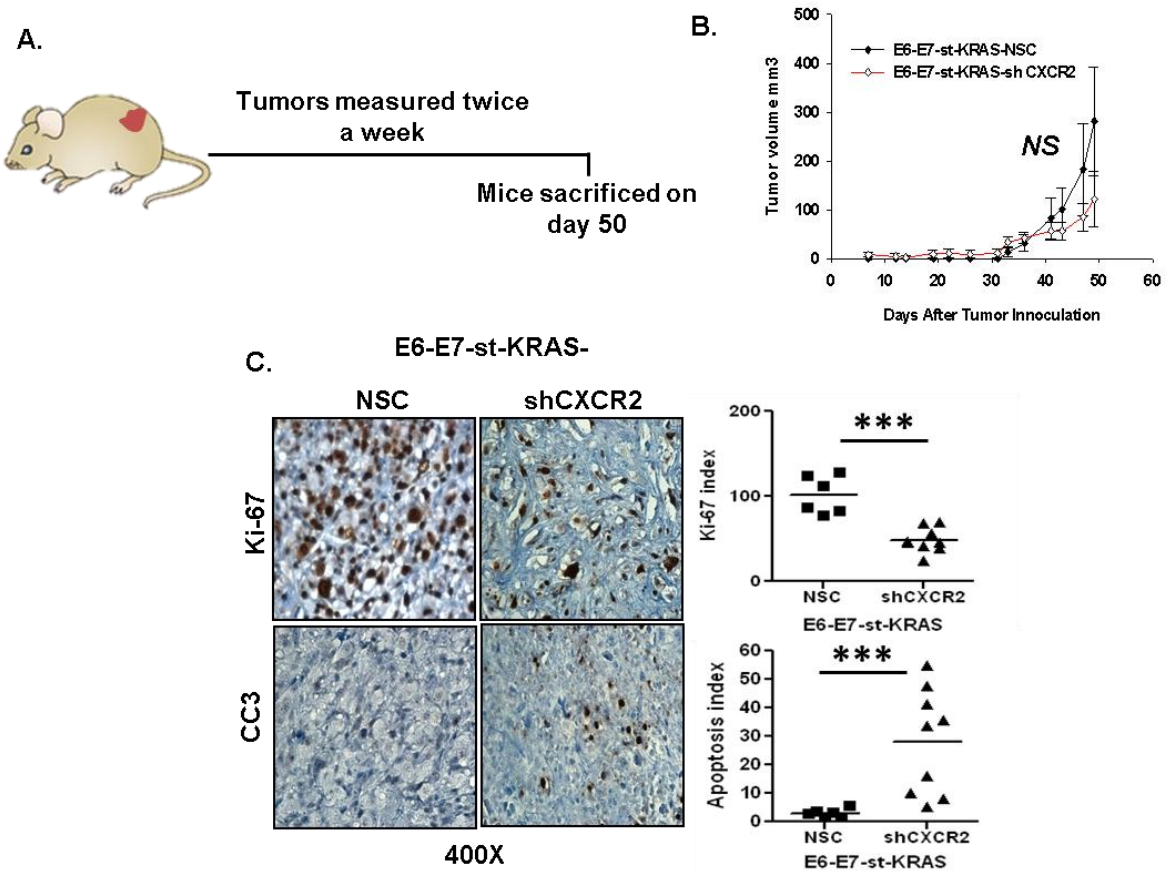
A.
Tumors measured twice a week
Mice sacrificed on day 50
B.
E6-E7-st-KRAS-NSC
E6-E7-st-KRAS-sh CXCR2
NS
Tumor volume mm3
Days After Tumor Innoculation
C.
E6-E7-st-KRAS-
NSC
shCXCR2
Ki-67
CC3
400X
Ki-67 index
***
NSC
shCXCR2
E6-E7-st-KRAS
Apoptosis index
***
NSC
shCXCR2
E6-E7-st-KRAS

Figure 4.5. Knock-down of CXCR2 results in inhibited growth of E6-E7-st-KRAS cells in the subcutaneous implants.

A) E6-E7-st-KRAS-NSC and E6-E7-st-KRAS-shCXCR2 cells were engrafted subcutaneously in the flanks of nude mice and tumors were measured twice weekly. **B)** Tumor growth represented by change in tumor volume of subcutaneous tumors at indicated time points after inoculation (*NS*). **C)** Representative immunohistochemical (IHC) staining for Ki-67 and cleaved caspase3 (CC3) in tumors of mice bearing E6-E7-st-KRAS-NSC or E6-E7-st-KRAS-shCXCR2 cells. IHC's were quantified as the average of positive cells in five independent fields per tumor at 400X. Error bars represent standard error of mean. Statistical significance determined by paired Student's t test (for tumor volume) and non-parametric Mann-Whitney *U* test. (* $p \leq 0.05$, ** $p \leq 0.01$, *** $p \leq 0.001$, *NS* $p > 0.05$).

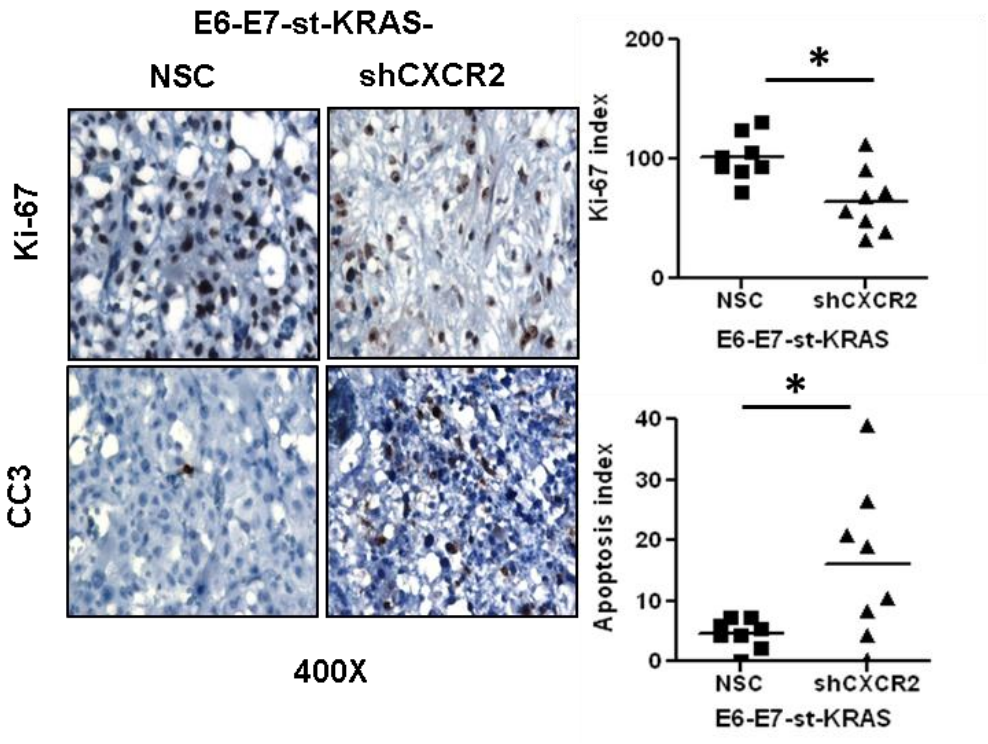
E6-E7-st-KRAS-
NSC
shCXCR2
Ki-67
CC3
400X
Ki-67 index
200
100
0
*
NSC
shCXCR2
E6-E7-st-KRAS
Apoptosis index
40
30
20
10
0
*
NSC
shCXCR2
E6-E7-st-KRAS

Figure 4.6. Orthotopic implants of CXCR2 knock-down cells demonstrate inhibited proliferation of tumor cells.

Representative immunohistochemistry (IHC) images and quantified stain score for Ki-67 and cleaved caspase 3 (CC3). IHC's were quantified as the average of positive cells in five independent fields per tumor at 400X. Statistical significance determined by paired Student's t test (* $p \leq 0.05$, ** $p \leq 0.01$, *** $p \leq 0.001$, *NS* $p > 0.05$).

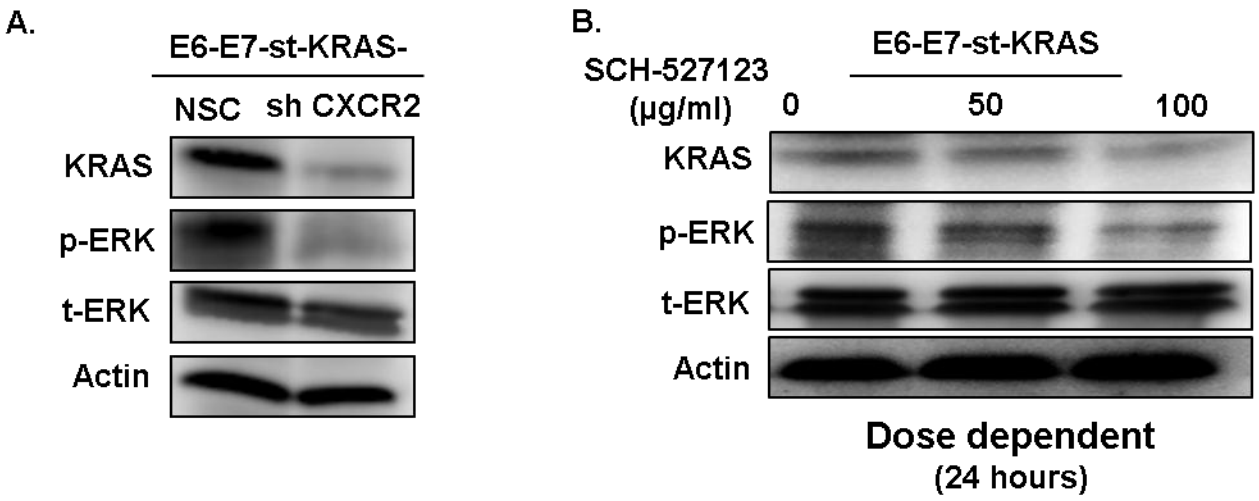
A.
E6-E7-st-KRAS-
NSC
sh CXCR2
KRAS
p-ERK
t-ERK
Actin
B.
SCH-527123
(μg/ml)
E6-E7-st-KRAS
0
50
100
KRAS
p-ERK
t-ERK
Actin
Dose dependent
(24 hours)

Figure 4.7. CXCR2 regulates levels of KRAS as a feed-forward loop. Western blots on whole cell lysates of **A)** E6-E7-st-KRAS-NSC and E6-E7-st-KRAS-shCXCR2 cells and **B)** E6-E7-st-KRAS cells treated with indicated doses of SCH-527123 for 24 hours demonstrating the protein levels of KRAS, p-ERK and T ERK. Actin serves as a loading control.

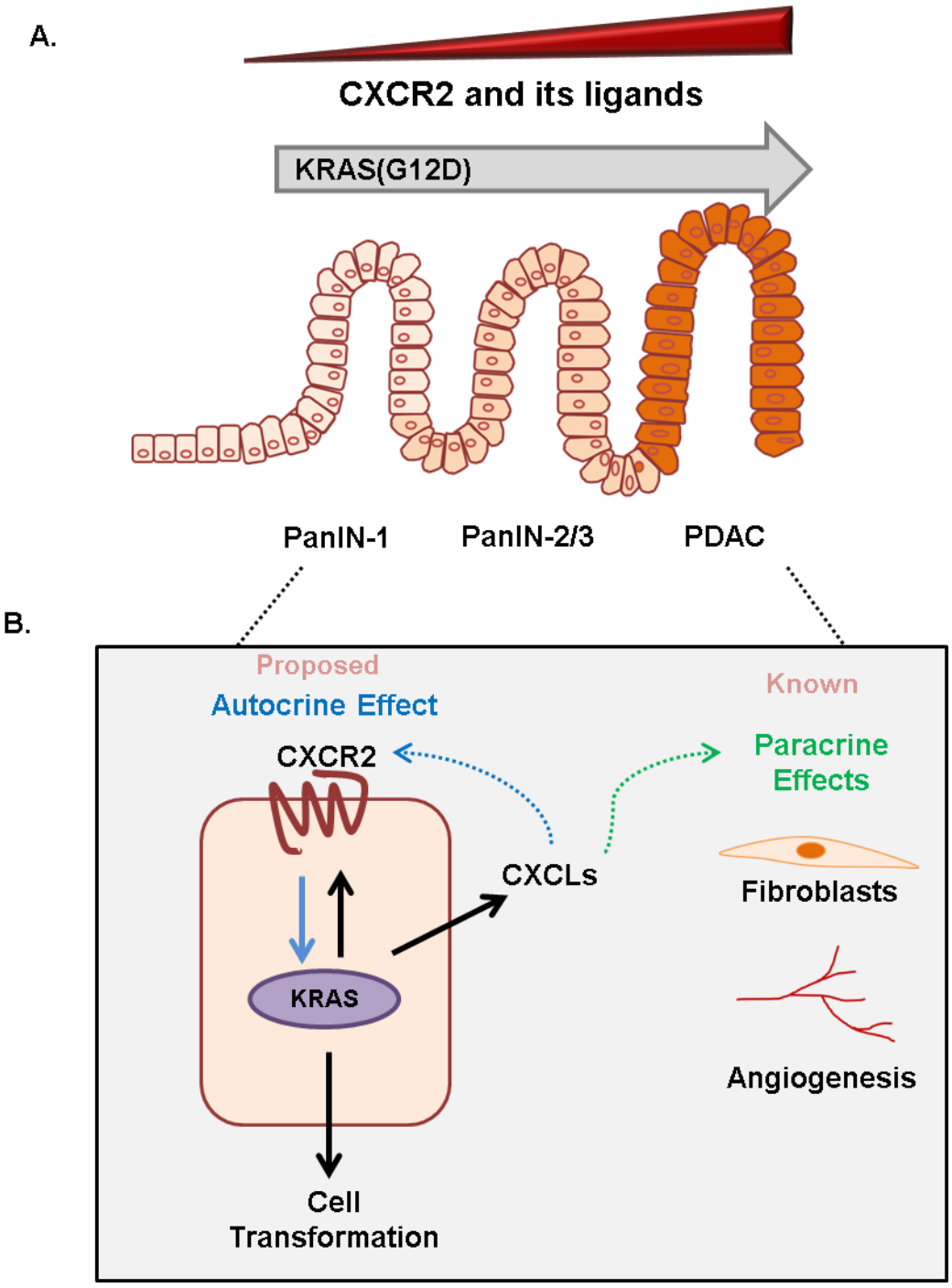
A.
CXCR2 and its ligands
KRAS(G12D)
PanIN-1
PanIN-2/3
PDAC
B.
Proposed
Autocrine Effect
CXCR2
KRAS
CXCLs
Cell
Transformation
Known
Paracrine
Effects
Fibroblasts
Angiogenesis

Figure 4.8. Role of CXCR2 signaling in *KRAS*$^{(G12D)}$-induced development of pancreatic cancer.

Based on data in the current study and previously published reports we can summarize the role of CXCR2 signaling in *KRAS*$^{(G12D)}$-induced initiation and progression of pancreatic cancer as follows: **A)** CXCR2 and its ligands are induced by the point mutation (G12D) in the KRAS gene. Their expression is detected early and further enhances as the precursor lesions advance to pancreatic ductal adenocarcinoma (PDAC). **B)** The enhanced KRAS activity inside the ductal cell induces the expression of both CXCR2 and CXCLs. Previous reports in pancreatic cancer identify how CXCR2 ligands indirectly alter the tumor progression by effecting endothelial cells and fibroblasts. In the current study we propose a novel cell-autonomous model where these upregulated CXCLs bind to CXCR2 receptors on the surface of the ductal cells. This CXCR2-CXCL autocrine loop in turn reinforces the expression of KRAS protein and enhances the growth of tumor cells.

Chapter 5

The role of host CXCR2 in regulating the growth of pancreatic cancer

Abstract:

Pancreatic cancer (PC) is a lethal disease with an aggressive tumor growth and early metastasis. Dense tumor microenvironment (TME) is a distinguishing feature of PC. The TME is composed of a heterogeneous population of cells including fibroblasts, immune and endothelial cells derived from the host. As CXCR2 is known to be expressed by a majority of these cell types, we examined the role of host CXCR2 in remodeling the TME during PC progression. Deletion of host *Cxcr2* (*Cxcr2*$^{-/-}$) did not affect the total tumor burden in the mice, but did enhance liver metastasis. Furthermore, we observed increased apoptosis in primary tumors; however, its overall impact on tumor burden was neutralized by increased fibrosis in these tumors. Interestingly, increased fibrosis in *Cxcr2*$^{-/-}$ mice was found to be a distinct characteristic of the pancreatic parenchyma, as this response was not observed in subcutaneous tumors. Tumors from *Cxcr2*$^{-/-}$ mice demonstrated reduced angiogenesis. Spleens from *Cxcr2*$^{-/-}$ mice had extramedullary hematopoiesis (EMH) with specifically increased expansion of polymorphonuclear (myeloid precursor) cells. These data suggested a systemic immune suppression in the *Cxcr2*$^{-/-}$ host. Taken together, these findings demonstrate that host *Cxcr2* signaling may contribute to PC progression by functioning both as a tumor promoter and suppressor. Therefore, careful discretion regarding the systemic targeting of CXCR2 in PC patients is suggested.

Introduction:

PC is the fourth leading cause of cancer-related death in both men and women in the USA (Siegel et al., 2015). One of the characteristic features of PC is the presence of a dense stromal reaction, referred to as desmoplasia, within the TME (Erkan et al., 2010). The contribution of TME in PC highlights the significance of the host responses during PC development. TME is chiefly composed of fibroblasts, extracellular matrix, endothelial cells and immune cells (Erkan et al., 2010). The overall development of PC is an outcome of the multiple reciprocal interactions among all these cellular entities. Therefore, in order to develop novel therapies for PC, it is essential to understand the role of any molecular marker in affecting not just the tumor cells but also the surrounding host milieu.

CXCR2 and its ligands have been implicated in the regulation of tumor growth, angiogenesis and metastasis in various cancers (Desurmont et al., 2015; Sharma et al., 2015; Zhou et al., 2012). Several studies have confirmed the presence of CXCR2 and its ligands in human PC tissues and cell lines (Li et al., 2011c; Matsuo et al., 2009c; Oliveira Frick et al., 2008; Wang et al., 2013b). Furthermore, expression of CXCR2 has been reported on PC fibroblasts (Ijichi et al., 2011b). CXCR2 signaling is also documented as a mediator of angiogenesis in PC (Ijichi et al., 2011a; Matsuo et al., 2009b; Matsuo et al., 2009c). Furthermore, CXCR2 is also known to orchestrate immune responses in various diseases including cancer (Acharyya et al., 2012; Chapman et al., 2009). Taken together, the literature summarized above provides evidence for the presence of

CXCR2 in the cellular entities of TME. Therefore, we hypothesized that CXCR2 signaling plays a critical role in mediating tumor-stromal interactions in PC.

Targeting CXCR2 can have a multitude of paradoxical outcomes on the biology of the host. For instance, binding of a ligand to CXCR2 expressed on different cell types in the host including the TME might result in either redundant or antagonizing effects inside the tumor. In such a scenario, effective targeting of CXCR2 for the better therapeutic outcome can be achieved by identifying the specific pathological role of CXCR2 in each cellular entity of the TME. This approach might further enable the specific targeting of these components resulting in reduced side effects. In this study, we evaluated host CXCR2-mediated effects during PC progression.

The primary objective of the current study was to identify how host *Cxcr2* signaling alters a) pancreatic parenchyma reprogramming and b) systemic responses in context of developing PC. To achieve this objective, we employed a syngeneic immunocompetent mouse model with a *Cxcr2* deletion in the host but intact CXCR2 expression on the tumor cells. This model enabled us to specifically study the role of CXCR2 inside the TME as well as its role in mediating systemic responses.

Results:

Deletion of host *Cxcr2* makes no impact on tumor burden but increases liver metastasis.

In this section of the study we sought to investigate the role of host *Cxcr2* in regulating PC tumor growth. To accomplish this objective we developed an immunocompetent orthotopically implanted murine model of PC. C57BL6 mice having WT or *Cxcr2* depleted genetic background were utilized for this study. We used two murine cell lines for the *in vivo* studies: I) KRAS-PDAC cells are derived from the ductal lesions of Pdx1-cre;LSL-*Kras*$^{(G12D)}$ mice. These cells express CXCR2 and its ligands at both mRNA and protein levels **(Chapter IV).** KRAS-PDAC cells were transduced to express a GFP-firefly luciferase vector **(Fig. 5.1A)**. II) Panc02: CXCR2 and its ligands were detected in these cells at the mRNA level **(Fig. 5.4A)**. Panc02 cells were transduced with GFP-GLUC expression vector **(Fig. 5.4B)**.

For our first experiment, KRAS-PDAC ($25x10^4$) were implanted orthotopically in the pancreas of WT or *Cxcr2*$^{-/-}$ C57BL6 mice. Mice were sacrificed after eight weeks **(Fig. 5.1B)**. We did not observe any change in the tumor weight of mice with different genotypes **(Fig. 5.1C)**. Also, there was no difference in the tumor incidence in mice with different genotypes **(Fig. 5.1D).** Figure 5.1E represents the histopathology of the tumors derived from mice with different genotypes.

We next examined the role of host *Cxcr2* in PC metastasis. KRAS-PDAC cells (25×10^4) were injected to the spleens of WT or *Cxcr2*$^{-/-}$ mice and liver metastasis was evaluated after four weeks **(Fig. 5.1F)**. Quantitation of macro metastases revealed that *Cxcr2*$^{-/-}$ mice developed greater (more and larger) metastatic lesions in comparison to WT mice **(Fig. 5.1G)**. To find a possible

explanation to this observation we evaluated the levels of CXCR2 ligands in the serum of tumor-bearing WT and *Cxcr2*$^{-/-}$ mice. Our results demonstrate that the levels of mCXCL2 were upregulated in the serum of *Cxcr2*$^{-/-}$ mice compared with the WT tumor-bearing mice **(Fig. 5.3).** Therefore, taken together we have observed no change in tumor burden but enhanced metastasis in the KRAS-PDAC PC models generated by us.

To extend our studies we used a second cell line. We implanted Panc02-GFP cells (1x10^6 cells) orthotopically and detected a higher GLUC activity in the blood of *Cxcr2*$^{-/-}$ mice compared with the WT tumor-bearing mice **(Fig. 5.4C)**. We believe that this secreted GLUC activity was representative of not just the primary tumor but also the metastatic burden in these mice.

Enhanced apoptosis in tumors of *Cxcr2*$^{-/-}$ mice.

We performed IHC for Ki-67 and CC3 on tumors derived from KRAS-PDAC-GFP-bearing WT and *Cxcr2*$^{-/-}$ mice. We quantified the staining to evaluate the proliferation and apoptosis index respectively. Our data demonstrated no change in the proliferation index in the WT versus *Cxcr2*$^{-/-}$ mice **(Fig. 5.2A)**. *Cxcr2*$^{-/-}$ mice tumors demonstrated an increased apoptosis compared with the WT group **(Fig. 5.2B).** We also determined the expression of apoptosis-related genes in these tumors by RT-PCR. Expression of *Bcl2* (anti-apoptotic) transcripts were higher in *Cxcr2*$^{-/-}$ mice tumors versus the WT mice tumors whereas the expression of *Bax* (pro-apoptotic) transcripts were higher in the *Cxcr2*$^{-/-}$ host tumors. No change was observed in the transcript levels of *Apo-2* in the two

groups **(Fig. 5.2C)**. We also observed similar results in the Panc02 PC model **(Fig. 5.4D and E).** Collectively, these data show that host CXCR2 signaling does not affect tumor cell proliferation but supports tumor growth by inhibiting tumor cell apoptosis.

Alteration of stromal responses in the tumor microenvironment of *Cxcr2*$^{-/-}$ hosts.

After identifying the overall impact of deleting host *Cxcr2* on tumor growth, we next wanted to gain an insight into the role of CXCR2 signaling in regulating the characteristic stromal responses in PC. Therefore, we evaluated angiogenesis and fibrosis in these tumors. Figure 5.5A shows the representative photomicrographs of Masson's trichrome staining on tumors. Quantitation of the blue stain in arbitrary units revealed that *Cxcr2*$^{-/-}$ hosts have higher fibrosis in the TME **(Fig. 5.5A)**. We evaluated the vessel density by performing IHC for CD31. Our data shows that *Cxcr2*$^{-/-}$ mice demonstrate significantly inhibited tumor angiogenesis **(Fig. 5.5B).**

Different effect of host *Cxcr2* deletion on the fibrotic response in orthotopic versus subcutaneous tumors.

The organ microenvironment itself can be an important determinant in regulating desmoplasia in PC. In order to evaluate whether CXCR2 signaling has any role in regulating the organ-specific response in PC, we implanted KRAS-PDAC ($25x10^4$) cells subcutaneously in WT or *Cxcr2*$^{-/-}$ C57BL6 mice. Interestingly, our data demonstrated that when PC cells were implanted

subcutaneously there was a reduction in tumor weight **(Fig. 5.6A)** and proliferation **(Fig. 5.6C)** in *Cxcr2*$^{-/-}$ hosts compared with WT. Furthermore, unlike the orthotopically implanted tumors, we observed no change in the fibrosis in the tumors derived from animals with different genotypes **(Fig. 5.6D)**. These results indicate that deletion of host *Cxcr2* exerts organ-specific variations in the fibroblasts of the TME.

Increased accumulation of immature myeloid precursors in the spleens of tumor-bearing *Cxcr2*$^{-/-}$ mice.

Gross anatomical evaluation of spleens derived from tumor-bearing mice demonstrated increased spleen size **(Fig. 5.7A)** and weight (splenomegaly) **(Fig. 5.7B)** in the *Cxcr2*$^{-/-}$ mice versus the WT mice. Histopathological evaluation of H&E stained spleens of tumor-bearing mice by a pathologist showed higher EMH in the spleens of *Cxcr2*$^{-/-}$ mice versus the WT genotype. Furthemore, WT and *Cxcr2*$^{-/-}$ mice showed differences in the ratios of the expanding populations. Inside the follicular zone in the spleens of WT tumor-bearing mice the ratio of myeloid to erythroid and lymphoid precursors was 1:3. However, in *Cxcr2*$^{-/-}$ tumor-bearing mice the follicular zones showed much higher expansion of immature myeloid precursor cells with a myeloid to erythroid and lymphoid precursors ratio of 3:1 (data not shown). Hema3 staining on splenocytes demonstrated an enhanced accumulation of polymorphonuclear cells in the spleens of *Cxcr2*$^{-/-}$ tumor-bearing mice compared with the WT tumor-bearing group. It is important to note that non-tumor-bearing *Cxcr2*$^{-/-}$ mice also have

increased populations of polymorphnuclear cells versus the WT mice. However, their accumulation is highest in the tumor-bearing *Cxcr2*$^{-/-}$ group **(Fig. 5.7C).**

Discussion:

The primary objective of this study was to identify the role of CXCR2 signaling in the PC TME. Our results demonstrate that deletion of host *Cxcr2* did not reduce the tumor burden despite enhancing apoptosis in orthotopic PC tumors. We believe that enhanced fibrosis in the tumors of *Cxcr2*$^{-/-}$ hosts limits the overall cell burden reduction thus reducing the impact caused by *Cxcr2* deletion. Importantly, enhanced fibrosis was not observed in tumors when inoculated subcutaneously, highlighting the specific role of CXCR2 signaling in the pancreatic parenchyma. Angiogenesis was significantly inhibited in tumors implanted in *Cxcr2*$^{-/-}$ mice. Furthermore, *Cxcr2*$^{-/-}$ mice had increased liver metastasis. These mice also demonstrated systemically enhanced expansion of myeloid progenitors in the spleens. Taken together, based on these results we conclude that deleting host *Cxcr2* causes both tumor-inhibiting and tumor-promoting effects.

Our first objective was to assess how the deletion of *Cxcr2* in the tumor-bearing host impacts the growth of tumor cells with intact CXCR2 signaling. Our results show that host *Cxcr2*$^{-/-}$ had no effect on the size of orthotopic tumors but enhanced metastatic dissemination of tumor cells. Further analysis revealed that abrogation of *Cxcr2* in the tumor parenchyma did not affect the proliferation of tumor cells but did enhance their apoptosis. These results suggest that host *Cxcr2* regulates the growth of tumor cells mainly by inhibiting apoptosis in them.

Recent research has shown that inhibiting *Cxcr2* in tumor-bearing host can either promote or inhibit the growth of PC tumors (Li et al., 2011b; Matsuo et al., 2009e). Treatment with a neutralizing anti-mouse CXCR2 antibody significantly reduced tumor volume, proliferation and angiogenesis in an orthotropic xenograft mouse model of PC (Matsuo et al., 2009e). Furthermore, in another report Li et al. showed that orthotopic inoculation of syngenic cells in mice with a *Cxcr2* deficient background led to reduced tumor volume (Li et al., 2011b). Contrary to these observations, a recent review by Hertzer et al. discussed unpublished data supporting our observations. They observed larger tumors in *Cxcr2*$^{-/+}$ mice versus the WT. Similarly, they also observed larger tumors in an orthotopic xenograft rodent model treated with the CXCR2 antagonist Reparixin (Hertzer et al., 2013). In the current study we observed no change in the overall size of the tumor but enhanced disease burden due to increased liver metastasis in *Cxcr2*$^{-/-}$ mice compared with WT.

To gain insight into the role of CXCR2 in regulating the characteristic stromal responses in PC we evaluated angiogenesis and fibrosis. Tumors from *Cxcr2*$^{-/-}$ mice had increased fibrosis and reduced angiogenesis. Interestingly, in the subcutaneously inoculated PC cells, *Cxcr2* deletion in the host did not affect the fibrosis. This observation strongly suggested a pancreatic parenchyma specific role of CXCR2 in regulating the fibrotic response in tumors. Expression of CXCR2 has been reported on PC fibroblasts (Ijichi et al., 2011b). In a recent report, Takamori et al. demonstrated that subcutaneous implants of a mixture of PC cells with fibroblasts showed faster tumor growth compared with only PC

cells. More importantly, CXCR2 knock-down in fibroblasts inhibited subcutaneous tumor growth while CXCR2 knock-down in the tumor cells caused no effect (Takamori et al., 2000). In the current study we demonstrate for the first time the impact of deleting CXCR2 in fibroblasts *in vivo*, inside the surrounding organ microenvironment. Furthermore, we also compared the effect of host *Cxcr2* deletion on tumors implanted orthotopically versus subcutaneously. This approach helped us to identify the role of CXCR2 in fibroblasts that is unique to the pancreatic parenchyma and how it alters the tissue programming in response to PC. Our results led us to the conclusion that CXCR2 is a negative regulator of fibrosis in pancreatic tumors.

The CXCR2 signaling axis has been well appreciated for its role in mediating angiogenesis in various cancers including PC. Moritz et al. reported the angiogenic activity of CXCR2 in PC by evaluating angiogenesis induced by culture supernatants of PC cell lines *in vivo* using the corneal micropocket assay (Wente et al., 2006). A recent study by Li et al. reported that tumor-bearing *Cxcr2*$^{-/-}$ mice demonstrated a reduction in the levels of bone marrow-derived endothelial progenitor cells (EPCs) in bone marrow and blood. Congruent with this observation, the authors show that CXCR2 knock-out reduced the proliferation and capillary tube formation of bone marrow derived cells *in vitro* (Li et al., 2011a). Our observation of reduced angiogenesis in *Cxcr2*$^{-/-}$ *mice* is in accordance with the aforementioned reports. However, the overall impact of reduced angiogenesis and enhanced fibrosis on tumor progression is hard to

predict as PC is known to be hypo vascular (Feig et al., 2012) and fibrosis is currently an area of contention in PC (Özdemir et al., 2014).

One of the key findings of this section of the study was enhanced EMH resulting in the accumulation of immature polymorphonuclear cells in the spleens of *Cxcr2*$^{-/-}$ tumor-bearing mice. Based on this observation we hypothesize that CXCR2 deficiency in host may lead to systemic immunosuppression. EMH has been identified in cancer patients. EMH is important for the increased demand of TALs in cancer (Cortez-Retamozo et al., 2012). A recent study demonstrated that splenectomy can delay the tumor growth in the KP model of lung cancer (Cortez-Retamozo et al., 2012). This study identified extramedullary stem and progenitor cells as targets of drug therapy (Cortez-Retamozo et al., 2012). EMH can result from the switching on of dormant hematopoietic precursor stem cells in the spleens or can be a secondary phenomenon following the filtration of hematopoietic precursor cells into the spleens (Conor O'keane et al., 1989). *Cxcr2*$^{-/-}$ mice have been shown to have expansion of myeloid progenitor cells in spleens, blood and bone marrow (Rollins, 1999). Therefore, we concluded that it is important to evaluate the dynamics of immune responses in spleens and inside the tumors of host *Cxcr2*$^{-/-}$ PC model generated by us.

Taken together, these data reveal novel roles of CXCR2 in mediating host responses during the development of PC. The model system employed by us illustrates the impact of the absence of CXCR2 signaling in the entire host compartment. This model helped us to identify the cumulative effect of *Cxcr2* depletion in host. Further experimentation in an advanced model systems can

help refine the information generated in this study. For instance, in future studies employment of mouse models with *Cxcr2* depletion in specific host cellular compartments can help identify the most suitable target cell(s) for inhibiting CXCR2 signaling in PC.

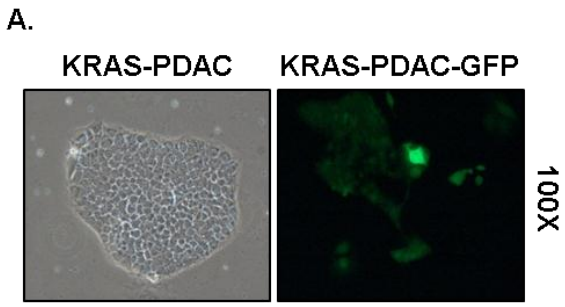

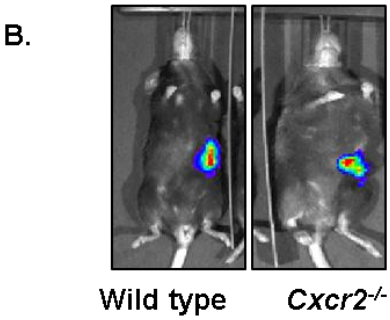

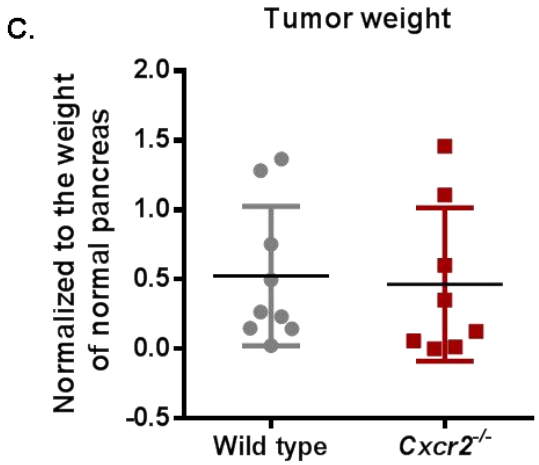

D.

Tumor Incidence	
Wild type	9/9
Cxcr2$^{-/-}$	7/8

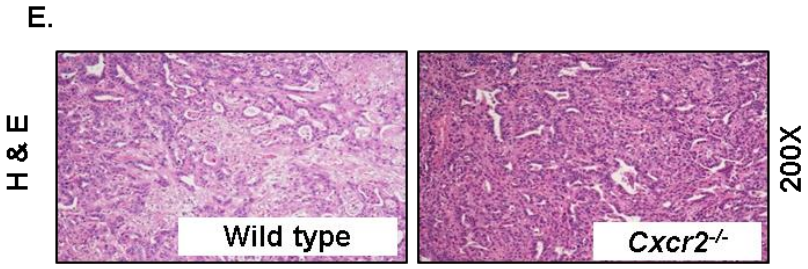

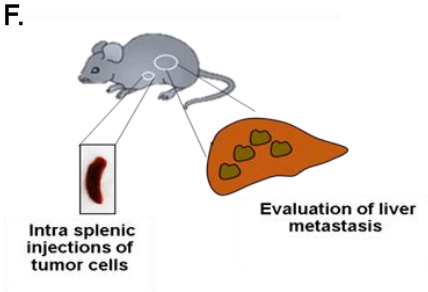

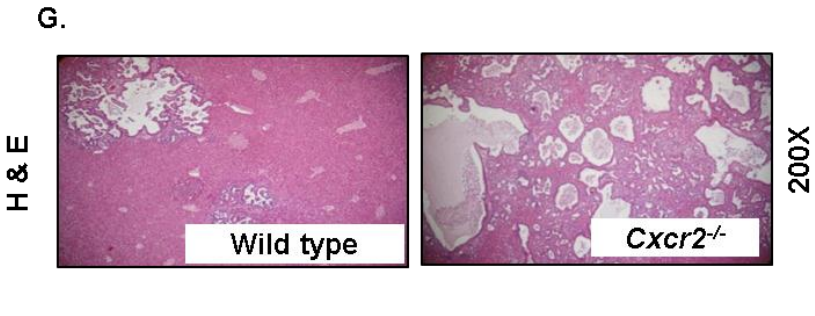

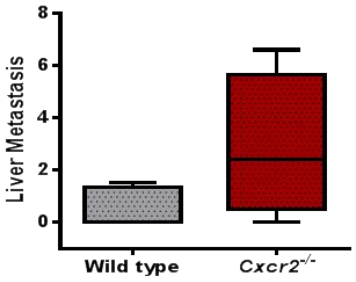

Figure 5.1. Deletion of host *Cxcr2* does not affect tumor growth but enhances liver metastasis.

A) Representative photographs showing expression of GFP in transduced KRAS-PDAC-GFP cells. **B)** Intravital luciferase images demonstrating the development of orthotopic tumors in wild type (n = 9) and *Cxcr2*$^{-/-}$ (n = 8) mice inoculated with KRAS-PDAC-GFP cells. **C)** Weight of tumors harvested from wild type and *Cxcr2*$^{-/-}$ mice. Each dot on the graph represents data point from an individual animal. **D)** Tumor incidence in wild type and *Cxcr2*$^{-/-}$ mice. **E)** Representative photographs of H&E staining showing the histopathology of tumors. **F)** A schematic depicting the procedure of the experimental metastasis assay. **G)** Representative images of H&E staining of livers demonstrating metastatic lesions in livers and corresponding graphs quantitating metastasis in wild type and *Cxcr2*$^{-/-}$ mice. Error bars represent standard deviation.

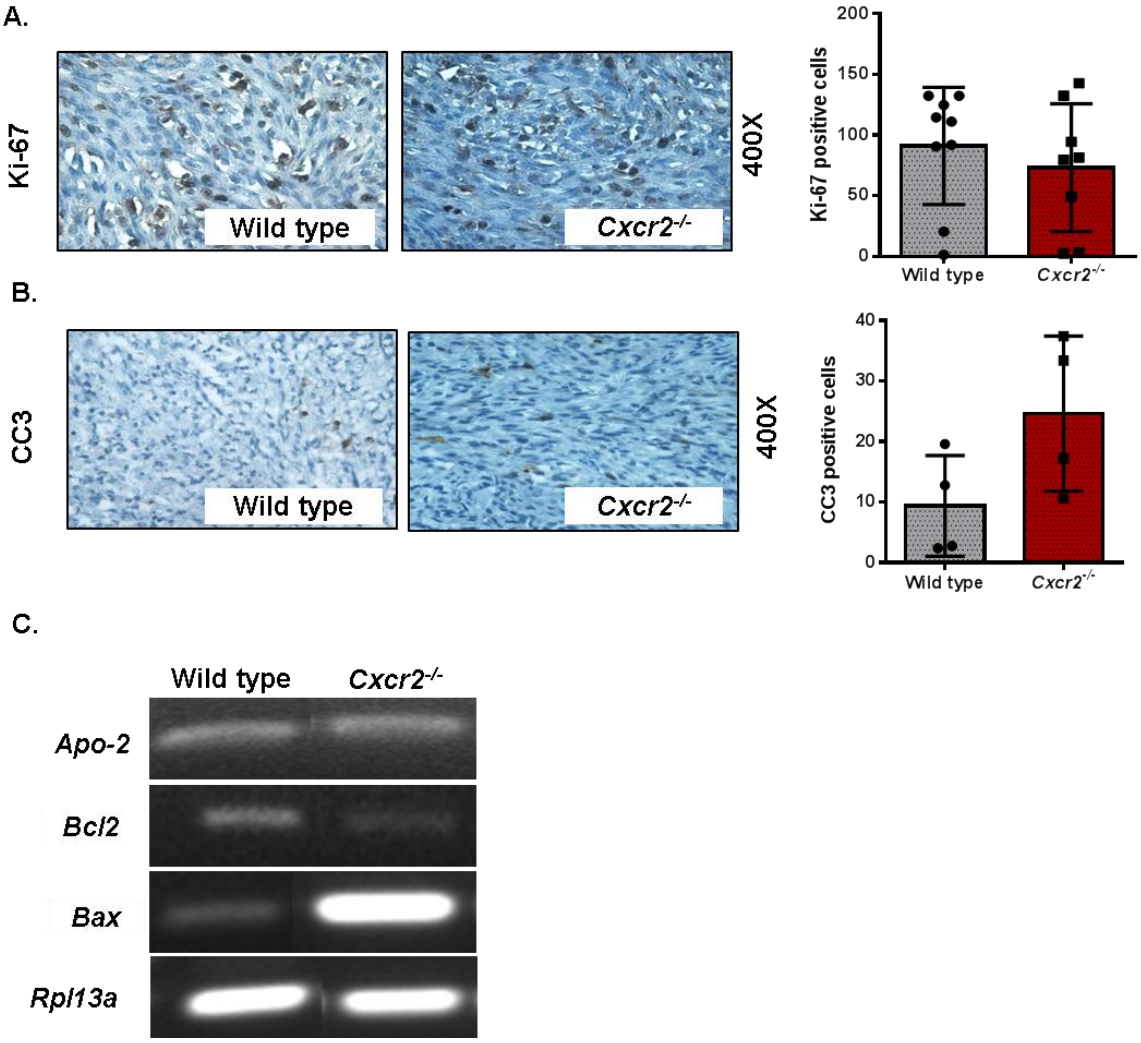
A.
Ki-67
Wild type
Cxcr2-/-
400X
Ki-67 positive cells
200
150
100
50
0
Wild type
Cxcr2-/-
B.
CC3
Wild type
Cxcr2-/-
400X
CC3 positive cells
40
30
20
10
0
Wild type
Cxcr2-/-
C.
Wild type
Cxcr2-/-
Apo-2
Bcl2
Bax
Rpl13a

Figure 5.2. Knock-out of host *Cxcr2* enhances apoptosis in tumors.

Representative photographs at 400X and graphs representing quantitation of **A)** Ki-67 and **B)** Cleaved caspase 3 (CC3) immunohistochemical staining. Each dot on the graph represents data point from an individual animal. Error bars represent standard deviation. **C)** PCR showing expression of *Apo2*, *Bcl2*, *Bax* and *Rpl13a* mRNA in tumors.

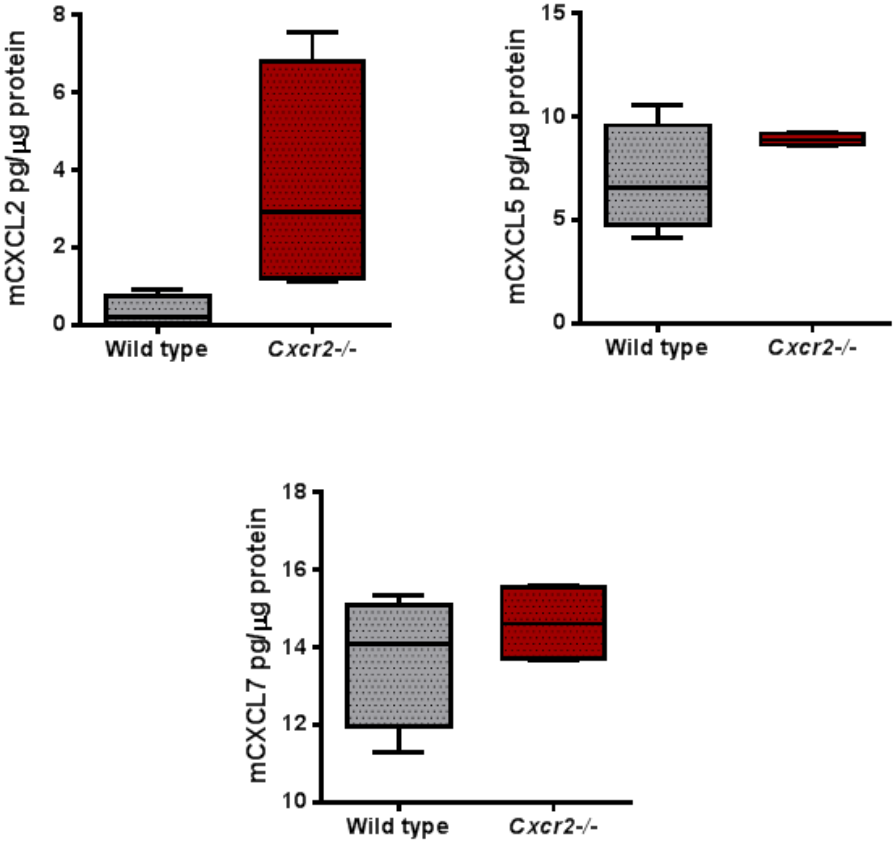
mCXCL2 pg/µg protein
8
6
4
2
0
Wild type
Cxcr2-/-
mCXCL5 pg/µg protein
15
10
5
0
Wild type
Cxcr2-/-
mCXCL7 pg/µg protein
18
16
14
12
10
Wild type
Cxcr2-/-

Figure 5.3. Deletion of host *Cxcr2* enhances serum levels of mCXCL2.

Expression levels of **A)** mCXCL2, **B)** mCXCL5 and **C)** mCXCL7 in serum of tumor-bearing wild type and *Cxcr2*$^{-/-}$ mice. Error bars represent standard deviation.

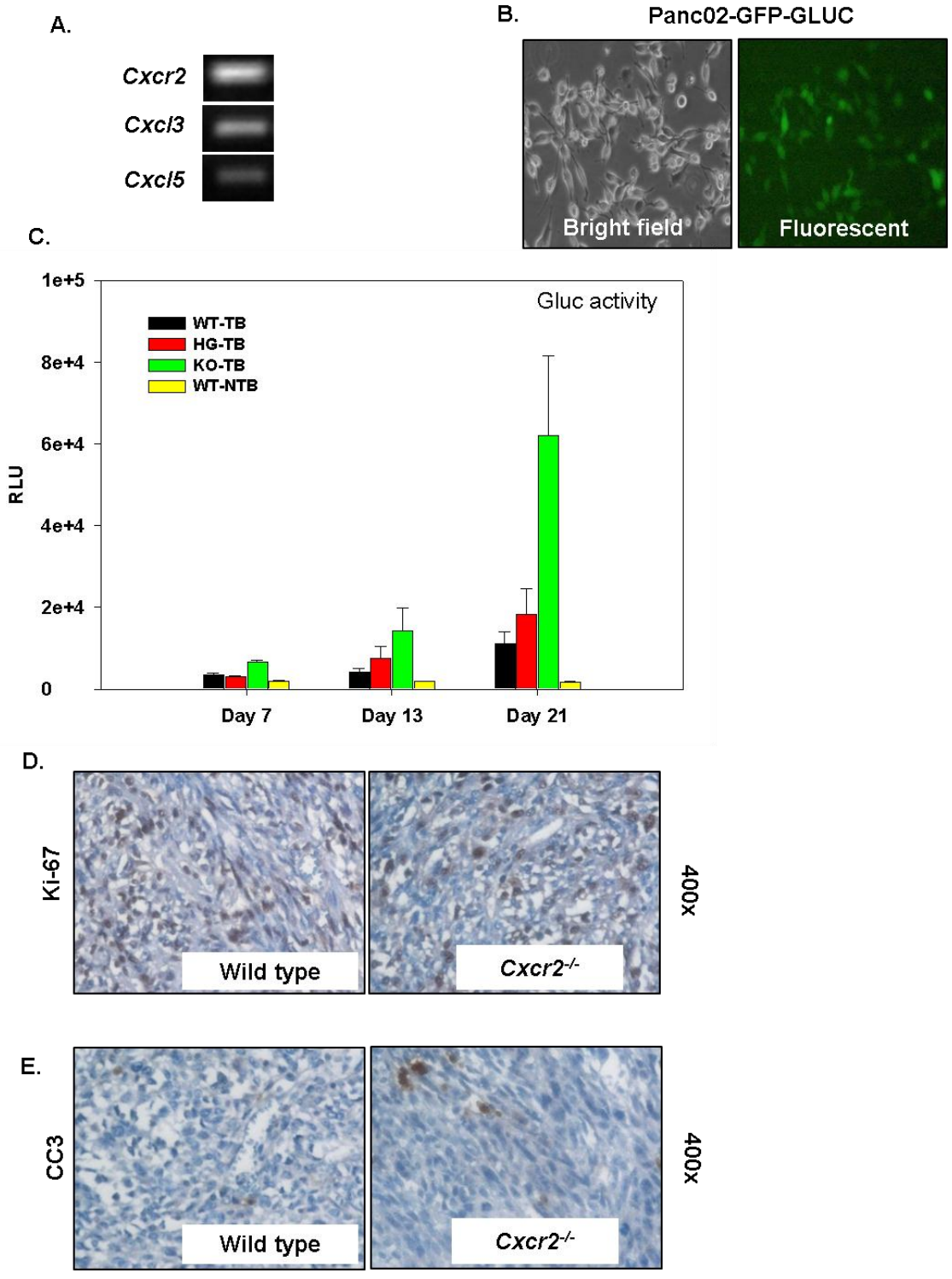
A.
Cxcr2
Cxcl3
Cxcl5
B.
Panc02-GFP-GLUC
Bright field
Fluorescent
C.
Gluc activity
WT-TB
HG-TB
KO-TB
WT-NTB
RLU
1e+5
8e+4
6e+4
4e+4
2e+4
0
Day 7
Day 13
Day 21
D.
Ki-67
Wild type
Cxcr2-/-
400x
E.
CC3
Wild type
Cxcr2-/-
400x

Figure 5.4. Growth of Panc02 tumors in *Cxcr2*$^{-/-}$ mice.

A) Detection of *Cxcl2*, *Cxcl3* and *Cxcl*5 in Panc02 cells by RT-PCR **B)** Representative images of Panc02 cells transduced with GLUC-GFP **C)** Higher GLUC activity in the blood of Panc02 tumors in *Cxcr2*$^{-/-}$ versus the wild type mice. Representative photographs of immunohistochemical staining and quantitative graphs of **D)** Ki-67 and **E)** Cleaved caspase 3 (CC3). Error bars represent standard error of mean.

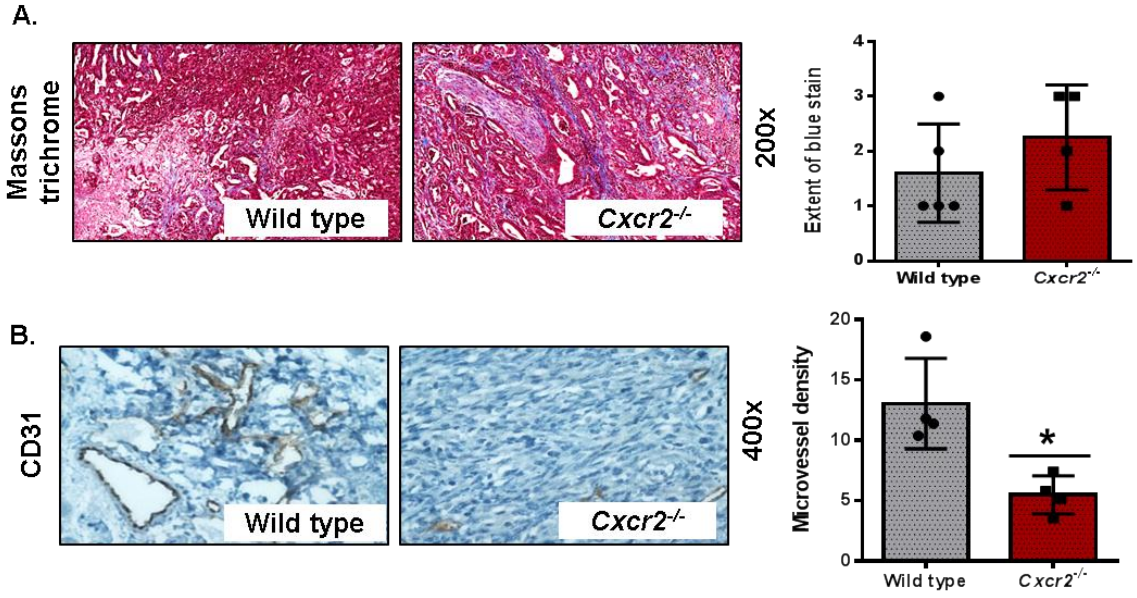
A.
Massons trichrome
Wild type
Cxcr2-/-
200x
Extent of blue stain
4
3
2
1
0
Wild type
Cxcr2-/-
B.
CD31
Wild type
Cxcr2-/-
400x
Microvessel density
20
15
10
5
0
*
Wild type
Cxcr2-/-

Figure 5.5. Increased fibrotic response and decreased angiogenesis in tumors of *Cxcr2*$^{-/-}$ mice.

A) Photomicrographs demonstrating Masson's trichrome staining for the assessment of fibrosis in wild type and *Cxcr2*$^{-/-}$ tumor-bearing mice and graph quantitating the extent of blue staining in arbitrary units **B)** Representative photographs of immunohistochemical staining for CD31 and quantitation for evaluating the microvessel density. Each dot on the graph represents data point from an individual animal. Error bars represent standard deviation. Statistical significance determined by paired Student's t test (* $p \leq 0.05$, ** $p \leq 0.01$, *** $p \leq 0.001$, *NS* $p > 0.05$).

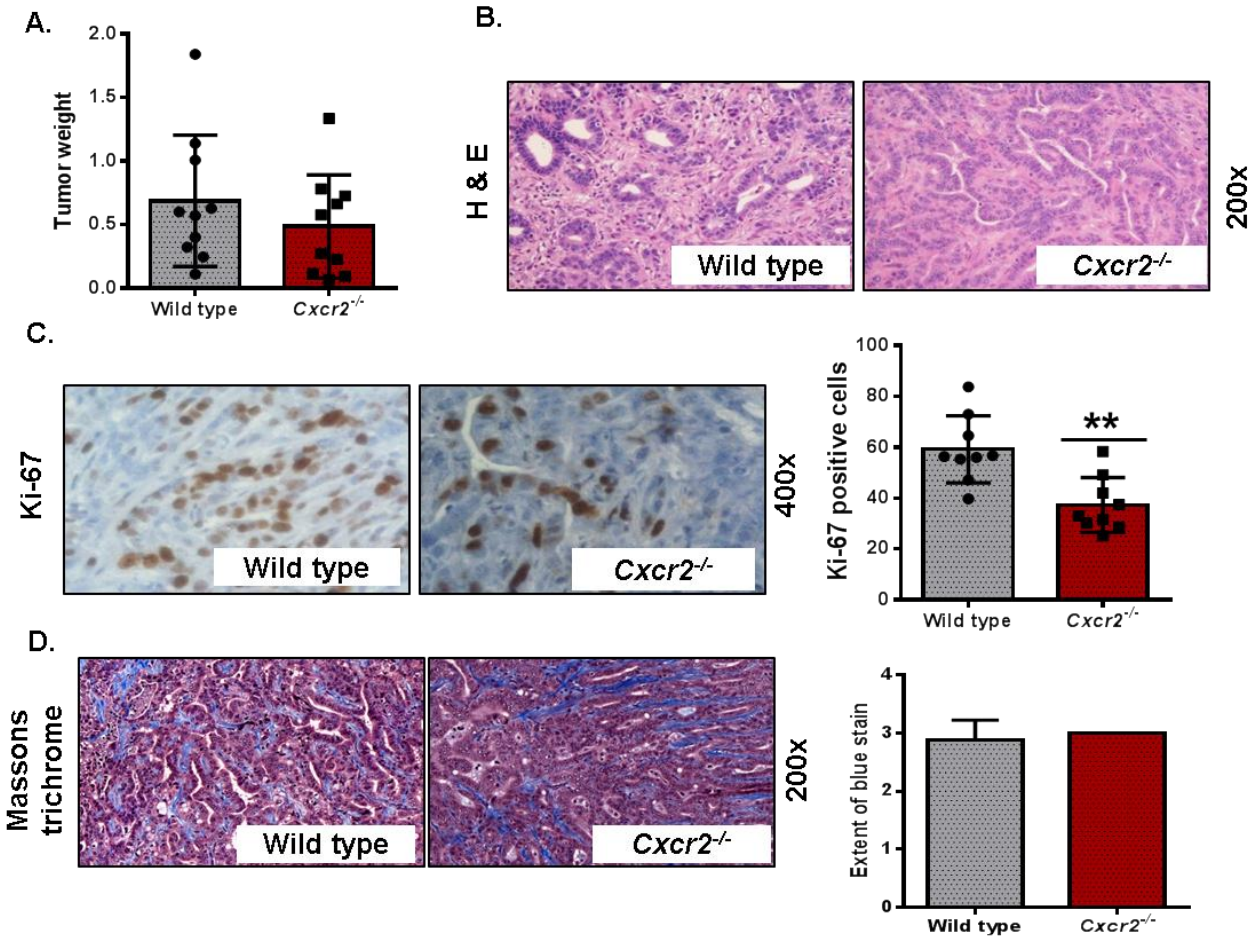
A.
Tumor weight
2.0
1.5
1.0
0.5
0.0
Wild type
Cxcr2-/-
B.
H & E
Wild type
Cxcr2-/-
200x
C.
Ki-67
Wild type
Cxcr2-/-
400x
Ki-67 positive cells
100
80
60
40
20
0
**
Wild type
Cxcr2-/-
D.
Massons trichrome
Wild type
Cxcr2-/-
200x
Extent of blue stain
4
3
2
1
0
Wild type
Cxcr2-/-

Figure 5.6. Host *Cxcr2* depletion inhibits the growth of pancreatic cancer cells at ectopic sites.

A) Weight of tumors (gms) developed by subcutaneous inoculation of KRAS-PDAC-GFP cells in wild type and *Cxcr2*$^{-/-}$ mice. **B)** H&E stained sections of subcutaneous tumors from wild type and *Cxcr2*$^{-/-}$ mice. **C)** Representative pictures of immunohistochemistry for Ki-67 (400X) and its quantitation. **D)** Photomicrographs of Masson's trichrome staining for assessment of fibrosis in wild type and *Cxcr2*$^{-/-}$ tumor-bearing mice. Each dot on the graph represents data point from an individual animal. Error bars represent standard deviation. Statistical significance determined by paired Student's t test (* $p \leq 0.05$, ** $p \leq 0.01$, *** $p \leq 0.001$, *NS* $p > 0.05$).

.

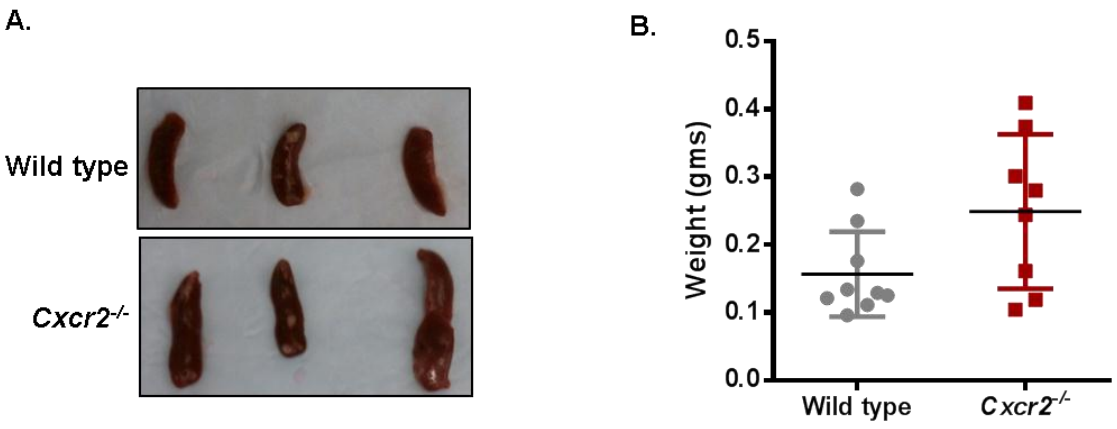
A.
Wild type
Cxcr2-/-
B.
Weight (gms)
0.5
0.4
0.3
0.2
0.1
0.0
Wild type
Cxcr2-/-
C.
Non-tumor-bearing
Tumor-bearing
Wild type
Cxcr2-/-
400x

Figure 5.7. Splenomegaly in *Cxcr2*$^{-/-}$ tumor-bearing mice.

A) Representative images of spleens resected from tumor-bearing wild type and *Cxcr2*$^{-/-}$ mice. **B)** Increased spleen weight in the tumor-bearing *Cxcr2*$^{-/-}$ mice versus the wild type group. Each dot on the graph represents data point from an individual animal. **C)** Representative pictures of Hema3 staining of cytospins prepared from the splenocytes of wild type and *Cxcr2*$^{-/-}$ non-tumor-bearing and tumor-bearing mice.

Chapter 6

CXCR2 biological axis in regulating host immune responses to pancreatic cancer

Abstract:

The presence of immunosuppressive cells inside the tumors as well as systemically in pancreatic cancer (PC)-bearing host is well documented. However, mechanisms regulating these immune responses remain unclear. In the previous chapter, we demonstrated that *Cxcr2* deletion in host leads to extramedullary hematopoiesis (EMH) and specific expansion of myeloid precursor cells in the spleens. Our objective for this section of the study was to elaborate the role of CXCR2 in regulating the dynamics of immune responses both locally (inside tumors) and systemically in PC. A higher intensity of CXCR2 was observed on MDSCs and dendritic cells located in the tumors versus the spleens. Deletion of host *Cxcr2* resulted in an enhanced accumulation of MDSCs in the spleens but inhibited their recruitment to the tumors. This altered dynamics of MDSCs was paralleled by increased frequency of cytotoxic T cells inside the tumors. Spleens in *Cxcr2*$^{-/-}$ mice demonstrated reduced cytotoxic T cells to MDSC ratio, suggesting a systemic immune suppression in *Cxcr2*$^{-/-}$ hosts. We also observed an increased accumulation of the antigen-presenting dendritic cell populations inside the tumors. Also, the changes in the levels of cytokines were evaluated in the immune cell populations inside the tumors of *Cxcr2*$^{-/-}$ hosts. Overall, this study for the first time defines the role of CXCR2 in altering the landscape of immune responses in PC.

Introduction:

The immune system in PC patients is severely impaired (Clark et al., 2007b). PC tumors are known to contain infiltrates of immune cells that help to suppress the anti-tumor responses (Clark et al., 2007c; Evans and Costello, 2012; Wörmann et al., 2014). Such immune infiltrates are composed of both myeloid- and lymphoid- lineages that include MDSCs, macrophages and Tregs (Wörmann et al., 2014). Apart from the local immune suppression at the tumor sites, immune responses in PC are also known to be ineffective systemically (von Bernstorff et al., 2001). In cancer patients, spleens are known to serve as reservoirs for tumor-associated immune cells and EMH (Cortez-Retamozo et al., 2012). By continuous proliferation of splenic hematopoietic stem cells, the constant demand of TALs is met (Cortez-Retamozo et al., 2012). Tumor-released factors in cancer stimulate myelopoiesis but block the differentiation of immature myeloid cells (IMCs) to mature myeloid cells like macrophages, dendritic cells and granulocytes. This IMC population is further activated by another group of factors resulting in the generation of immunosuppressive cells collectively known as MDSCs. MDSCs are known to have increased levels of ROS, arginase, and/or NO (Gabrilovich and Nagaraj, 2009). A spontaneous murine model of PC was shown to have a significant accumulation of MDSCs in their spleens at PanINs and PDAC stages (Clark et al., 2007c). Therefore, the authors suggested that MDSCs in PC are expanded systemically and recruited to the sites of tumors. It is important to note that MDSCs have the ability to cause immune suppression both locally and systemically (Nagaraj and Gabrilovich, 2008).

These findings implicate MDSCs as one of the key cells involved in systemic immune suppression in PC.

In order to develop effective immunotherapies for PC, it is important to shed light on mechanisms that are involved in regulating the production of immune cells as well as their relocation to the tumors. In PC mechanisms controlling these alterations are not yet elaborated. CXCR2 can be an important target for immunotherapy in light of the numerous scientific reports identifying CXCR2 as a key regulator of immune responses in several diseases (Chapman et al., 2009) including cancer (Highfill et al., 2014; Katoh et al., 2013).

In the previous chapter, we demonstrated that deletion of CXCR2 in the host resulted in no effect on the size of the primary tumor but enhanced the metastatic burden in these mice. We also observed altered hematopoietic responses in the *Cxcr2*$^{-/-}$ host at the spleens. Therefore, in this section of the study our objective was to evaluate how CXCR2 regulated immune responses contribute to the tumor-associated phenotypes in PC.

Results:

CXCR2-positive myeloid cell populations are present in the pancreas and spleens of tumor-bearing mice.

CXCR2 is known to be expressed by myeloid cell populations including macrophages, MDSCs, mast cells and dendritic cells. We identified the presence of CXCR2^{+} MDSCs, macrophages and dendritic cells in the syngeneic orthotopic PC murine model generated by us. To evaluate the significance of CXCR2 in the

recruitment of myeloid cell populations the tumors, we firstly we examined the intensity of CXCR2 expression on immune (myeloid-lineage) cells located in the tumors versus similar cells in spleens. Our results demonstrates that the intensity of CXCR2 expression is higher in MDSCs ($CD11b^{+}Ly6C^{+}G^{+}$), macrophages ($CD11b^{+}F480^{+}$) and dendritic cells ($CD11b^{+}$) located in tumors versus the spleens **(Fig. 6.2A and B)**. These data suggest that CXCR2 signaling is likely to mediate the infiltration of these immune populations from spleens to the tumor site.

Depletion of host *Cxcr2* inhibits the infiltration of MDSCs to the tumors but causes their splenic expansion.

We next assessed the frequencies of myeloid cell populations in the tumors and spleens of tumor-bearing WT and *Cxcr2*$^{-/-}$ host mice. We firstly evaluated the frequency of MDSCs, macrophages and dendritic cells in tumors of WT versus *Cxcr2*$^{-/-}$ hosts. As illustrated in **(Fig. 6.3A and 6.4A)**, we observed that *Cxcr2*$^{-/-}$ in the hosts decreased the frequency of MDSCs inside the tumors. We found no change in the infiltration of macrophages **(Fig. 6.3B and 6.4B)**. However, the frequency of dendritic cells was increased in tumors of *Cxcr2*$^{-/-}$ hosts **(Fig. 6.3C)**. These results suggest that while CXCR2 mediates the recruitment of MDSCs to the tumors, it does not seem to be the central player in the recruitment of macrophage population. Furthermore, *Cxcr2*$^{-/-}$ may also cause the sequestration of antigen-presenting dendritic cells in the tumors.

In the previous chapter, we showed that the *Cxcr2*$^{-/-}$ mice have larger spleens versus WT tumor-bearing mice. Spleens are known to be sites of EMH and serve as reservoirs for supplying TALs in cancer. Therefore, we evaluated the alterations in the frequencies of myeloid cell populations inside the spleens of *Cxcr2*$^{-/-}$ tumor-bearing hosts. Our data demonstrated that *Cxcr2* deletion increased the frequency of MDSCs inside the spleens **(Fig. 6.3D and 6.4C and D)**; however, we observed no change in the frequencies of macrophages **(Fig. 6.3E)** and dendritic cells **(Fig. 6.3F)** in the spleens.

Host *Cxcr2* depletion increases the cytotoxic T cell frequency inside the tumors but decreases the same inside the spleens.

We evaluated the effect of deleting host *Cxcr2* on the populations of T cell subsets in the TME. We observed that the tumors in *Cxcr2*$^{-/-}$ mice demonstrated increased populations of T helper (Th) cells (CD3+CD4+CD25-) and cytotoxic T cells (CD3+CD4-CD8+) cells versus the WT group **(Fig. 6.5A).** We also evaluated the effect of *Cxcr2* deletion on the population of Treg cells (CD3+CD4-CD25+). *Cxcr2*$^{-/-}$ mice demonstrated inhibition in the recruitment of immunosuppressive Treg population **(Fig. 6.5A)**. In spleens we observed no change in the frequency of Th cells (CD3+CD4+CD25-) **(Fig. 6.5B)**. The frequencies of cytotoxic T cells (CD3+CD4-CD8+) were lower in the spleens of *Cxcr2*$^{-/-}$ tumor-bearing mice **(Fig. 6.5B)**. No alteration in the population of Treg cells (CD3+CD4-CD25+) was observed inside the spleens **(Fig. 6.5B).**

To further elaborate our data we calculated the ratio of cytotoxic T cells to MDSCs in tumors as well as the spleens. We found that the ratio of cytotoxic T cells to MDSCs increased in the tumors of *Cxcr2*$^{-/-}$ mice suggesting that these tumors demonstrate enhanced anti-tumor immunity **(Fig. 6.6A)**. However, this ratio was reduced in the spleens of *Cxcr2*$^{-/-}$ tumor-bearing hosts **(Fig. 6.6B)**.These results support our hypothesis of systemic inhibition in the *Cxcr2*$^{-/-}$ hosts.

Host *Cxcr2* depletion alters the levels of cytokines in tumor-associated lymphocytes and the spleens.

As a next step, we evaluated the alterations in the gene expression of cytokines in the TALs isolated from WT and *Cxcr2*$^{-/-}$ tumors. The TALs isolated from *Cxcr2*$^{-/-}$ mice demonstrated enhanced expression of *Ccl2, 5* and *3* **(Fig. 6.7A)**. Furthermore, the expression of *TNF-α*, cytotoxic T cell effector cytokine *IFNγ* and its inducer *IL-12* was increased in the *Cxcr2*$^{-/-}$ TALs population **(Fig. 6.7B)**.

Discussion:

In the current section, we aimed to establish the role of CXCR2 biological axis in regulating the host immune responses to PC. We examined the effect of *Cxcr2* ablation in the host on intratumoral and systemic immune responses during PC progression. Based on our results we conclude that CXCR2 differentially regulates immune responses to PC inside the tumors versus peripherally in the host system. Our findings in favor of this notion are as follows:

i) Impaired recruitment of MDSCs and Tregs in the tumors of *Cxcr2*$^{-/-}$ mice. ii) Increased recruitment of cytotoxic T cells in tumors of *Cxcr2*$^{-/-}$ hosts. iii) Splenic accumulation of MDSCs in the *Cxcr2*$^{-/-}$ hosts. iv). Decreased cytotoxic T cells/ MDSCs ratio in the spleens. Taken together, these findings elaborate a novel role of CXCR2 in regulating local and systemic immunological mechanisms in PC.

One of the key findings of this study was the inhibited recruitment of MDSCs to the tumors of *Cxcr2*$^{-/-}$ hosts and their paralleled expansion in the spleens. In the previous chapter we observed identical results of increased splenic accumulation of immature polymorphonuclear (myeloid) cell populations in the *Cxcr2*$^{-/-}$ hosts. Our findings in this section have refined our knowledge from the previous chapter by confirming the phenotype of these cells as MDSCs ($CD11b^{+}$ $Ly6C^{+}Ly6G^{+}$). MDSCs are a phenotypically heterogeneous population of immature myeloid cells. MDSCs are known to express CXCR2 and several studies have elaborated the role of CXCR2 signaling axis in MDSC trafficking in various cancers including breast (Acharyya et al., 2012), colon (Katoh et al., 2013) and rhabdomyosarcoma (Highfill et al., 2014). Resembling our observation of higher CXCR2 intensity on Ly6G-C populations in tumors versus in spleen, a report in melanoma identified higher levels of chemokines CXCL1-3, 5, 7 and 8 on MDSCs located in tumors compared with the MDSC population in bone marrow (Wang et al., 2015). More importantly recent report by Highfill et al. also demonstrated similar results that CXCR2 deficiency inhibited the granulocytic MDSCs trafficking to the tumors in murine rhabdomyosarcoma resulting in their

compensatory accumulation in the spleens and blood stream. They further concluded that $CXCR2^{+}$ granulocytic MDSCs mediate local immunosuppression in murine rhabdomyosarcoma and inhibiting CXCR2 signaling can enhance the efficacy of checkpoint inhibitors (Highfill et al., 2014). Collectively, our data clearly demonstrates that CXCR2 is essential for the migration of MDSCs from the spleens to the tumors in PC. Furthermore, we also show that inhibition of host *Cxcr2* causes the systemic expansion of MDSCs in the spleens of tumor-bearing hosts.

We observed no effect of host *Cxcr2* ablation on the recruitment of macrophages. These observations are in agreement with previous reports demonstrating no effect of CXCR2 activation on monocyte chemotaxis (Bailey et al., 2007). Another detrimental effect of host *Cxcr2* depletion on tumor progression can be mediated by dendritic cell's sequestration. We observed higher frequency of dendritic cell populations in the tumors, which suggest a possible sequestration of these cells inside the tumors resulting in poor antigen presentation and impediment of dendritic cell activated anti-tumor T cell responses (Feijoó et al., 2005). Thus, our data suggests that there can be a number of mechanisms that can compensate for the anti-tumor effect caused by reduced infiltration of MDSCs to the tumors of *Cxcr2*$^{-/-}$ hosts.

As we found an altered frequency on MDSCs in the tumors and spleens of *Cxcr2*$^{-/-}$ hosts, we were prompted to next examine the effect of *Cxcr2* deletion on the frequencies of various T cell populations both in spleens and tumors. Clark et al. (2007) provided a direct evidence for the role of MDSCs in regulating T cell

responses. They demonstrated that lack of tumor-infiltrating effector T cells strongly correlated with the presence of intratumoral MDSCs (Clark et al., 2007b). Also, MDSCs are also known to cause indirect immunosuppression by promoting the recruitment of Tregs and by blocking the entry of effector T cells to the tumor sites (Goedegebuure et al., 2011). Matching our hypothesis, we observed an increased ratio of cytotoxic T cells to MDSCs in the pancreas and decreased frequency of Tregs. Conversely, in spleens the ratio of cytotoxic T cells to MDSCs was reduced. MDSCs are known to suppress the proliferation and activation of T cells by inhibiting the expression of MHC class II on antigen presenting cells and CD3-ζ chains on T cells respectively, primarily by the production of iNOS and arginase 1 (Fujimura et al., 2010; Gabrilovich and Nagaraj, 2009; Goedegebuure et al., 2011; Nagaraj and Gabrilovich, 2008). However, in the peripheral tissues MDSCs function as antigen-presenting cells and induce ROS-mediated T cell suppression during the antigen specific interaction between MDSCs and T cells (Nagaraj and Gabrilovich, 2008). Thus, these findings suggested a systemic immune suppression in the *Cxcr2*$^{-/-}$ hosts.

Cytokines are important for mediating the communication and action of immune cells and mounting the inflammatory immune responses to tumors (Candido and Hagemann, 2013). Therefore, we evaluated the alteration in the cytokine profile of TAL's. Cytokines are known to play dual roles in tumor biology (Burkholder et al., 2014). Our data demonstrate that *Cxcr2*$^{-/-}$ TALs have enhanced expression of transcripts of *IL-12*, *IL-10*, *IFNγ* and *TNFα*. IFNγ is essential for antigen-specific immune responses of $CD4^+$ Th and $CD8^+$ cytotoxic

T cells (Burkholder et al., 2014).TNFα is known to mediate the recruitment and cytotoxic activation of $CD4^+$ T cells (Burkholder et al., 2014). We also observed an increased transcript expression of *Ccl2, 3* and *5*. These chemokines have been implicated for their roles in the recruitment of T cells to tumors (Lança et al., 2013).

Based on these data, we postulate that although *Cxcr2* deletion in the host inhibits the recruitment of MDSCs to the tumors yet it causes the expansion of MDSC populations in the spleen leading to systemic immune suppression in these mice. This systemic immunosuppression caused by the accumulation of MDSCs in *Cxcr2*$^{-/-}$ mice compensates for the tumor-inhibitory effect of decreased trafficking of MDSC populations to the tumors. Our study provides an overview of the novel roles of CXCR2 altering the landscape of host immune responses to the PC. However, we have employed an orthotopically implanted PC murine model generated by surgeries. Also, all the data for alterations in the frequencies of immune cells presented by us did not reach statistical significance. Further experimenting in spontaneous PC murine models may help in refining the results generated in this study.

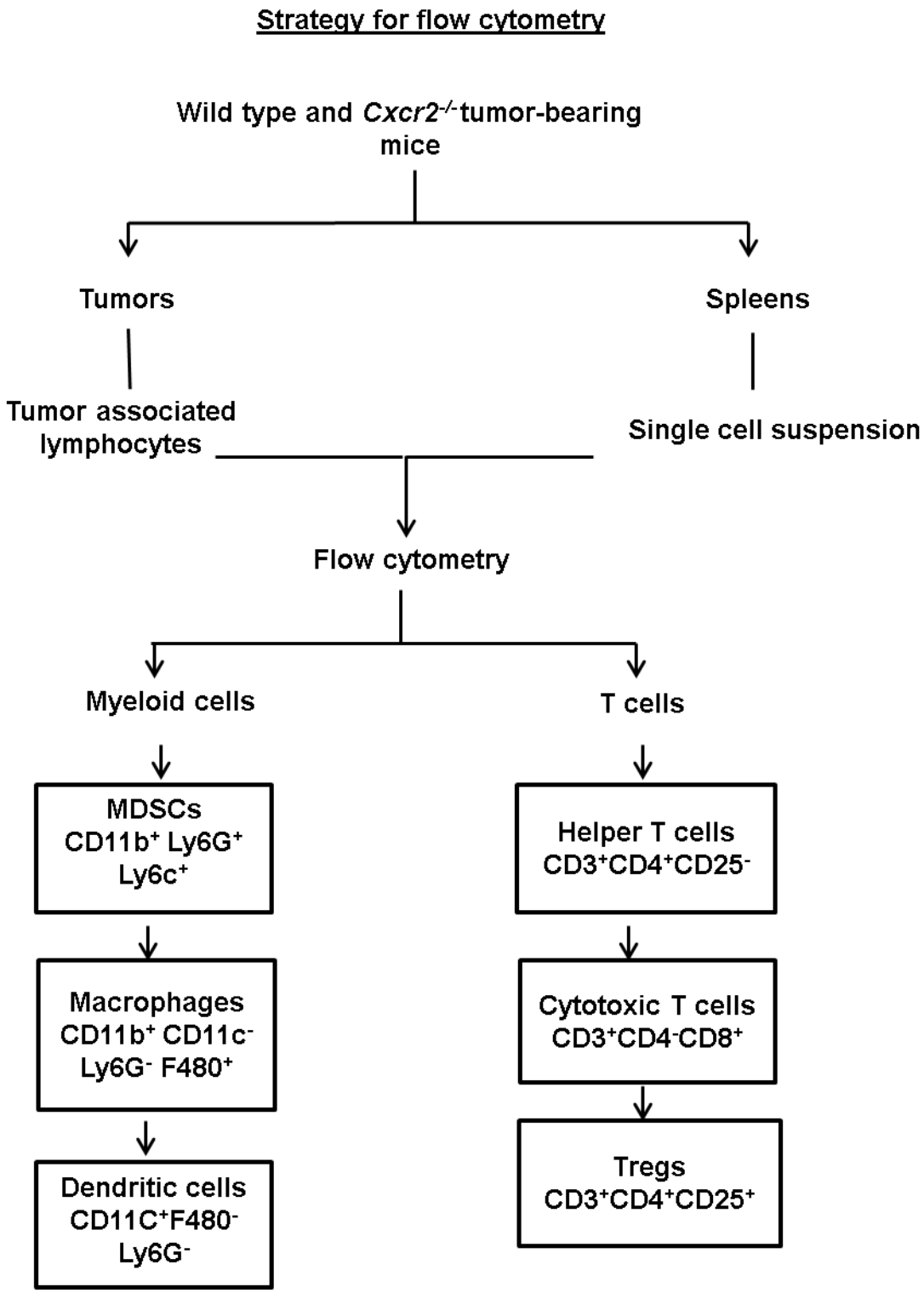
Strategy for flow cytometry
Wild type and Cxcr2-/- tumor-bearing mice
Tumors
Spleens
Tumor associated lymphocytes
Single cell suspension
Flow cytometry
Myeloid cells
T cells
MDSCs CD11b+ Ly6G+ Ly6c+
Macrophages CD11b+ CD11c- Ly6G- F480+
Dendritic cells CD11C+F480- Ly6G-
Helper T cells CD3+CD4+CD25-
Cytotoxic T cells CD3+CD4-CD8+
Tregs CD3+CD4+CD25+

Figure 6.1. Outline of the experimental approach used to characterize infiltrating immune cells.

Schematic representation of the experimental approach and the details of markers employed to characterize the immune infiltrates by flow cytometry.

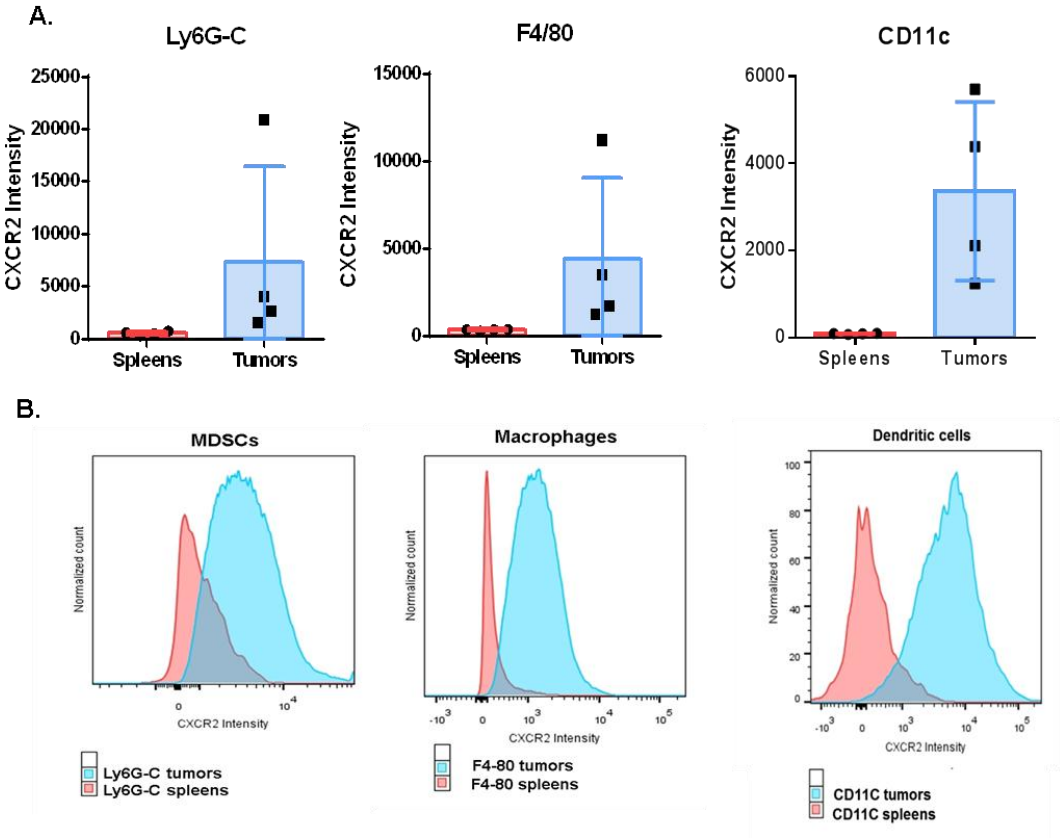
A.
Ly6G-C
F4/80
CD11c
CXCR2 Intensity
25000
20000
15000
10000
5000
0
Spleens
Tumors
15000
10000
5000
0
Spleens
Tumors
6000
4000
2000
0
Spleens
Tumors
B.
MDSCs
Macrophages
Dendritic cells
Normalized count
CXCR2 Intensity
Ly6G-C tumors
Ly6G-C spleens
F4-80 tumors
F4-80 spleens
CD11C tumors
CD11C spleens

Figure 6.2. The intensity of CXCR2 on the myeloid cell population in spleens versus the pancreas.

A) Comparison of the average mean fluorescence intensity of CXCR2 expression on myeloid-derived suppressor cells (MDSCs) ($CD11b^{+}Ly6G^{+}Ly6C^{+}$), macrophages ($CD11b^{+}F480^{+}$) and dendritic cells ($CD11c^{+}$) isolated from the pancreas and spleens of tumor-bearing wild type and *Cxcr2*$^{-/-}$ mice. Each dot on the graph represents data point from an individual animal. Error bars represent standard deviation. **B)** Representative histograms demonstrating mean fluorescence intensity for MDSCs, macrophages and dendritic cells in tumors versus spleens chart.

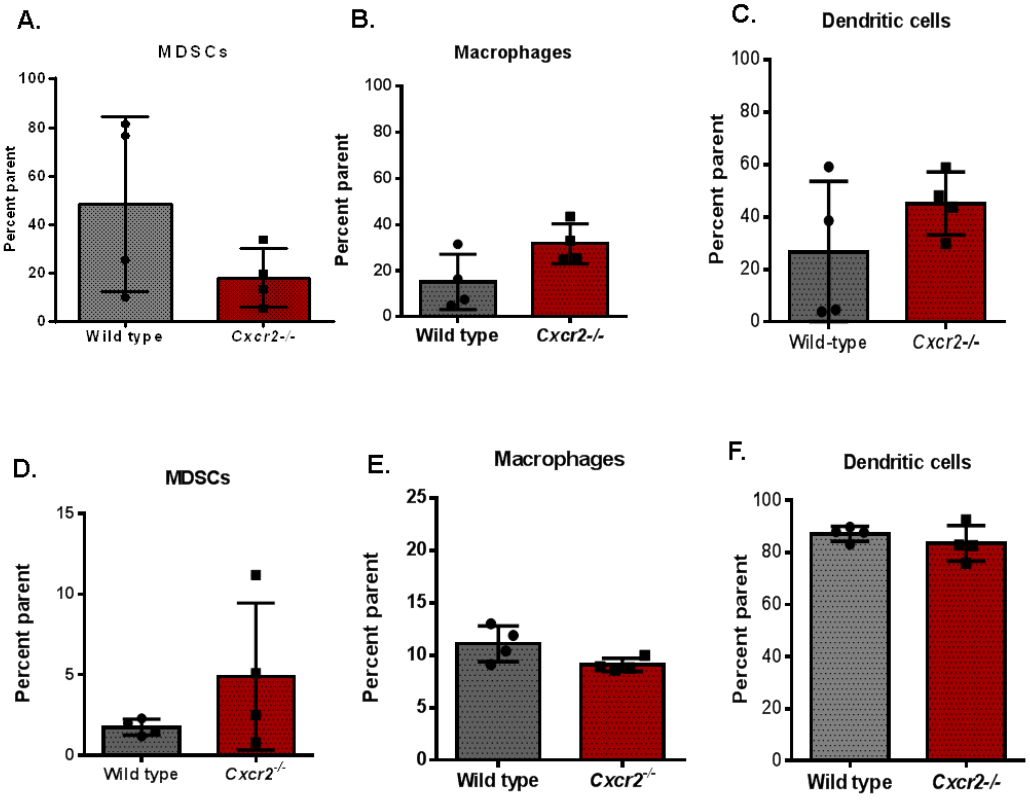
A.
MDSCs
Percent parent
100
80
60
40
20
0
Wild type
Cxcr2-/-
B.
Macrophages
Percent parent
100
80
60
40
20
0
Wild type
Cxcr2-/-
C.
Dendritic cells
Percent parent
100
80
60
40
20
0
Wild-type
Cxcr2-/-
D.
MDSCs
Percent parent
15
10
5
0
Wild type
Cxcr2-/-
E.
Macrophages
Percent parent
25
20
15
10
5
0
Wild type
Cxcr2-/-
F.
Dendritic cells
Percent parent
100
80
60
40
20
0
Wild type
Cxcr2-/-

Figure 6.3. Effect of host *Cxcr2* deletion on the frequencies of myeloid cells in the pancreas and spleens of tumor-bearing mice.

Effect of *Cxcr2* deletion on the percentages of MDSCs, macrophages and dendritic cells in **A)** pancreas and **B)** spleens of wild type and *Cxcr2*$^{-/-}$ mice. Each dot on the graph represents data point from an individual animal. Error bars represent standard deviation.

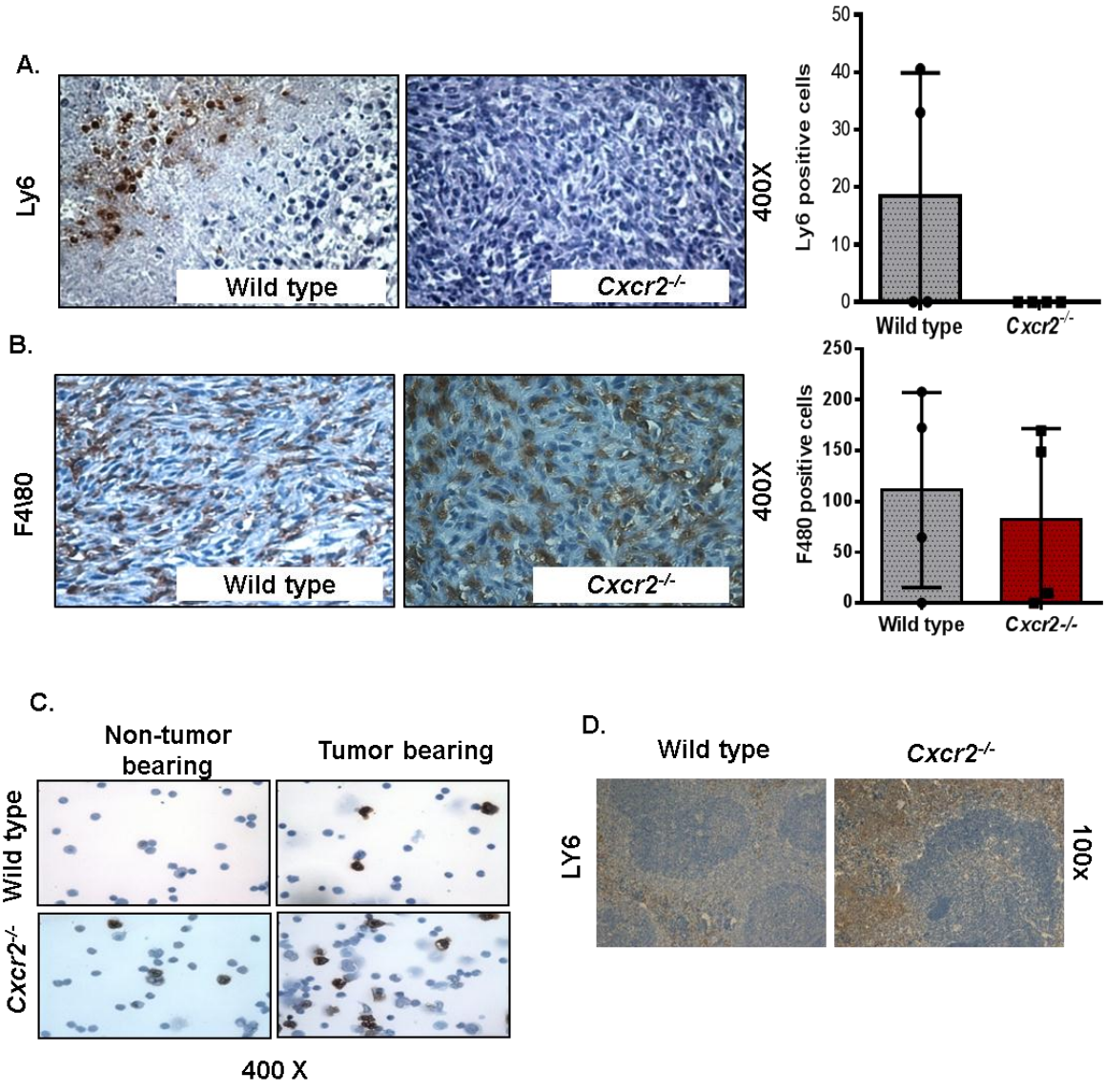
A.
Ly6
Wild type
Cxcr2-/-
400X
Ly6 positive cells
50
40
30
20
10
0
Wild type
Cxcr2-/-
B.
F4180
Wild type
Cxcr2-/-
400X
F480 positive cells
250
200
150
100
50
0
Wild type
Cxcr2-/-
C.
Non-tumor bearing
Tumor bearing
Wild type
Cxcr2-/-
400 X
D.
Wild type
Cxcr2-/-
LY6
100x

Figure 6.4. Effect of host *Cxcr2* deletion on the frequencies of myeloid cells in the pancreas and spleens of tumor-bearing mice.

Representative photomicrographs demonstrating immunohistochemical (IHC) staining its quantitation for **A)** Ly6 in the tumors and **B)** F4/80 in tumors of wild type and *Cxcr2*$^{-/-}$ tumor-bearing mice. Each dot on the graph represents data point from an individual animal. Error bars represent standard deviation. IHC for Ly6 in **C)** cytospins prepared from splenocytes and **D)** spleens of wild type and *Cxcr2*$^{-/-}$ tumor-bearing mice.

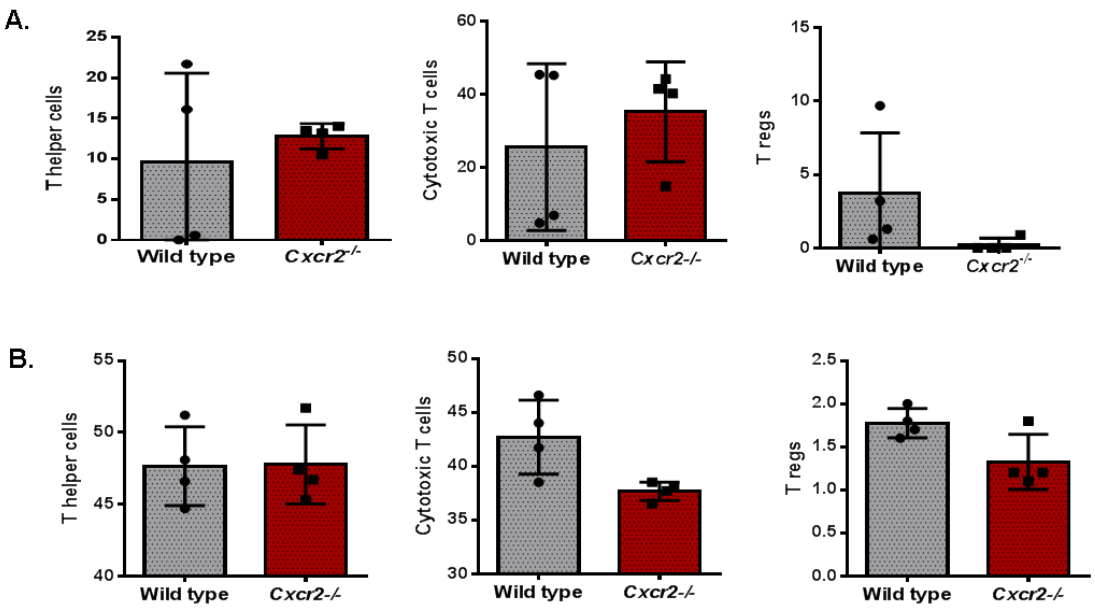
A.
T helper cells
25
20
15
10
5
0
Wild type
Cxcr2-/-
Cytotoxic T cells
60
40
20
0
Wild type
Cxcr2-/-
T regs
15
10
5
0
Wild type
Cxcr2-/-
B.
T helper cells
55
50
45
40
Wild type
Cxcr2-/-
Cytotoxic T cells
50
45
40
35
30
Wild type
Cxcr2-/-
T regs
2.5
2.0
1.5
1.0
0.5
0.0
Wild type
Cxcr2-/-

Figure 6.5. Effect of host *Cxcr2* deletion on the frequencies of T cell subset populations in the pancreas and spleens of tumor-bearing mice.

Percentages of T helper cells ($CD3^+CD4^+CD25^-$%$CD3^+$), cytotoxic T cells ($CD3^+CD4^-CD8^+$%$CD3^+$) and T regulatory cells (Tregs) ($CD3^+CD4^+CD25^-$ %$CD3^+$) in **A)** pancreas and **B)** spleens of wild type and *Cxcr2*$^{-/-}$ mice. Each dot on the graph represents data point from an individual animal. Error bars represent standard deviation.

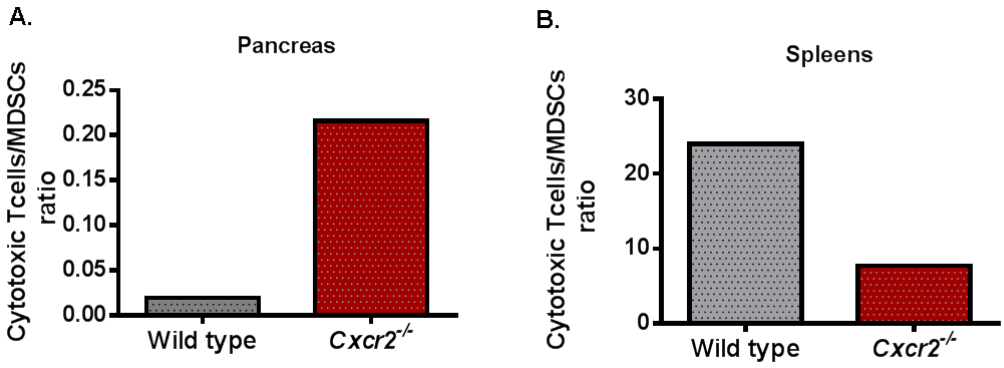
A.
Pancreas
Cytotoxic Tcells/MDSCs ratio
0.25
0.20
0.15
0.10
0.05
0.00
Wild type
Cxcr2-/-
B.
Spleens
Cytotoxic Tcells/MDSCs ratio
30
20
10
0
Wild type
Cxcr2-/-

Figure 6.6. Effect of host *Cxcr2* deletion on the ratio of cytotoxic T cell to myeloid-derived suppressor cell populations in the pancreas and spleens of tumor-bearing mice.

Comparison of the ratios of myeloid-derived suppressor cells (MDSCs) and cytotoxic T cells in the **A)** pancreas or **B)** spleens of tumor-bearing wild type versus *Cxcr2*$^{-/-}$ mice groups.

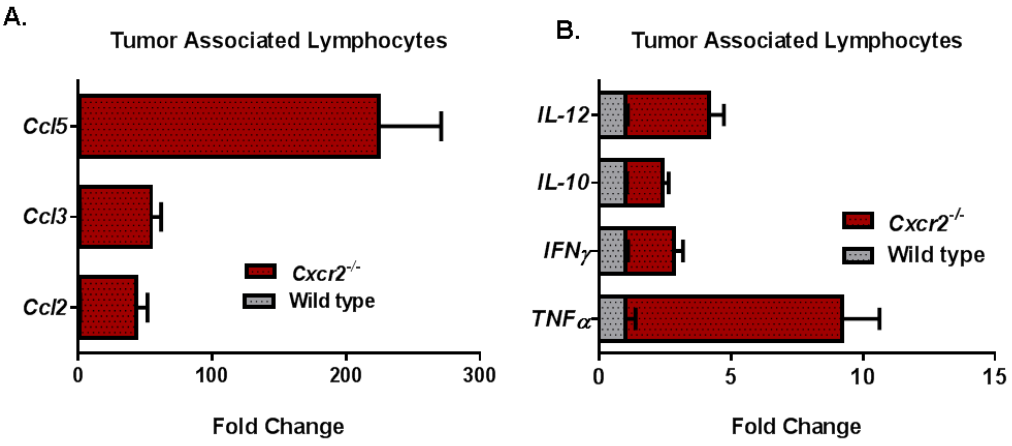
A.
Tumor Associated Lymphocytes
Ccl5
Ccl3
Ccl2
Cxcr2-/-
Wild type
0
100
200
300
Fold Change
B.
Tumor Associated Lymphocytes
IL-12
IL-10
IFNγ
TNFα
Cxcr2-/-
Wild type
0
5
10
15
Fold Change

Figure 6.7. Expression profile of cytokines in tumor-associated lymphocytes.

Real time PCR data representing fold change in the levels of mRNA expression of **A)** *Ccl2*, *Ccl3* and *Ccl5* **B)** *IL-12*, *IL-10*, *IFNγ* and *TNFα* in the lymphocytes isolated from the tumors (pancreas) of *Cxcr2*$^{-/-}$ versus the wild type mice groups. Error bars represent standard deviation.

Chapter 7

Evaluation of CXCR2 antagonist as a therapeutic agent in preclinical models of pancreatic cancer

Abstract:

Pancreatic cancer (PC) is known to have a poor prognosis. There is an urgent need for novel therapies for PC. We and others have shown the aberrant expression of CXCR2 and its ligands in PC. CXCR2 antagonists are currently in clinical trials for chronic obstructive pulmonary diseases. Therefore, targeting CXCR2 appears to be an attractive strategy. Our objective for this section of the study was to evaluate the therapeutic utility of CXCR2 antagonist in the preclinical models of PC. We investigated the effect of intraperitoneal administration of the CXCR2 antagonist (SCH-479833) in orthotopically implanted (syngeneic or xenogeneic) PC murine models. Our results demonstrate that systemic administration of CXCR2 antagonist had both tumor-promoting and -inhibiting effect on PC. CXCR2 antagonist inhibited the proliferation of tumor cells. Furthermore, mirroring our results from host *Cxcr2*$^{-/-}$ study we observed increased accumulation of Ly6-positive cells in the spleens of CXCR2 antagonist-treated mice. To the best of our knowledge, the current study is the first effort to evaluate the impact of pharmacological inhibition of CXCR2 in preclinical models of PC.

Introduction:

PC is in dire need of novel therapies. Results from the previous chapters provide evidence for the aberrant expression of CXCR2 and its ligands in PC. Analysis of human specimens demonstrated upregulation of CXCR2 and its ligands in PC tumor cells as well as the surrounding stroma. Furthermore, we identified an important role of this signaling axis in regulating *KRAS*$^{(G12D)}$-induced autocrine growth of PC cells. Taken together, these findings suggest that CXCR2 can be a promising therapeutic target for PC.

Previous reports from our laboratory and others have demonstrated the utility of CXCR2 antagonists as anti-cancer agents in various cancer types. Treatment with CXCR2 antagonists inhibited the *in vitro* cell proliferation and chemotaxis of melanoma cells (Singh et al., 2009). Furthermore, administration of CXCR2 antagonists to nude mice having subcutaneous melanoma implants inhibited tumor growth and angiogenesis (Singh et al., 2007). In another report, we have shown the effectivity of CXCR2 antagonists as anti-metastatic therapeutics preclinically in human colon cancer (Varney et al., 2011). Besides reports from our laboratory, a recent study reported that CXCR2 antagonist (SCH-527123) further sensitized colorectal cancer cells to oxaliplatin treatment (Ning et al., 2012a). In the previous sections of this dissertation, we have evaluated the therapeutic efficacy of CXCR2 antagonists in the context of *KRAS*$^{(G12D)}$ mutation *in vitro* on PC cells. Treatment of PC cells with CXCR2 antagonists (SCH-527123 and SCH-479833) inhibited the *in vitro* growth and

migration of *KRAS*$^{(G12D)}$ mutation-bearing PC cell lines. However, our *in vivo* PC model with *Cxcr2*$^{-/-}$ host demonstrated no effect on tumor cell proliferation but had enhanced liver metastasis. Taken together, results from previous chapters suggested that CXCR2 inhibition *in vivo* in PC may have both tumor inhibitory and promoting effects. Therefore, based on our findings from preceding sections we were prompted to evaluate the impact of inhibiting CXCR2 pharmacologically in a preclinical murine model of PC.

Results:

Administration of CXCR2 antagonist to immunocompetent syngeneic pancreatic cancer murine model reduces tumor cell proliferation.

In order to evaluate the effect of CXCR2 antagonist in a preclinical model of PC, we used a syngeneic orthotopically implanted murine PC model. KRAS-PDAC-GFP cells (10 x 10^4) were injected into the pancreas of C57BL6 WT female mice by performing surgeries **(Fig. 7.1A)**. A week after the surgeries, mice were assigned randomly to receive either control solvent HPβCD (100 µl) (n = 4) or the CXCR2 antagonist (SCH479833; 100 mg/kg body weight) once a day for seven days a week **(Fig. 7.1A)**. Treatment with CXCR2 antagonist led to a minor increase in the tumor weight **(Fig. 7.1B)**. This observation was consistent with our previous results in the host *Cxcr2* deletion model. We observed no change in the histopathology of the tumors from the two treatment groups **(Fig. 7.1D)**. The frequency and weight of peritoneal metastasis were decreased in the CXCR2 antagonist-treated group. Tumor growth was assessed by performing IHC for Ki-67. We observed that treatment of PC-bearing mice with CXCR2

antagonists resulted in decreased tumor cell proliferation **(Fig. 7.2A and B).** Therefore, we conclude that systemic administration of CXCR2 antagonists slows the growth of tumor cells in orthotopically implanted model but did not reduce the tumor weight.

Tumors from CXCR2 antagonist treated mice show reduced angiogenesis.

CXCR2 signaling axis has been widely implicated as a regulator of angiogenesis in PC. However, the impact of therapeutic inhibition of CXCR2 signaling on angiogenesis has not yet been evaluated in preclinical murine PC model. We observed significant inhibition of angiogenesis in tumors of mice treated with CXCR2 antagonist compared with the control HPβCD-treated group **(Fig. 7.3A)**.

We next investigated the ability of CXCR2 antagonist treatment to impact fibrosis in murine PC. We performed Masson's trichrome staining in these tumors. Consistent with our results in the host *Cxcr2*$^{-/-}$ model, we observed increased fibrosis in the tumors derived from mice treated with the CXCR2 antagonist **(Fig. 7.3B)**.

Treatment with CXCR2 antagonist induces splenic accumulation of Ly6^{+} cells.

In the previous section, we observed enhanced accumulation of Ly6^{+} cells in the spleens of tumor-bearing *Cxcr2*$^{-/-}$ hosts. We, therefore, evaluated the impact of CXCR2 antagonist treatment on the frequency of Ly6^{+} cells in the spleens. We observed no change in the weight and histological architecture of

spleens derived from CXCR2 antagonist treated mice **(Fig. 7.4A and B)**. However, we found an enhanced accumulation of $Ly6^+$ populations in the follicular zone of the spleens of tumor-bearing mice treated with CXCR2 antagonist compared with the control HPβCD group **(Fig. 7.5A and B)**.

Treatment with CXCR2 antagonist reduces tumor weight but enhances metastasis in the pancreatic cancer nude mouse model:

Based on our results thus far, we next attempted to evaluate the effect of treating immunodeficient mice bearing human PC cells with CXCR2 antagonist. For this purpose, we used two different human PC cell lines, CD18/HPAF and E6-E6-st-KRAS. The first model employed by us was generated by injecting CD18/HPAF cells in the pancreas of nude mice by performing surgeries. As shown in the figure 7.6 A, on day 7 of the surgeries mice were randomly divided into two groups. The control group (n = 4) received IP injections of 100 μl HPβCD for five continuous days a week. The treatment group received CXCR2 antagonist (SCH-479833; 100 mg/kg body weight) diluted in 100 μl HPβCD. Mice were sacrificed when they developed palpable tumors (day 28).

Treatment with CXCR2 antagonists decreased the weight of primary tumors **(Fig 7.6B).** There was no difference in the histopathology of the tumors derived from the two different groups **(Fig 7.6C).** Both HPβCD and CXCR2 antagonist-treated groups developed metastasis **(Fig 7.6D and E)**. Similarly, we developed another xenograft model by injecting E6-E7-st-KRAS cells in nude mice **(Fig 7.7A)**. Treatment with CXCR2 antagonist decreased the weight of

primary tumors **(Fig 7.7B).** There was no difference in the histopathology of the tumors derived from the two different groups **(Fig 7.7C).**

Discussion:

In this section of the study, we conclude that treatment of PC-bearing mice with CXCR2 antagonists has both anti- and pro-tumorigenic effects on the development of PC. Our findings in favor of this notion are as follows: tumors of mice treated with CXCR2 antagonist demonstrates i) inhibited tumor cell proliferation, ii) decreased angiogenesis, iii) enhanced fibrosis and iv) increased splenic accumulation of Ly6+ cells.

We have previously (Chapter 4) demonstrated a growth inhibitory effect of CXCR2 antagonists on *KRAS*$^{(G12D)}$- bearing PC cells *in vitro*. In this study, we found that IP administration of CXCR2 antagonist to immunocompetent mice bearing syngeneic PC cells inhibited tumor cell proliferation but did not affect the tumor size. An explanation of this discrepancy was provided by enhanced fibrosis in the SCH-479833 treated group. It is important to note that tumors in PC are composed of a heterogeneous population of cells including fibroblasts, immune and endothelial cells (Feig et al., 2012). The difference in responses of other cancers like colon (Singh et al., 2009) and melanoma (Varney et al., 2011) to CXCR2 antagonists versus PC could be due to the organ-specific microenvironment and host-induced responses.

In the previous sections, we demonstrated that *Cxcr2* depletion in the host caused EMH and splenic expansion of MDSC population. Mirroring these

findings we have observed an increased population of $Ly6^+$ cells in the spleens of CXCR2 antagonist-treated mice. Therefore, we conclude that systemic inhibition of CXCR2 by pharmacological as well as genetic approaches causes immunosuppression in the host.

CXCR2 is expressed by various cell types in the body. Furthermore, as CXCR2 has multiple ligands, it can affect different cell types and distinct ways. Therefore, the systemic administration of CXCR2 antagonists in PC needs to be carefully weighed.

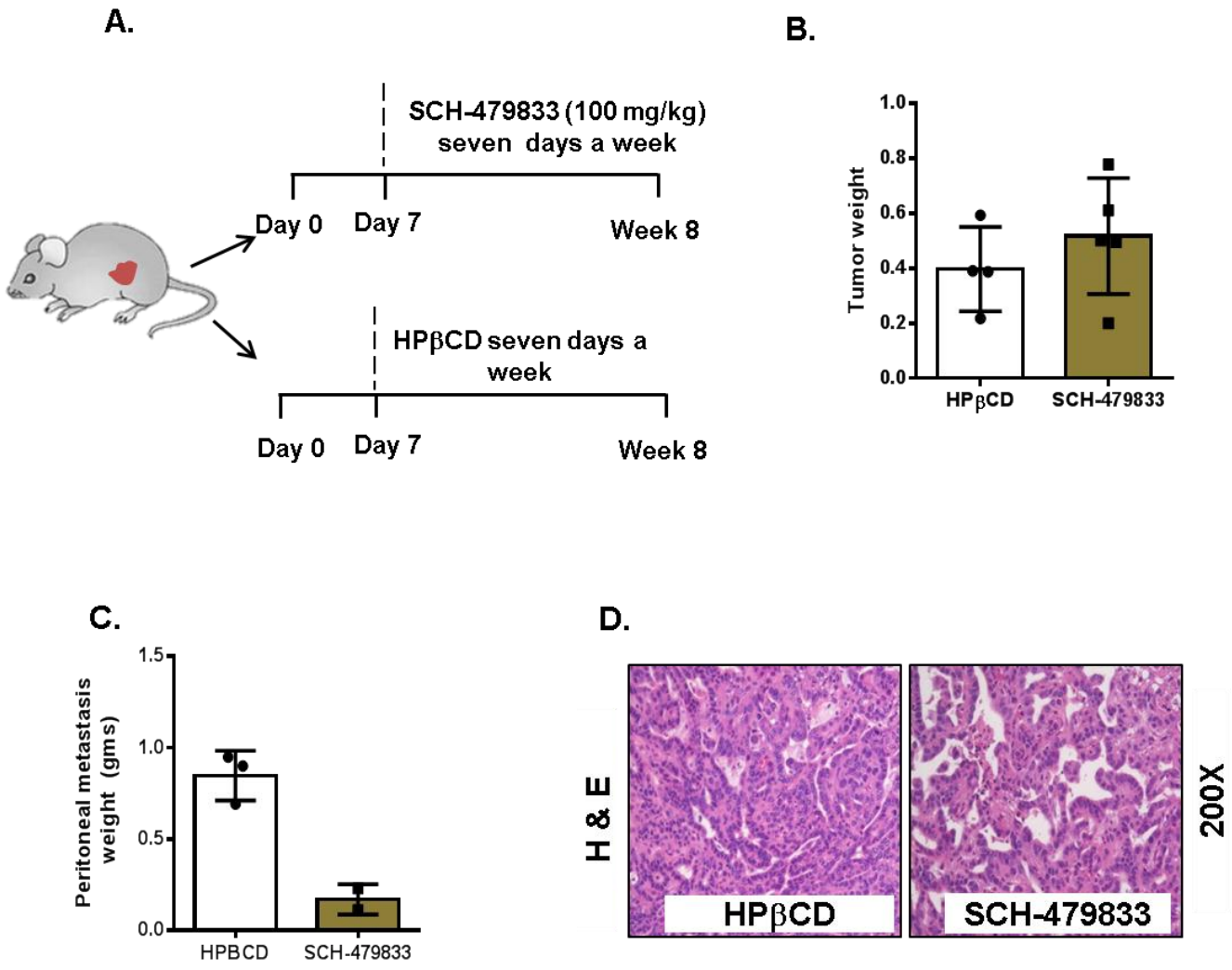
A.
SCH-479833 (100 mg/kg)
seven days a week
Day 0
Day 7
Week 8
HPβCD seven days a
week
Day 0
Day 7
Week 8
B.
Tumor weight
1.0
0.8
0.6
0.4
0.2
0.0
HPβCD
SCH-479833
C.
Peritoneal metastasis
weight (gms)
1.5
1.0
0.5
0.0
HPBCD
SCH-479833
D.
H & E
HPβCD
SCH-479833
200X

Figure 7.1. Administration of CXCR2 antagonist to immunocompetent, syngeneic pancreatic cancer mouse model.

A) Experimental design for treatment of orthotopic pancreatic cancer mouse model with HPβCD (control) or SCH-479833 (CXCR2 antagonist). **B)** Weight (gms) of KRAS-PDAC-GFP tumors derived from mice treated with HPβCD or SCH-479833. **C)** Weight of peritoneal metastasis in the two treatment groups. **D)** Representative photomicrographs of H&E staining demonstrating the histopathology of tumors resected from the HPβCD- and SCH-479833-treated groups. Each dot on the graph represents data point from an individual animal. Error bars represent standard deviation.

A.

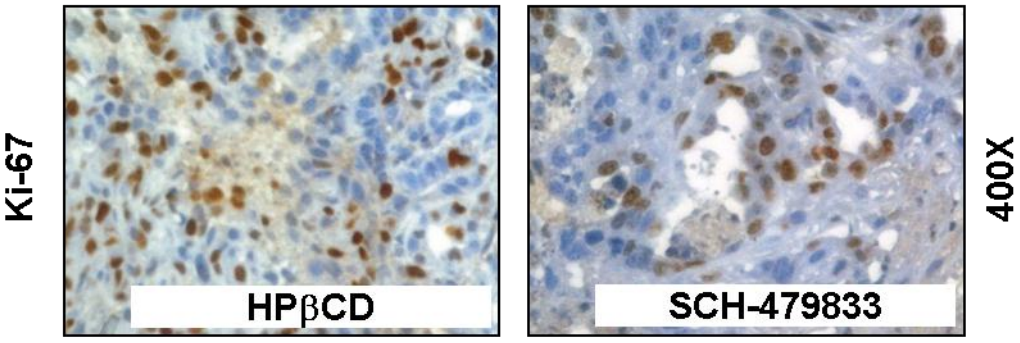
Ki-67
HPβCD
SCH-479833
400X

B.

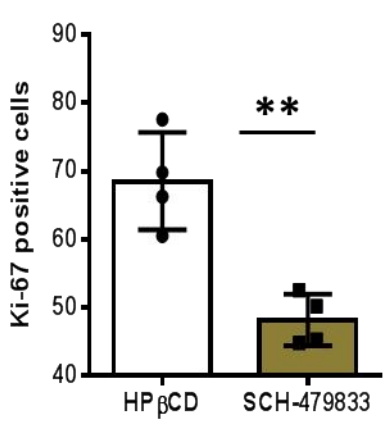
Ki-67 positive cells
90
80
70
60
50
40
**
HPβCD
SCH-479833

Figure 7.2. Systemic administration of CXCR2 antagonist inhibits tumor cell proliferation.

A) Representative photomicrographs demonstrating immunohistochemistry for Ki-67 in the tumor of HPβCD and SCH-479833 (CXCR2 antagonist) treated mice groups (n = 4). **B)** Comparison of the proliferation index of tumors from the two groups. Each dot on the graph represents data point from an individual animal. Error bars represent standard deviation. Statistical significance determined by Student's t-test (* $p \leq 0.05$, ** $p \leq 0.01$, *** $p \leq 0.001$, *NS* $p > 0.05$).

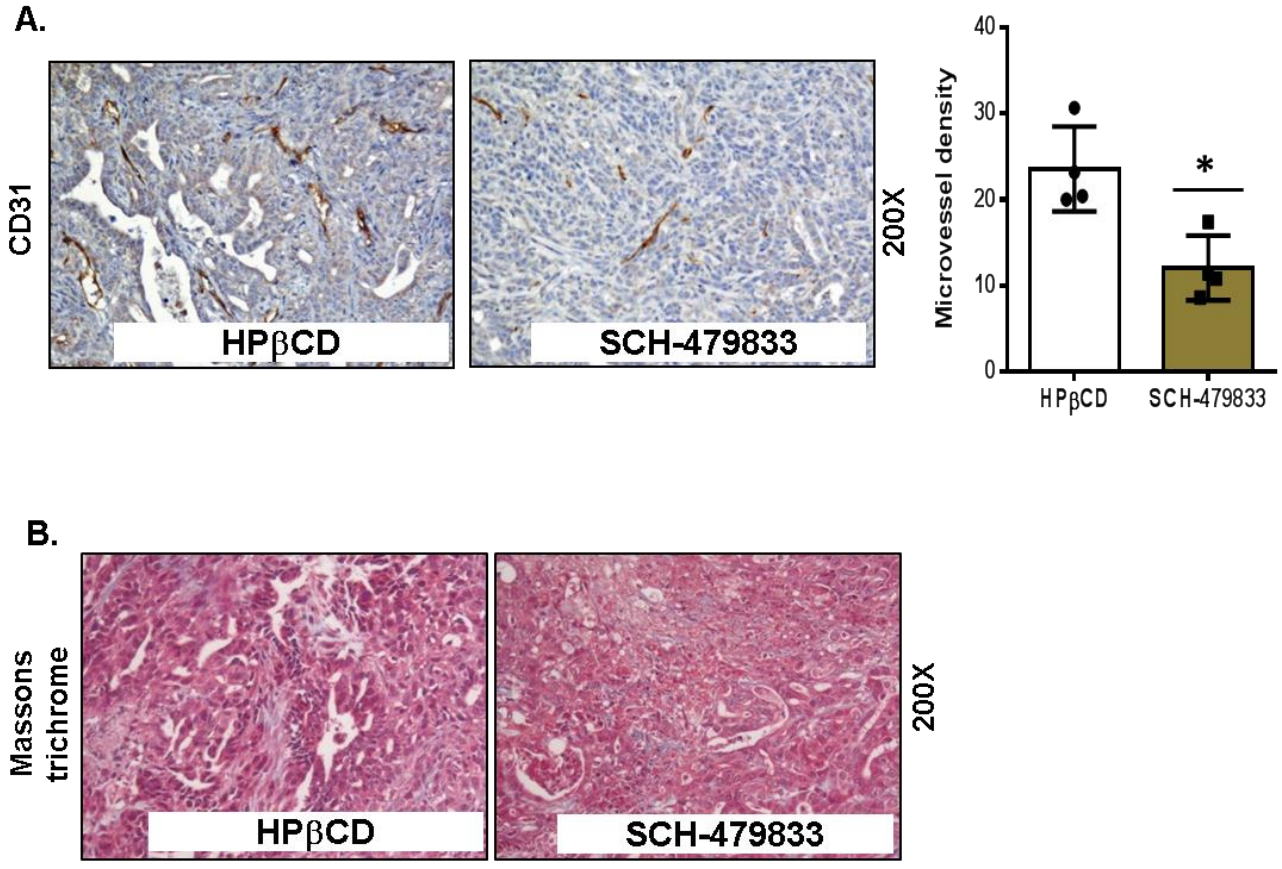
A.
CD31
HPβCD
SCH-479833
200X
Microvessel density
40
30
20
10
0
*
HPβCD
SCH-479833
B.
Massons trichrome
HPβCD
SCH-479833
200X

Figure 7.3. Decreased angiogenesis and enhanced fibrosis in CXCR2 antagonist treated mice.

A) Representative CD31 immunohistochemistry photographs and evaluation of microvessel density **B)** Masson's trichrome staining on tumors derived from HPβCD and SCH-479833 (CXCR2 antagonist) treated mice groups (n = 4). Each dot on the graph represents data point from an individual animal. Error bars represent standard deviation. Statistical significance determined by Student's t-test (* $p \leq 0.05$, ** $p \leq 0.01$, *** $p \leq 0.001$, *NS* $p > 0.05$).

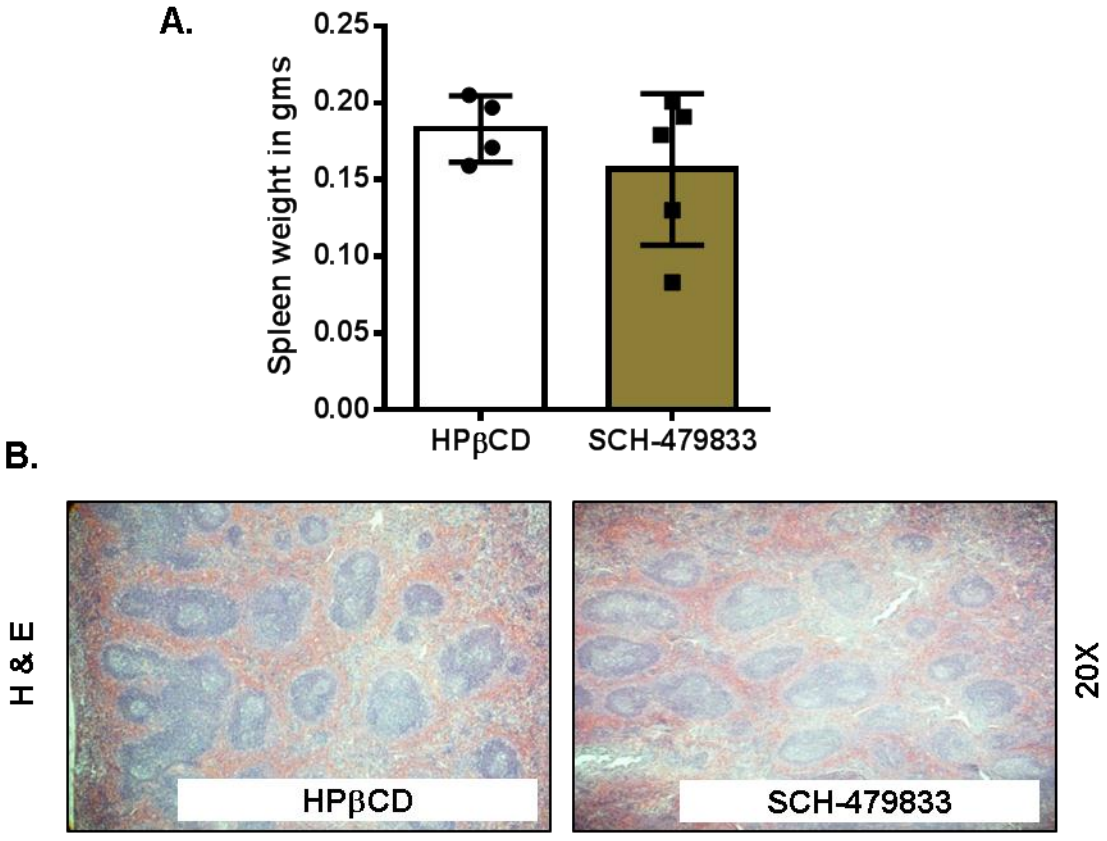
A.
Spleen weight in gms
0.25
0.20
0.15
0.10
0.05
0.00
HPβCD
SCH-479833
B.
H & E
HPβCD
SCH-479833
20X

Figure 7.4. No effect on the weight and histological architecture of spleens in HPβCD and CXCR2 antagonist treated mice.

A) Weight (gms) and **B)** histological architecture of the spleens isolated from mice treated with HPβCD (n = 4) or CXCR2 antagonist (SCH-479833) (n = 5). Each dot on the graph represents data point from an individual animal. Error bars represent standard deviation.

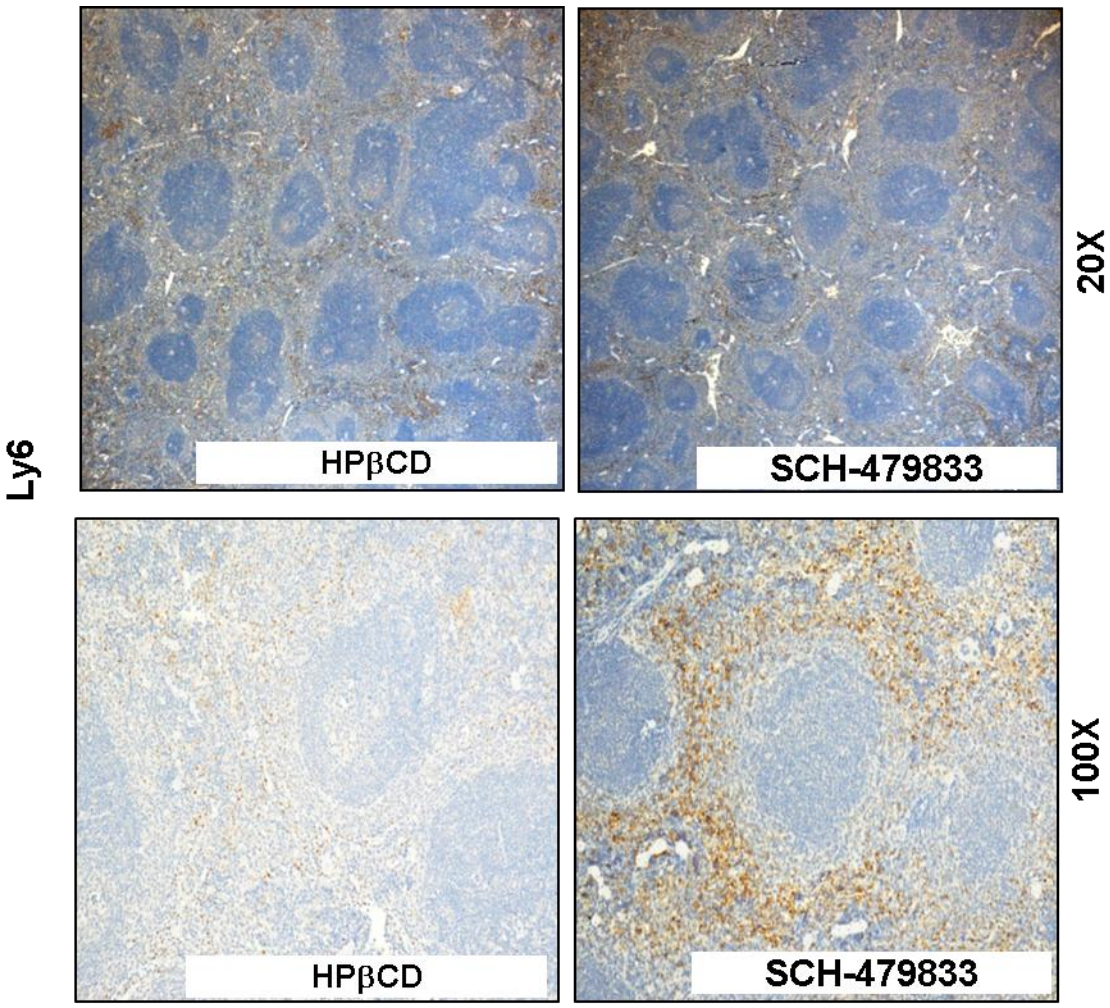
Ly6
HPβCD
SCH-479833
20X
HPβCD
SCH-479833
100X

Figure 7.5. Treatment with CXCR2 antagonist induces splenic accumulation of Ly6^{+} cells.

Images showing the immunohistochemistry for Ly6 in spleens of HPβCD- and CXCR2 antagonist (SCH-479833)-treated mice.

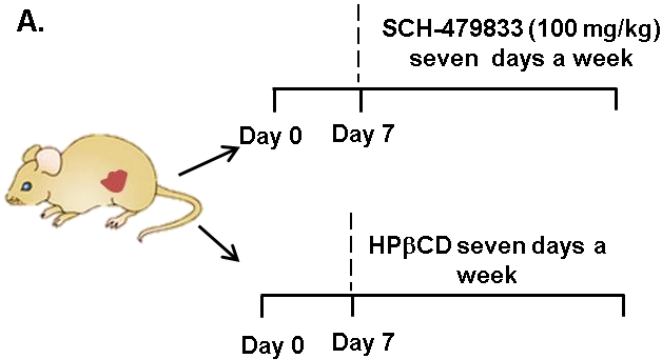

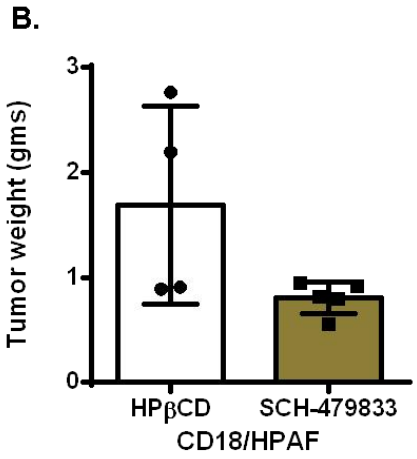

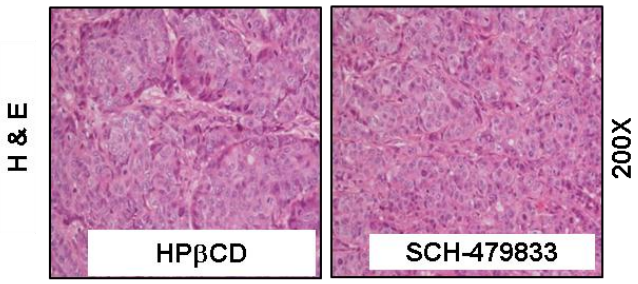

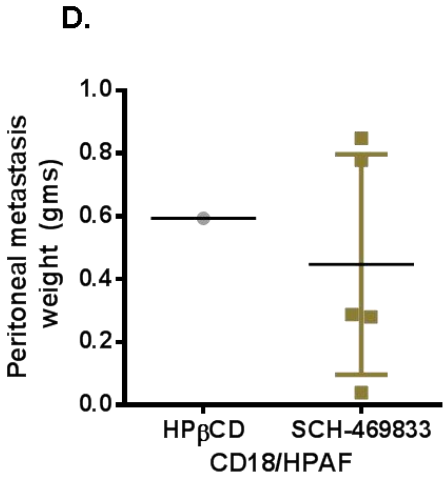

E.

	1	2	3	4	5
HPβCD	Mets all over intestine	Mets in intestine	Mets in liver, peritoneum and intestine	No mets visible	-
SCH479833	Mets in stomach and peritoneum	Peritoneum and stomach	Peritoneum and stomach	Peritoneum and stomach	Peritoneum and stomach

Figure 7.6. Administration of CXCR2 antagonist to immunocompromised nude mouse model bearing CD18/HPAF xenograft tumors reduces tumor weight but enhances peritoneal metastasis.

A) Experimental design for treatment of orthotopic pancreatic cancer mouse model with HPβCD (control) or CXCR2 antagonist (SCH-479833). **B)** Weight of CD18/HPAF tumors derived from mice treated with HPβCD or SCH-479833. **C)** Representative photomicrographs of H&E staining of tumors. **D)** Weight of peritoneal metastasis in the two treatment groups. **E)** Table summarizing the incidence of metastasis in mice treated with HPβCD or SCH-479833. Each dot on the graph represents data point from an individual animal. Error bars represent standard deviation.

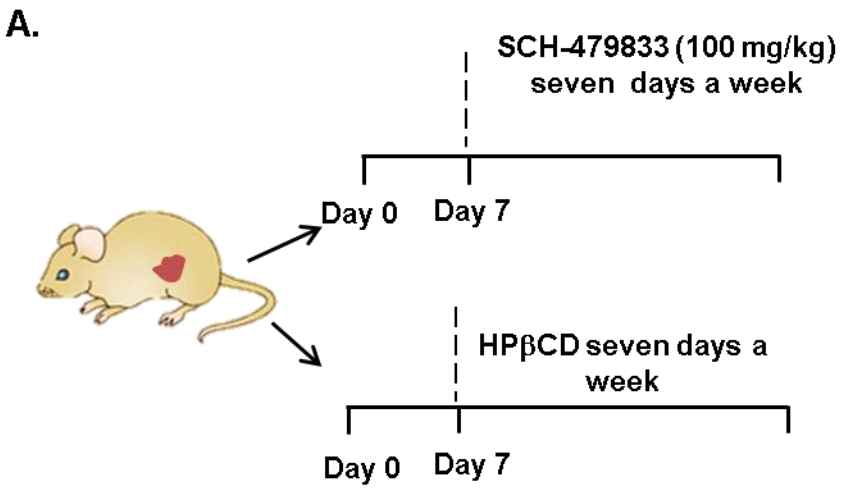
A.
SCH-479833 (100 mg/kg)
seven days a week
Day 0
Day 7
HPβCD seven days a
week
Day 0
Day 7

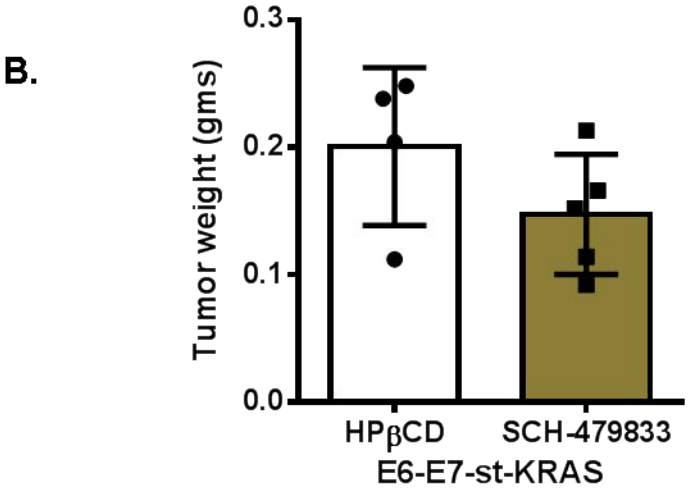
B.
Tumor weight (gms)
0.3
0.2
0.1
0.0
HPβCD
SCH-479833
E6-E7-st-KRAS

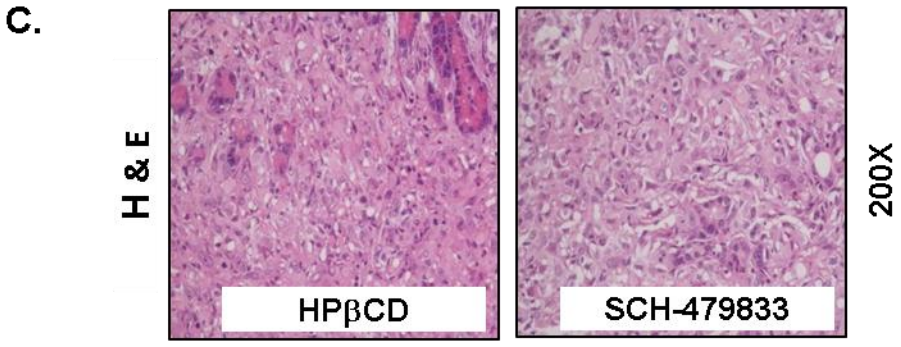
C.
H & E
HPβCD
SCH-479833
200X

Figure 7.7. Administration of CXCR2 antagonist to immunocompromised nude mouse model bearing E6-E7-st-KRAS xenograft tumors.

A) Experimental design for treatment of orthotopic pancreatic cancer mouse model with HPβCD (control) or CXCR2 antagonist (SCH-479833) **B)** Weight of E6-E7-st-KRAS tumors derived from mice treated with HPβCD or SCH-479833. **C)** Representative photomicrographs of H&E staining of tumors. Each dot on the graph represents data point from an individual animal. Error bars represent standard deviation.

Chapter 8

Major Conclusions and Future Directions

CXCR2 a double-edged sword in pancreatic cancer: a perspective

PC is a complex disease that arises in a multi-step manner and involves several players regulating its pathogenesis. The unbridled growth and spread of the cancer cells is backed up by not just the genetic alterations in the tumor cells but also by active support from the cancer-bearing host. Targeted therapies have emerged as the new face of cancer treatment. Unlike standard chemotherapies that inhibit tumor growth by killing rapidly dividing cells, targeted therapies exert their effect by interfering with the activity of an identified target. An ideal target has differentially higher expression in the cancer cells. However, these proteins can be expressed by many of the healthy cells of the host as well. In such a scenario, there is the possibility of off-target effects that can create substantial unwanted outcomes. This emphasizes the need to analyze the impact of inhibiting any potential molecular target in the context of cancer cell versus normal noncancerous cells. Several published reports and our preliminary data have suggested the potential of CXCR2 as a “molecular target” for PC therapies. The purpose of the research presented in this dissertation was to identify the role(s) of CXCR2, a G-protein coupled receptor, in malignant PC tumor cells as well as in host-tumor interactions. Based on the results generated in this study we conclude that CXCR2 serves as a double-edged sword during PC progression **(Fig. 8.1)**. Our conclusion is based on several observations upon inhibition of CXCR2 either in the tumor cells or in the cancer-bearing host. The first section of this chapter is a summary of the major findings and conclusions of

this dissertation. In the later section I present the future directions for this project by discussing the uninvestigated questions and suggestions of experiments to answer them.

Summary and conclusions.

Where and when are CXCR2 and its ligands expressed in PC?

i) In human PC tissues hCXCR2 and its ligands hCXCL1 and hCXCL3 are expressed in the normal pancreas as well as in PC. In PC tissues their expression is located on both malignant ducts and stroma. Acinar cells in normal pancreas express CXCR2; however, ducts in the normal pancreas are negative for this signaling.

ii) In mice, only PDAC tissues express mCXCR2 and its ligands mCXCL1 and mCXCL5 while the normal pancreas remains negative.

iii) Upregulation of the CXCR2 signaling axis is an early event during PC development and is directly linked with the *KRAS*$^{(G12D)}$ mutation *in vitro* and *in vivo.*

What is the significance of CXCR2 signaling in tumor cell autonomous growth in the context of the KRAS$^{(G12D)}$ *mutation?*

i) The CXCR2 signaling axis mediates *KRAS*$^{(G12D)}$-induced autocrine growth *in vitro* and *in vivo* in PDAC cells.

ii) CXCR2 antagonists specifically inhibit the growth of *KRAS*$^{(G12D)}$-bearing cells versus control counterparts having WT *KRAS*.

iii) Inhibiting CXCR2 signaling in PDAC cells down-regulates the protein levels of KRAS and inhibits the activation of the ERK pathway.

iv) A KRAS-CXCR2 feed-forward loop amplifies autocrine growth promoting signals in PDAC cells.

What is the significance of CXCR2 in tumor-host interaction during the progression of PC?

i) Depletion of host *Cxcr2* did not affect the growth of PC cells but enhanced their apoptosis. Therefore, host CXCR2 mainly regulates the survival of tumor cells.

ii) Overall, host *Cxcr2* depletion did not shrink the primary tumor.

iii) Enhanced fibrosis in the tumors of *Cxcr2*$^{-/-}$ hosts compensates for any tumor size reduction due to the decreased survival of tumor cells. Therefore, we did not observe any tumor shrinkage in *Cxcr2*$^{-/-}$ hosts.

iv) Enhanced fibrosis in tumors of *Cxcr2*-depleted host was specific to pancreatic parenchyma.

v) Host *Cxcr2* deletion increases metastasis to livers.

vi) Decreased angiogenesis in tumors derived from *Cxcr2*$^{-/-}$ hosts.

vii) Splenomegaly was observed in tumor-bearing *Cxcr2*$^{-/-}$ hosts.

viii) Enhanced splenic accumulation of immature polymorphonuclear cells in tumor-bearing *Cxcr2*$^{-/-}$ hosts suggests increased EMH of myeloid precursors in these mice.

What is the significance of CXCR2 signaling in altering the dynamics of local and systemic immune responses to PC?

i) CXCR2 is important for the recruitment of myeloid populations to the tumor and CXCR2 positive myeloid cells including MDSCs, macrophages, and dendritic cells are present in orthotopically implanted tumors.

ii) Knock-down of host *Cxcr2* results in the inhibited recruitment of MDSCs from spleens to the tumors.

iii) Decreased frequency of MDSCs inside the tumors is accompanied with reduction in the populations of Treg cells.

iv) Knocking-down of host *Cxcr2* has no effect on the recruitment of macrophages.

v) Knock-down of host *Cxcr2* leads to the expansion of MDSCs in spleens.

vi) Treatment of syngeneic immunocompetent mouse model with CXCR2 antagonist also led to the expansion of $Ly6^+$ populations inside the spleens.

vii) Overall, knock-down of *Cxcr2* in the host generates an anti-tumor immune response inside the TME but causes systemic immune suppression in the host.

Figure 8.1 provides a synopsis of conclusions of this dissertation.

Directions for future work on this project:

i) *What are the pathways downstream of KRAS$^{(G12D)}$ that upregulate the expression of CXCR2?*

Previous studies have reported that KRAS-induced upregulation of CXCR2 ligands is mediated by pathways like ERK or AKT. We here identify a direct connection between *KRAS$^{(G12D)}$* mutation and expression of CXCR2. However, the pathways downstream of KRAS that induce the expression of CXCR2 remain unidentified. Therefore, as a next step we can identify activation of the pathways downstream of KRAS that cause the upregulation of CXCR2. In order to accomplish this objective we will treat human and mouse PC cell lines having *KRAS$^{(G12D)}$* mutation with inhibitors for various signaling pathways, for example: ERK inhibitor (PD98590), PI3K/Akt pathway inhibitor (Wortmannin).

ii) *What is the contribution of the individual ligands of CXCR2 in KRAS$^{(G12D)}$ -induced PC*?

Reports suggest that KRAS-induced expression of CXCR2 ligands can exert functionally different outcomes in different cell types. For instance, CXCL1 was shown to induce senescence in fibroblasts while CXCL8 was found to be angiogenic. For future research, the role of an individual ligand in regulating *KRAS$^{(G12D)}$* **-**induced autocrine and paracrine tumor-promoting roles in PC should be studied. This can help in mitigating the side effects generated by systemic inhibition of CXCR2.

iii) What will be the effect of deleting Cxcr2 specifically in the ductal cells of a spontaneous PC mouse model?

To study the autocrine roles of CXCR2 in *KRAS*$^{(G12D)}$-induced PC, we have used orthotopic and subcutaneous nude mouse models inoculated with PC cells having *Cxcr2* depletion. As a logical step, the effect of deleting *Cxcr2* at different time points in the ductal cells of a spontaneous PC model like Pdx1-cre;LSL-*Kras*$^{(G12D)}$ should be evaluated. Alternatively, ductal cells can be isolated from Pdx1-cre;LSL-*Kras*$^{(G12D)}$-*Cxcr2*$^{-/-}$ mice and cultured *in vitro*. *In vitro* tumor-associated phenotypes should be evaluated. Furthermore, these cells can be implanted in the pancreas of WT C57BL6 mice. C57BL6 mice having pancreatic implantation of KRAS-PDAC cells will serve as the control group.

iv) To evaluate how CXCR2 deletion in the host alters the frequency of mast cell infiltrations in the tumors?

In chapter 1 we discussed the roles of mast cells in the PC TME and also presented information regarding the importance of CXCR2 in mast cell biology. We have evaluated the role of CXCR2 in regulating the infiltration of MDSCs, macrophages and dendritic cell. Future studies should evaluate the significance of CXCR2 in altering the infiltration of mast cells in PC.

v) What will be the effect of deleting Cxcr2 in the bone marrow on the growth of PC?

We have employed a mouse model having *Cxcr2* deletion to study the host immune responses in PC. To specifically address the effect of *Cxcr2* depletion in

the myeloid cell compartment, bone marrow from *Cxcr2*$^{-/-}$ mice can be transplanted to a spontaneous PC mouse model like Pdx1-cre;LSL-*Kras*$^{(G12D)}$. Tumor growth should be evaluated. Once the mice are sacrificed the altered frequencies of immune cell populations in these tumors should be studied by flow cytometry and IHC.

vi) What will be the effect of splenectomizing mice at the time of implanting tumor cells in the pancreas?

Our results in this study have demonstrated a peripheral immune suppression in spleens of tumor-bearing *Cxcr2*$^{-/-}$ hosts. Therefore, it would be interesting to analyze the impact of splenectomizing the WT and *Cxcr2*$^{-/-}$ mice at the time of performing pancreatic surgeries to inoculate tumor cells.

vii) Will the precise delivery of CXCR2 antagonists to a specific cell type improve the therapeutic outcome?

By employing adjuvant or proper delivery systems for targeting CXCR2 antagonists to specific cell types, the side effects generated by overall systemic delivery of CXCR2 signaling can be reduced.

PC is in an urgent need of new molecular targets for designing improved therapeutics. In this dissertation we evaluated the significance of CXCR2 in PC pathology. The results presented here clearly suggest a dual tumor-promoting as wells as tumor-inhibiting role of CXCR2 in PC. We hope that these results will serve as a beacon for guiding the future research in this area. However, to reach an unequivocal conclusion further research efforts in this direction are essential.

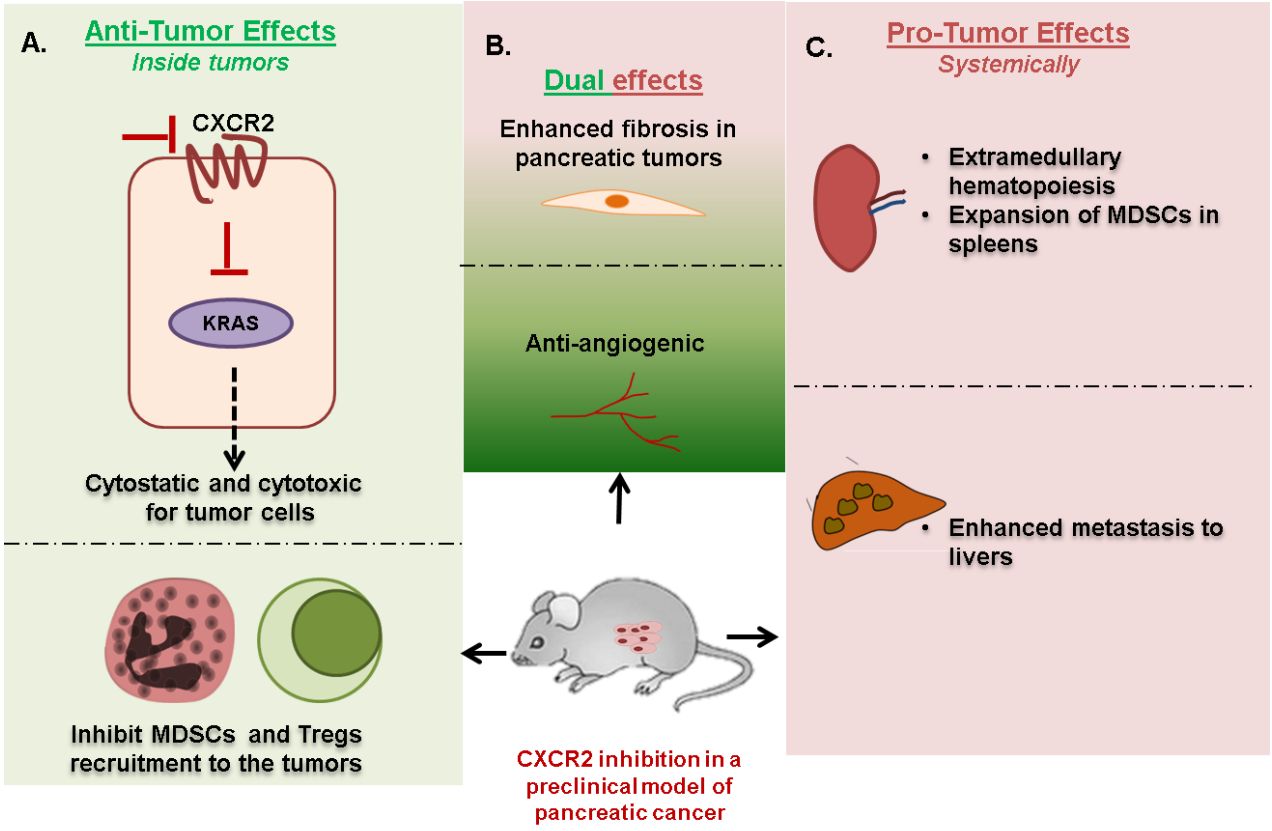
A.
Anti-Tumor Effects
Inside tumors
CXCR2
KRAS
Cytostatic and cytotoxic for tumor cells
Inhibit MDSCs and Tregs recruitment to the tumors
B.
Dual effects
Enhanced fibrosis in pancreatic tumors
Anti-angiogenic
CXCR2 inhibition in a preclinical model of pancreatic cancer
C.
Pro-Tumor Effects
Systemically
Extramedullary hematopoiesis
Expansion of MDSCs in spleens
Enhanced metastasis to livers

Figure 8.1. CXCR2 signaling a double-edged sword in pancreatic cancer.

Schematic representation of the effects of CXCR2 inhibition in a preclinical mouse model of pancreatic cancer. Systemic inhibition of CXCR2 results in differential tumor-promoting or –inhibiting effects in tumors versus the host. **A)** Anti-tumor effects of CXCR2 deletion are inhibition of tumor cell proliferation and reduced infiltration of myeloid-derived suppressor cells (MDSCs) and regulatory T cells (Tregs). **B)** The significance of fibrosis and angiogenesis are areas of contention in pancreatic cancer. Therefore, pro-fibrotic and anti-angiogenic effect of CXCR2 inhibition is classified as a dual effect (having pro- and anti-tumor impact). **C)** CXCR2 inhibition in the host causes extramedullary hematopoiesis of myeloid precursors and expansion of MDSCs inside the spleens resulting in systemic immune suppression and enhanced metastasis to livers.

Bibliography

Acharyya, S., Oskarsson, T., Vanharanta, S., Malladi, S., Kim, J., Morris, P.G., Manova-Todorova, K., Leversha, M., Hogg, N., and Seshan, V.E. (2012). A CXCL1 paracrine network links cancer chemoresistance and metastasis. Cell *150*, 165-178.

Ancrile, B.B., O'Hayer, K.M., and Counter, C.M. (2008). Oncogenic Ras–Induced Expression of Cytokines in Cancer. Molecular interventions *8*, 22.

Baggiolini, M. (1998). Chemokines and leukocyte traffic. Nature *392*, 565-568.

Baggiolini, M., Dewald, B., and Moser, B. (1994a). Interleukin-8 and related chemotactic cytokines--CXC and CC chemokines. Advances in Immunology *55*, 97-179.

Baggiolini, M., Moser, B., and Clark-Lewis, I. (1994b). Interleukin-8 and related chemotactic cytokines: the Giles Filley lecture. CHEST Journal *105*, 95S-98S.

Bailey, C., Negus, R., Morris, A., Ziprin, P., Goldin, R., Allavena, P., Peck, D., and Darzi, A. (2007). Chemokine expression is associated with the accumulation of tumour associated macrophages (TAMs) and progression in human colorectal cancer. Clinical & Experimental Metastasis *24*, 121-130.

Biedermann, T., Kneilling, M., Mailhammer, R., Maier, K., Sander, C.A., Kollias, G., Kunkel, S.L., Hültner, L., and Röcken, M. (2000). Mast cells control neutrophil recruitment during T cell–mediated delayed-type hypersensitivity reactions through tumor necrosis factor and macrophage inflammatory protein 2. The Journal of Experimental Medicine *192*, 1441-1452.

Bonecchi, R., Facchetti, F., Dusi, S., Luini, W., Lissandrini, D., Simmelink, M., Locati, M., Bernasconi, S., Allavena, P., and Brandt, E. (2000). Induction of

functional IL-8 receptors by IL-4 and IL-13 in human monocytes. The Journal of Immunology *164*, 3862-3869.

Bryant, K.L., Mancias, J.D., Kimmelman, A.C., and Der, C.J. (2014). KRAS: feeding pancreatic cancer proliferation. Trends in Biochemical Sciences *39*, 91-100.

Burkholder, B., Huang, R.-Y., Burgess, R., Luo, S., Jones, V.S., Zhang, W., Lv, Z.-Q., Gao, C.-Y., Wang, B.-L., and Zhang, Y.-M. (2014). Tumor-induced perturbations of cytokines and immune cell networks. Biochimica et Biophysica Acta (BBA)-Reviews on Cancer *1845*, 182-201.

Campbell, P.M., Groehler, A.L., Lee, K.M., Ouellette, M.M., Khazak, V., and Der, C.J. (2007). K-Ras promotes growth transformation and invasion of immortalized human pancreatic cells by Raf and phosphatidylinositol 3-kinase signaling. Cancer Research *67*, 2098-2106.

Candido, J., and Hagemann, T. (2013). Cancer-related inflammation. Journal of Clinical Immunology *33*, 79-84.

Cavanagh, L.L., and Von Andrian, U.H. (2002). Travellers in many guises: the origins and destinations of dendritic cells. Immunology and Cell Biology *80*, 448-462.

Chapman, R., Phillips, J., Hipkin, R., Curran, A., Lundell, D., and Fine, J. (2009). CXCR2 antagonists for the treatment of pulmonary disease. Pharmacology & Therapeutics *121*, 55-68.

Chen, L., Fan, J., Chen, H., Meng, Z., Chen, Z., Wang, P., and Liu, L. (2014). The IL-8/CXCR1 axis is associated with cancer stem cell-like properties and

correlates with clinical prognosis in human pancreatic cancer cases. Scientific Reports *4*.

Chen, Y., Shi, M., Yu, G.-Z., Qin, X.-R., Jin, G., Chen, P., and Zhu, M.-H. (2012). Interleukin-8, a promising predictor for prognosis of pancreatic cancer. World Journal of Gastroenterology: WJG *18*, 1123.

Cheng, W.-L., Wang, C.-S., Huang, Y.-H., Tsai, M.-M., Liang, Y., and Lin, K.-H. (2011). Overexpression of CXCL1 and its receptor CXCR2 promote tumor invasion in gastric cancer. Annals of Oncology, mdq739.

Chung, E., Yamashita, H., Au, P., Tannous, B.A., Fukumura, D., and Jain, R.K. (2009). Secreted Gaussia luciferase as a biomarker for monitoring tumor progression and treatment response of systemic metastases. PLoS One *4*, e8316.

Clark, C.E., Hingorani, S.R., Mick, R., Combs, C., Tuveson, D.A., and Vonderheide, R.H. (2007c). Dynamics of the immune reaction to pancreatic cancer from inception to invasion. Cancer Research *67*, 9518-9527.

Collington, S.J., Williams, T.J., and Weller, C.L. (2011). Mechanisms underlying the localisation of mast cells in tissues. Trends in Immunology *32*, 478-485.

Collins, M.A., Bednar, F., Zhang, Y., Brisset, J.-C., Galbán, S., Galbán, C.J., Rakshit, S., Flannagan, K.S., Adsay, N.V., and di Magliano, M.P. (2012). Oncogenic Kras is required for both the initiation and maintenance of pancreatic cancer in mice. The Journal of Clinical Investigation *122*, 639.

Conor O'keane, J., Wolf, B.C., and Neiman, R.S. (1989). The pathogenesis of splenic extramedullary hematopoiesis in metastatic carcinoma. Cancer *63*, 1539-1543.

Cortez-Retamozo, V., Etzrodt, M., Newton, A., Rauch, P.J., Chudnovskiy, A., Berger, C., Ryan, R.J., Iwamoto, Y., Marinelli, B., and Gorbatov, R. (2012). Origins of tumor-associated macrophages and neutrophils. Proceedings of the National Academy of Sciences *109*, 2491-2496.

Desurmont, T., Skrypek, N., Duhamel, A., Jonckheere, N., Millet, G., Leteurtre, E., Gosset, P., Duchene, B., Ramdane, N., and Hebbar, M. (2015). Overexpression of chemokine receptor CXCR2 and ligand CXCL7 in liver metastases from colon cancer is correlated to shorter disease-free and overall survival. Cancer Science *106*, 262-269.

Devalaraja, R.M., Nanney, L.B., Qian, Q., Du, J., Yu, Y., Devalaraja, M.N., and Richmond, A. (2000). Delayed wound healing in CXCR2 knockout mice. Journal of Investigative Dermatology *115*, 234-244.

Downward, J. (2003). Targeting RAS signalling pathways in cancer therapy. Nature Reviews Cancer *3*, 11-22.

Epstein, F.H., and Luster, A.D. (1998). Chemokines—chemotactic cytokines that mediate inflammation. New England Journal of Medicine *338*, 436-445.

Erkan, M., Reiser-Erkan, C., Michalski, C., and Kleeff, J. (2010). Tumor microenvironment and progression of pancreatic cancer. Exp Oncol *32*, 128-131.

Evans, A., and Costello, E. (2012). The role of inflammatory cells in fostering pancreatic cancer cell growth and invasion. Frontiers in Physiology *3*.

Feig, C., Gopinathan, A., Neesse, A., Chan, D.S., Cook, N., and Tuveson, D.A. (2012). The pancreas cancer microenvironment. Clinical Cancer Research *18*, 4266-4276.

Feijoó, E., Alfaro, C., Mazzolini, G., Serra, P., Peñuelas, I., Arina, A., Huarte, E., Tirapu, I., Palencia, B., and Murillo, O. (2005). Dendritic cells delivered inside human carcinomas are sequestered by interleukin-8. International Journal of Cancer *116*, 275-281.

Fesinmeyer, M.D., Austin, M.A., Li, C.I., De Roos, A.J., and Bowen, D.J. (2005). Differences in survival by histologic type of pancreatic cancer. Cancer Epidemiology Biomarkers & Prevention *14*, 1766-1773.

Fujimura, T., Mahnke, K., and Enk, A.H. (2010). Myeloid derived suppressor cells and their role in tolerance induction in cancer. Journal of Dermatological Science *59*, 1-6.

Gabrilovich, D.I., and Nagaraj, S. (2009). Myeloid-derived suppressor cells as regulators of the immune system. Nature Reviews Immunology *9*, 162-174.

Garassino, M., Marabese, M., Rusconi, P., Rulli, E., Martelli, O., Farina, G., Scanni, A., and Broggini, M. (2011). Different types of K-Ras mutations could affect drug sensitivity and tumour behaviour in non-small-cell lung cancer. Annals of Oncology *22*, 235-237.

Gerszten, R.E., Garcia-Zepeda, E.A., Lim, Y.-C., Yoshida, M., Ding, H.A., Gimbrone, M.A., Luster, A.D., Luscinskas, F.W., and Rosenzweig, A. (1999). MCP-1 and IL-8 trigger firm adhesion of monocytes to vascular endothelium under flow conditions. Nature *398*, 718-723.

Gillitzer, R., and Goebeler, M. (2001). Chemokines in cutaneous wound healing. Journal of Leukocyte Biology *69*, 513-521.

Goedegebuure, P., Mitchem, J., Porembka, M., Tan, M., Belt, B., Wang-Gillam, A., Gillanders, W., Hawkins, W., and Linehan, D. (2011). Myeloid-derived suppressor cells: general characteristics and relevance to clinical management of pancreatic cancer. Current Cancer Drug Targets *11*, 734.

Gordon, S. (2003). Alternative activation of macrophages. Nature Reviews Immunology *3*, 23-35.

Gumbs, A., Moore, P., Falconi, M., Bassi, C., Beghelli, S., Modlin, I., and Scarpa, A. (2002). Review of the clinical, histological, and molecular aspects of pancreatic endocrine neoplasms. Journal of Surgical Oncology *81*, 45-53.

Hallgren, J., Jones, T.G., Abonia, J.P., Xing, W., Humbles, A., Austen, K.F., and Gurish, M.F. (2007). Pulmonary CXCR2 regulates VCAM-1 and antigen-induced recruitment of mast cell progenitors. Proceedings of the National Academy of Sciences *104*, 20478-20483.

Haskill, S., Peace, A., Morris, J., Sporn, S.A., Anisowicz, A., Lee, S.W., Smith, T., Martin, G., Ralph, P., and Sager, R. (1990). Identification of three related human GRO genes encoding cytokine functions. Proceedings of the National Academy of Sciences *87*, 7732-7736.

Hertzer, K.M., Donald, G.W., and Hines, O.J. (2013). CXCR2: a target for pancreatic cancer treatment? Expert Opinion on Therapeutic Targets *17*, 667-680.

Highfill, S.L., Cui, Y., Giles, A.J., Smith, J.P., Zhang, H., Morse, E., Kaplan, R.N., and Mackall, C.L. (2014). Disruption of CXCR2-mediated MDSC tumor trafficking enhances anti-PD1 efficacy. Science Translational Medicine *6*, 237ra267-237ra267.

Hingorani, S.R., Petricoin, E.F., Maitra, A., Rajapakse, V., King, C., Jacobetz, M.A., Ross, S., Conrads, T.P., Veenstra, T.D., and Hitt, B.A. (2003a). Preinvasive and invasive ductal pancreatic cancer and its early detection in the mouse. Cancer Cell *4*, 437-450.

Hingorani, S.R., Wang, L., Multani, A.S., Combs, C., Deramaudt, T.B., Hruban, R.H., Rustgi, A.K., Chang, S., and Tuveson, D.A. (2005). Trp53R172H and KrasG12D cooperate to promote chromosomal instability and widely metastatic pancreatic ductal adenocarcinoma in mice. Cancer Cell *7*, 469-483.

Hirooka, S., Yanagimoto, H., Satoi, S., Yamamoto, T., Toyokawa, H., Yamaki, S., Yui, R., Inoue, K., Michiura, T., and Kwon, A.-H. (2011). The role of circulating dendritic cells in patients with unresectable pancreatic cancer. Anticancer Research *31*, 3827-3834.

Holmes, W.E., Lee, J., Kuang, W.-J., Rice, G.C., and Wood, W.I. (1991). Structure and functional expression of a human interleukin-8 receptor. Science *253*, 1278-1280.

Holz, O., Khalilieh, S., Ludwig-Sengpiel, A., Watz, H., Stryszak, P., Soni, P., Tsai, M., Sadeh, J., and Magnussen, H. (2010). SCH527123, a novel CXCR2 antagonist, inhibits ozone-induced neutrophilia in healthy subjects. European Respiratory Journal *35*, 564-570.

Hruban, R.H., Goggins, M., Parsons, J., and Kern, S.E. (2000). Progression model for pancreatic cancer. Clinical Cancer Research *6*, 2969-2972.

Hruban, R.H., Maitra, A., and Goggins, M. (2008). Update on pancreatic intraepithelial neoplasia. International Journal of Clinical and Experimental Pathology *1*, 306.

Hruban, R.H., Takaori, K., Klimstra, D.S., Adsay, N.V., Albores-Saavedra, J., Biankin, A.V., Biankin, S.A., Compton, C., Fukushima, N., and Furukawa, T. (2004). An illustrated consensus on the classification of pancreatic intraepithelial neoplasia and intraductal papillary mucinous neoplasms. The American Journal of Surgical Pathology *28*, 977-987.

Ijichi, H., Chytil, A., Gorska, A.E., Aakre, M.E., Bierie, B., Tada, M., Mohri, D., Miyabayashi, K., Asaoka, Y., and Maeda, S. (2011a). Inhibiting Cxcr2 disrupts tumor-stromal interactions and improves survival in a mouse model of pancreatic ductal adenocarcinoma. The Journal of Clinical Investigation *121*, 4106.

Kamohara, H., Takahashi, M., Ishiko, T., Ogawa, M., and Baba, H. (2007). Induction of interleukin-8 (CXCL-8) by tumor necrosis factor-α and leukemia inhibitory factor in pancreatic carcinoma cells: Impact of CXCL-8 as an autocrine growth factor. International Journal of Oncology *31*, 627-632.

Katoh, H., Wang, D., Daikoku, T., Sun, H., Dey, S.K., and DuBois, R.N. (2013). CXCR2-expressing myeloid-derived suppressor cells are essential to promote colitis-associated tumorigenesis. Cancer Cell *24*, 631-644.

Kaur, M., and Singh, D. (2013). Neutrophil chemotaxis caused by chronic obstructive pulmonary disease alveolar macrophages: the role of CXCL8 and the

receptors CXCR1/CXCR2. Journal of Pharmacology and Experimental Therapeutics *347*, 173-180.

Keane, M.P., Belperio, J.A., Xue, Y.Y., Burdick, M.D., and Strieter, R.M. (2004). Depletion of CXCR2 inhibits tumor growth and angiogenesis in a murine model of lung cancer. The Journal of Immunology *172*, 2853-2860.

Khazaie, K., Blatner, N.R., Khan, M.W., Gounari, F., Gounaris, E., Dennis, K., Bonertz, A., Tsai, F.-N., Strouch, M.J., and Cheon, E. (2011). The significant role of mast cells in cancer. Cancer and Metastasis Reviews *30*, 45-60.

Kitamura, T., and Pollard, J.W. (2015). Therapeutic potential of chemokine signal inhibition for metastatic breast cancer. Pharmacological Research *100*, 266-270.

Krishnaswamy, G., Kelley, J., Yerra, L., Smith, J.K., and Chi, D.S. (1999). Human endothelium as a source of multifunctional cytokines: molecular regulation and possible role in human disease. Journal of Interferon & Cytokine Research *19*, 91-104.

Kuwada, Y., Sasaki, T., Morinaka, K., Kitadai, Y., Mukaida, N., and Chayama, K. (2003). Potential involvement of IL-8 and its receptors in the invasiveness of pancreatic cancer cells. International Journal of Oncology *22*, 765-771.

Lança, T., Costa, M.F., Gonçalves-Sousa, N., Rei, M., Grosso, A.R., Penido, C., and Silva-Santos, B. (2013). Protective role of the inflammatory CCR2/CCL2 chemokine pathway through recruitment of type 1 cytotoxic γδ T lymphocytes to tumor beds. The Journal of Immunology *190*, 6673-6680.

Lazennec, G., and Richmond, A. (2010). Chemokines and chemokine receptors: new insights into cancer-related inflammation. Trends in Molecular Medicine *16*, 133-144.

Le, X., Shi, Q., Wang, B., Xiong, Q., Qian, C., Peng, Z., Li, X.-C., Tang, H., Abbruzzese, J.L., and Xie, K. (2000). Molecular regulation of constitutive expression of interleukin-8 in human pancreatic adenocarcinoma. Journal of Interferon & Cytokine Research *20*, 935-946.

Lee, H.J., Song, I.-C., Yun, H.-J., Jo, D.-Y., and Kim, S. (2014). CXC chemokines and chemokine receptors in gastric cancer: From basic findings towards therapeutic targeting. World Journal of Gastroenterology: WJG *20*, 1681.

Lee, J.-W., Kim, H., Wei, J.-D., Seo, J.-M., Park, S.Y., Park, G.-S., Lee, A.-J., and Kim, J.-H. (2011). Proinflammatory cytokine IL-1β stimulates IL-8 synthesis in mast cells via a leukotriene B4 receptor 2-linked pathway, contributing to angiogenesis. Cancer Research *71*, 404-404.

Li, A., Cheng, X.J., Moro, A., Singh, R.K., Hines, O.J., and Eibl, G. (2011a). CXCR2-dependent endothelial progenitor cell mobilization in pancreatic cancer growth. Translational Oncology *4*, 20-28.

Li, A., King, J., Moro, A., Sugi, M.D., Dawson, D.W., Kaplan, J., Li, G., Lu, X., Strieter, R.M., and Burdick, M. (2011c). Overexpression of CXCL5 is associated with poor survival in patients with pancreatic cancer. The American Journal of Pathology *178*, 1340-1349.

Li, A., Varney, M.L., and Singh, R.K. (2001). Expression of interleukin 8 and its receptors in human colon carcinoma cells with different metastatic potentials. Clinical Cancer Research *7*, 3298-3304.

Li, M., Zhang, Y., Feurino, L.W., Wang, H., Fisher, W.E., Brunicardi, F.C., Chen, C., and Yao, Q. (2008). Interleukin-8 increases vascular endothelial growth factor and neuropilin expression and stimulates ERK activation in human pancreatic cancer. Cancer Science *99*, 733-737.

Lin, A.M., Rubin, C.J., Khandpur, R., Wang, J.Y., Riblett, M., Yalavarthi, S., Villanueva, E.C., Shah, P., Kaplan, M.J., and Bruce, A.T. (2011). Mast cells and neutrophils release IL-17 through extracellular trap formation in psoriasis. The Journal of Immunology *187*, 490-500.

Lippert, U., Artuc, M., Grützkau, A., Möller, A., Kenderessy-Szabo, A., Schadendorf, D., Norgauer, J., Hartmann, K., Schweitzer-Stenner, R., and Zuberbier, T. (1998). Expression and functional activity of the IL-8 receptor type CXCR1 and CXCR2 on human mast cells. The Journal of Immunology *161*, 2600-2608.

Lowenfels, A.B., and Maisonneuve, P. (2006). Epidemiology and risk factors for pancreatic cancer. Best Practice & Research Clinical Gastroenterology *20*, 197-209.

Luppi, F., Longo, A., De Boer, W., Rabe, K., and Hiemstra, P. (2007). Interleukin-8 stimulates cell proliferation in non-small cell lung cancer through epidermal growth factor receptor transactivation. Lung Cancer *56*, 25-33.

Maltby, S., Khazaie, K., and McNagny, K.M. (2009). Mast cells in tumor growth: angiogenesis, tissue remodelling and immune-modulation. Biochimica et Biophysica Acta (BBA)-Reviews on Cancer *1796*, 19-26.

Mantovani, A., Allavena, P., Sozzani, S., Vecchi, A., Locati, M., and Sica, A. (2004a). Chemokines in the recruitment and shaping of the leukocyte infiltrate of tumors. Paper presented at: Seminars in Cancer Biology (Elsevier).

Mantovani, A., Sica, A., Sozzani, S., Allavena, P., Vecchi, A., and Locati, M. (2004b). The chemokine system in diverse forms of macrophage activation and polarization. Trends in Immunology *25*, 677-686.

Matsuo, Y., Campbell, P.M., Brekken, R.A., Sung, B., Ouellette, M.M., Fleming, J.B., Aggarwal, B.B., Der, C.J., and Guha, S. (2009a). K-Ras promotes angiogenesis mediated by immortalized human pancreatic epithelial cells through mitogen-activated protein kinase signaling pathways. Molecular Cancer Research *7*, 799-808.

Matsuo, Y., Ochi, N., Sawai, H., Yasuda, A., Takahashi, H., Funahashi, H., Takeyama, H., Tong, Z., and Guha, S. (2009d). CXCL8/IL-8 and CXCL12/SDF-1α co-operatively promote invasiveness and angiogenesis in pancreatic cancer. International Journal of Cancer *124*, 853-861.

Matsuo, Y., Raimondo, M., Woodward, T.A., Wallace, M.B., Gill, K.R., Tong, Z., Burdick, M.D., Yang, Z., Strieter, R.M., and Hoffman, R.M. (2009e). CXC-chemokine/CXCR2 biological axis promotes angiogenesis in vitro and in vivo in pancreatic cancer. International Journal of Cancer *125*, 1027-1037.

Melillo, R., Guarino, V., Avilla, E., Galdiero, M., Liotti, F., Prevete, N., Rossi, F., Basolo, F., Ugolini, C., and de Paulis, A. (2010). Mast cells have a protumorigenic role in human thyroid cancer. Oncogene *29*, 6203-6215.

Moser, B., Barella, L., Mattei, S., Schumacher, C., Boulay, F., Colombo, M., and Baggiolini, M. (1993). Expression of transcripts for two interleukin 8 receptors in human phagocytes, lymphocytes and melanoma cells. Biochemistry Journal *294*, 285-292.

Murdoch, C., Giannoudis, A., and Lewis, C.E. (2004). Mechanisms regulating the recruitment of macrophages into hypoxic areas of tumors and other ischemic tissues. Blood *104*, 2224-2234.

Nagaraj, S., and Gabrilovich, D.I. (2008). Tumor escape mechanism governed by myeloid-derived suppressor cells. Cancer Research *68*, 2561-2563.

Nakao, S., Kuwano, T., Tsutsumi-Miyahara, C., Ueda, S.-i., Kimura, Y.N., Hamano, S., Sonoda, K.-h., Saijo, Y., Nukiwa, T., and Strieter, R.M. (2005). Infiltration of COX-2–expressing macrophages is a prerequisite for IL-1β–induced neovascularization and tumor growth. Journal of Clinical Investigation *115*, 2979.

Nilsson, G., Mikovits, J.A., Metcalfe, D.D., and Taub, D.D. (1999). Mast cell migratory response to interleukin-8 is mediated through interaction with chemokine receptor CXCR2/Interleukin-8RB. Blood *93*, 2791-2797.

Ning, Y., Labonte, M.J., Zhang, W., Bohanes, P.O., Gerger, A., Yang, D., Benhaim, L., Paez, D., Rosenberg, D.O., and Venkata, K.C.N. (2012a). The CXCR2 antagonist, SCH-527123, shows antitumor activity and sensitizes cells to

oxaliplatin in preclinical colon cancer models. Molecular Cancer Therapeutics *11*, 1353-1364.

O'Hayer, K.M., Brady, D.C., and Counter, C.M. (2009). ELR+ CXC chemokines and oncogenic Ras-mediated tumorigenesis. Carcinogenesis *30*, 1841-1847.

Ochi, A., Nguyen, A.H., Bedrosian, A.S., Mushlin, H.M., Zarbakhsh, S., Barilla, R., Zambirinis, C.P., Fallon, N.C., Rehman, A., and Pylayeva-Gupta, Y. (2012). MyD88 inhibition amplifies dendritic cell capacity to promote pancreatic carcinogenesis via Th2 cells. The Journal of Experimental Medicine *209*, 1671-1687.

Oliveira Frick, V., Rubie, C., Wagner, M., Graeber, S., Grimm, H., Kopp, B., Rau, B.M., and Schilling, M.K. (2008). Enhanced ENA-78 and IL-8 expression in patients with malignant pancreatic diseases. Pancreatology *8*, 488-497.

Ostrand-Rosenberg, S., and Sinha, P. (2009). Myeloid-derived suppressor cells: linking inflammation and cancer. The Journal of Immunology *182*, 4499-4506.

Özdemir, B.C., Pentcheva-Hoang, T., Carstens, J.L., Zheng, X., Wu, C.-C., Simpson, T.R., Laklai, H., Sugimoto, H., Kahlert, C., and Novitskiy, S.V. (2014). Depletion of carcinoma-associated fibroblasts and fibrosis induces immunosuppression and accelerates pancreas cancer with reduced survival. Cancer Cell *25*, 719-734.

Patel, L., Charlton, S., Chambers, J., and Macphee, C. (2001). Expression and functional analysis of chemokine receptors in human peripheral blood leukocyte populations. Cytokine *14*, 27-36.

Pinzon-Charry, A., Maxwell, T., and Lopez, J.A. (2005). Dendritic cell dysfunction in cancer: a mechanism for immunosuppression. Immunology and Cell Biology *83*, 451-461.

Porembka, M.R., Mitchem, J.B., Belt, B.A., Hsieh, C.-S., Lee, H.-M., Herndon, J., Gillanders, W.E., Linehan, D.C., and Goedegebuure, P. (2012). Pancreatic adenocarcinoma induces bone marrow mobilization of myeloid-derived suppressor cells which promote primary tumor growth. Cancer Immunology, Immunotherapy *61*, 1373-1385.

Proost, P., De Wolf-Peeters, C., Conings, R., Opdenakker, G., Billiau, A., and Van Damme, J. (1993). Identification of a novel granulocyte chemotactic protein (GCP-2) from human tumor cells. In vitro and in vivo comparison with natural forms of GRO, IP-10, and IL-8. The Journal of Immunology *150*, 1000-1010.

Raimondi, S., Maisonneuve, P., and Lowenfels, A.B. (2009). Epidemiology of pancreatic cancer: an overview. Nature Reviews Gastroenterology and Hepatology *6*, 699-708.

Richmond, A., and Thomas, H.G. (1988). Melanoma growth stimulatory activity: isolation from human melanoma tumors and characterization of tissue distribution. Journal of Cellular Biochemistry *36*, 185-198.

Rollins, B. (1999). Chemokines and cancer (Springer Science & Business Media).

Saintigny, P., Massarelli, E., Lin, S., Ahn, Y.-H., Chen, Y., Goswami, S., Erez, B., O'Reilly, M.S., Liu, D., and Lee, J.J. (2013). CXCR2 expression in tumor cells is a

poor prognostic factor and promotes invasion and metastasis in lung adenocarcinoma. Cancer Research *73*, 571-582.

Salazar, N., Castellan, M., Shirodkar, S.S., and Lokeshwar, B.L. (2013). Chemokines and chemokine receptors as promoters of prostate cancer growth and progression. Critical Reviews™ in Eukaryotic Gene Expression *23*.

Sharma, B., Nannuru, K.C., Varney, M.L., and Singh, R.K. (2015). Host Cxcr2-dependent regulation of mammary tumor growth and metastasis. Clinical & Experimental Metastasis *32*, 65-72.

Siegel, R.L., Miller, K.D., and Jemal, A. (2015). Cancer statistics, 2015. CA: a Cancer Journal for Clinicians *65*, 5-29.

Singh, S., Sadanandam, A., Nannuru, K.C., Varney, M.L., Mayer-Ezell, R., Bond, R., and Singh, R.K. (2009). Small-molecule antagonists for CXCR2 and CXCR1 inhibit human melanoma growth by decreasing tumor cell proliferation, survival, and angiogenesis. Clinical Cancer Research *15*, 2380-2386.

Singh, S., Varney, M., Mayer-Ezell, R., Bond, R., and Singh, R. (2007). Small molecule antagonists for CXCR1 and CXCR2 inhibit tumor growth of human melanoma by decreasing cell proliferation and angiogenesis and enhancing apoptosis. Cancer Research *67*, 5633-5633.

Slettenaar, V.I., and Wilson, J.L. (2006). The chemokine network: a target in cancer biology? Advanced Drug Delivery Reviews *58*, 962-974.

Sozzani, S., Luini, W., Borsatti, A., Polentarutti, N., Zhou, D., Piemonti, L., D'amico, G., Power, C.A., Wells, T., and Gobbi, M. (1997). Receptor expression

and responsiveness of human dendritic cells to a defined set of CC and CXC chemokines. The Journal of Immunology *159*, 1993-2000.

Sozzani, S., Sallusto, F., Luini, W., Zhou, D., Piemonti, L., Allavena, P., Van Damme, J., Valitutti, S., Lanzavecchia, A., and Mantovani, A. (1995). Migration of dendritic cells in response to formyl peptides, C5a, and a distinct set of chemokines. The Journal of Immunology *155*, 3292-3295.

Sparmann, A., and Bar-Sagi, D. (2004). Ras-induced interleukin-8 expression plays a critical role in tumor growth and angiogenesis. Cancer cell *6*, 447-458.

Takamori, H., Oades, Z.G., Hoch, R.C., Burger, M., and Schraufstatter, I.U. (2000). Autocrine growth effect of IL-8 and GROα on a human pancreatic cancer cell line, Capan-1. Pancreas *21*, 52-56.

Tannous, B.A. (2009). Gaussia luciferase reporter assay for monitoring biological processes in culture and in vivo. Nature Protocols *4*, 582-591.

Thompson, N., and Lyons, J. (2005). Recent progress in targeting the Raf/MEK/ERK pathway with inhibitors in cancer drug discovery. Current Opinion in Pharmacology *5*, 350-356.

Tjomsland, V., Niklasson, L., Sandström, P., Borch, K., Druid, H., Bratthäll, C., Messmer, D., Larsson, M., and Spångeus, A. (2011). The desmoplastic stroma plays an essential role in the accumulation and modulation of infiltrated immune cells in pancreatic adenocarcinoma. Clinical and Developmental Immunology *2011*.

Toh, B., Wang, X., Keeble, J., Sim, W.J., Khoo, K., Wong, W.-C., Kato, M., Prevost-Blondel, A., Thiery, J.-P., and Abastado, J.-P. (2011). Mesenchymal

transition and dissemination of cancer cells is driven by myeloid-derived suppressor cells infiltrating the primary tumor. PLoS Biology *9*, e1001162.

Torres, M.P., Rachagani, S., Souchek, J.J., Mallya, K., Johansson, S.L., and Batra, S.K. (2013a). Novel pancreatic cancer cell lines derived from genetically engineered mouse models of spontaneous pancreatic adenocarcinoma: applications in diagnosis and therapy. Plos One 20, 8(11)

Van Damme, J., Van Beeumen, J., Opdenakker, G., and Billiau, A. (1988). A novel, NH2-terminal sequence-characterized human monokine possessing neutrophil chemotactic, skin-reactive, and granulocytosis-promoting activity. The Journal of Experimental Medicine *167*, 1364-1376.

Varney, M.L., Johansson, S.L., and Singh, R.K. (2006). Distinct expression of CXCL8 and its receptors CXCR1 and CXCR2 and their association with vessel density and aggressiveness in malignant melanoma. American Journal of Clinical Pathology *125*, 209-216.

Varney, M.L., Singh, S., Li, A., Mayer-Ezell, R., Bond, R., and Singh, R.K. (2011). Small molecule antagonists for CXCR2 and CXCR1 inhibit human colon cancer liver metastases. Cancer Letters *300*, 180-188.

Vincent, A., Herman, J., Schulick, R., Hruban, R.H., and Goggins, M. (2011). Pancreatic cancer. Lancet *378*, 607-620.

von Bernstorff, W., Voss, M., Freichel, S., Schmid, A., Vogel, I., Jöhnk, C., Henne-Bruns, D., Kremer, B., and Kalthoff, H. (2001). Systemic and local immunosuppression in pancreatic cancer patients. Clinical Cancer Research *7*, 925s-932s.

Walz, A., and Baggiolini, M. (1989). A novel cleavage product of β-thromboglobulin formed in cultures of stimulated mononuclear cells activates human neutrophils. Biochemical and Biophysical Research Communications *159*, 969-975.

Walz, A., Burgener, R., Car, B., Baggiolini, M., Kunkel, S.L., and Strieter, R.M. (1991). Structure and neutrophil-activating properties of a novel inflammatory peptide (ENA-78) with homology to interleukin 8. The Journal of Experimental Medicine *174*, 1355-1362.

Walz, A., Peveri, P., Aschauer, H., and Baggiolini, M. (1987a). Purification and amino acid sequencing of NAF, a novel neutrophil-activating factor produced by monocytes. Biochemical and Biophysical Research Communications *149*, 755-761.

Walz, D.A., de Lamo, R., Dene, H., and McCoy, L.E. (1977). Primary structure of human platelet factor 4. Thrombosis Research *11*, 893-898.

Wang, D., Yang, W., Du, J., Devalaraja, M.N., Liang, P., Matsumoto, K., Tsubakimoto, K., Endo, T., and Richmond, A. (2000). MGSA/GRO-mediated melanocyte transformation involves induction of Ras expression. Oncogene *19*, 4647.

Wang, J., Yu, F., Jia, X., Iwanowycz, S., Wang, Y., Huang, S., Ai, W., and Fan, D. (2015). MicroRNA-155 deficiency enhances the recruitment and functions of myeloid-derived suppressor cells in tumor microenvironment and promotes solid tumor growth. International Journal of Cancer *136*, E602-E613.

Wang, S., Wu, Y., Hou, Y., Guan, X., Castelvetere, M.P., Oblak, J.J., Banerjee, S., Filtz, T.M., Sarkar, F.H., and Chen, X. (2013a). CXCR2 macromolecular complex in pancreatic cancer: a potential therapeutic target in tumor growth. Translational Oncology *6*, 216-225.

Wang, Y., and Thorlacius, H. (2005). Mast cell-derived tumour necrosis factor-α mediates macrophage inflammatory protein-2-induced recruitment of neutrophils in mice. British Journal of Pharmacology *145*, 1062-1068.

Wang, Z., and Storm, D.R. (2006). Extraction of DNA from mouse tails. BioTechniques *41*, 410, 412-410, 412.

Waugh, D.J., and Wilson, C. (2008). The interleukin-8 pathway in cancer. Clinical Cancer Research *14*, 6735-6741.

Weiss, J.M., Back, T.C., Scarzello, A.J., Subleski, J.J., Hall, V.L., Stauffer, J.K., Chen, X., Micic, D., Alderson, K., and Murphy, W.J. (2009). Successful immunotherapy with IL-2/anti-CD40 induces the chemokine-mediated mitigation of an immunosuppressive tumor microenvironment. Proceedings of the National Academy of Sciences *106*, 19455-19460.

Wente, M.N., Keane, M.P., Burdick, M.D., Friess, H., Büchler, M.W., Ceyhan, G.O., Reber, H.A., Strieter, R.M., and Hines, O.J. (2006). Blockade of the chemokine receptor CXCR2 inhibits pancreatic cancer cell-induced angiogenesis. Cancer Letters *241*, 221-227.

Wislez, M., Fujimoto, N., Izzo, J.G., Hanna, A.E., Cody, D.D., Langley, R.R., Tang, H., Burdick, M.D., Sato, M., and Minna, J.D. (2006). High expression of

ligands for chemokine receptor CXCR2 in alveolar epithelial neoplasia induced by oncogenic kras. Cancer Research *66*, 4198-4207.

Wörmann, S., Diakopoulos, K., Lesina, M., and Algül, H. (2014). The immune network in pancreatic cancer development and progression. Oncogene *33*, 2956-2967.

Wu, S., Singh, S., Varney, M.L., Kindle, S., and Singh, R.K. (2012). Modulation of CXCL-8 expression in human melanoma cells regulates tumor growth, angiogenesis, invasion, and metastasis. Cancer Medicine *1*, 306-317.

Wu, W., Sun, C., Xu, D., Zhang, X., Shen, W., Lv, Y., and Ma, T. (2015). Expression of CXCR2 and its clinical significance in human colorectal cancer. International journal of Clinical and Experimental Medicine *8*, 5883.

Xu, L., Warren, M., Rose, W., Gong, W., and Wang, J. (1996). Human recombinant monocyte chemotactic protein and other CC chemokines bind and induce directional migration of dendritic cells in vitro. Journal of Leukocyte Biology *60*, 365-371.

Yang, G., Rosen, D.G., Zhang, Z., Bast, R.C., Mills, G.B., Colacino, J.A., Mercado-Uribe, I., and Liu, J. (2006). The chemokine growth-regulated oncogene 1 (Gro-1) links RAS signaling to the senescence of stromal fibroblasts and ovarian tumorigenesis. Proceedings of the National Academy of Sciences *103*, 16472-16477.

Zheng, L., and Martins-Green, M. (2007). Molecular mechanisms of thrombin-induced interleukin-8 (IL-8/CXCL8) expression in THP-1-derived and primary human macrophages. Journal of Leukocyte Biology *82*, 619-629.

Zhou, S.L., Dai, Z., Zhou, Z.J., Wang, X.Y., Yang, G.H., Wang, Z., Huang, X.W., Fan, J., and Zhou, J. (2012). Overexpression of CXCL5 mediates neutrophil infiltration and indicates poor prognosis for hepatocellular carcinoma. Hepatology *56*, 2242-2254.

Zlotnik, A., and Yoshie, O. (2000). Chemokines: a new classification system and their role in immunity. Immunity *12*, 121-127.